| 1. Report No.<br><br>FHWA/TX-92/1148-2 | 2. Government Accession No. | 3. Recipient's Catalog No. | |
|---|---|---|---|
| 4. Title and Subtitle<br><br>TRAFFIC SIGNAL TIMING MODELS FOR OVERSATURATED SIGNALIZED INTERCHANGES | | 5. Report Date<br><br>January 1991<br>January 1992/Revised | |
| | | 6. Performing Organization Code | |
| 7. Author(s)<br><br>Youngchan Kim and Carroll J. Messer | | 8. Performing Organization Report No.<br><br>Research Report 1148-2 | |
| 9. Performing Organization Name and Address<br><br>Texas Transportation Institute<br>The Texas A&M University System<br>College Station, Texas 77843-3135 | | 10. Work Unit No. | |
| | | 11. Contract or Grant No.<br><br>Study No. 2-18-88-1148 | |
| 12. Sponsoring Agency Name and Address<br><br>Texas Department of Transportation<br>Transportation Planning Division<br>P.O. Box 5051<br>Austin, Texas 78763 | | 13. Type of Report and Period Covered<br><br>Interim-March 1989<br>January 1992 | |
| | | 14. Sponsoring Agency Code | |

| 15. Supplementary Notes |
|---|
| Research performed in cooperation with DOT, FHWA.<br>Study Title: Guidelines for Operational Control of Diamond Interchange. |

16. Abstract

This research report documents the development models for control of signalized diamond interchanges during oversaturated traffic conditions. Oversaturated traffic conditions occur when the average traffic demand exceeds the capacity of the signal system. The dynamic optimization model proposed is the principal product of this research. The control objective of the dynamic model is to provide maximum system productivity as well as minimum delay for a selected roadway system. A special feature predetermined upper limits. The dynamic model was developed for conventional diamond interchanges and three-level diamond interchanges. The model takes the form of mixed integer linear programming. The effectiveness of the control strategies generated by the dynamic model was compared to those derived from conventional signal timing models, using the TRAF-NETSIM microscopic simulation model.

It was found that the dynamic models produced optimal signal timing plans for the oversaturated signalized interchanges. The dynamic model consistently outperformed conventional models with respect to system productivity. This conclusion was drawn from the TRAF-NETSIM simulation. The dynamic model solutions significantly reduced total system delay for most test cases, while slightly increasing the delay for a few test cases.

| 17. Key Words<br><br>Dynamic optimization model, signalized interchanges TRAF-NETSIM, diamond interchange. | 18. Distribution Statement<br><br>No restrictions. This document is available to the public through the National Technical Information Service 5285 Port Royal Road. Springfield, VA 22161 | | |
|---|---|---|---|
| 19. Security Classif. (of this report)<br><br>Unclassified | 20. Security Classif. (of this page)<br><br>Unclassified | 21. No. of Pages<br><br>118 | 22. Price |

Form DOT F 1700.7 (8-69)

# TRAFFIC SIGNAL TIMING MODELS

# FOR OVERSATURATED SIGNALIZED INTERCHANGES

by

Youngchan Kim
Engineering Research Associate

and

Carroll J. Messer
Research Engineer

# METRIC (SI*) CONVERSION FACTORS

## APPROXIMATE CONVERSIONS TO SI UNITS

| Symbol | When You Know | Multiply By | To Find | Symbol |
|---|---|---|---|---|
| | **LENGTH** | | | |
| in | inches | 2.54 | centimetres | cm |
| ft | feet | 0.3048 | metres | m |
| yd | yards | 0.914 | metres | m |
| mi | miles | 1.61 | kilometres | km |
| | **AREA** | | | |
| in$^2$ | square inches | 645.2 | centimetres squared | cm$^2$ |
| ft$^2$ | square feet | 0.0929 | metres squared | m$^2$ |
| yd$^2$ | square yards | 0.836 | metres squared | m$^2$ |
| mi$^2$ | square miles | 2.59 | kilometres squared | km$^2$ |
| ac | acres | 0.395 | hectares | ha |
| | **MASS (weight)** | | | |
| oz | ounces | 28.35 | grams | g |
| lb | pounds | 0.454 | kilograms | kg |
| T | short tons (2000 lb) | 0.907 | megagrams | Mg |
| | **VOLUME** | | | |
| fl oz | fluid ounces | 29.57 | millilitres | mL |
| gal | gallons | 3.785 | litres | L |
| ft$^3$ | cubic feet | 0.0328 | metres cubed | m$^3$ |
| yd$^3$ | cubic yards | 0.0765 | metres cubed | m$^3$ |

NOTE: Volumes greater than 1000 L shall be shown in m$^3$.

### TEMPERATURE (exact)

| Symbol | When You Know | Multiply By | To Find | Symbol |
|---|---|---|---|---|
| °F | Fahrenheit temperature | 5/9 (after subtracting 32) | Celsius temperature | °C |

## APPROXIMATE CONVERSIONS TO SI UNITS

| Symbol | When You Know | Multiply By | To Find | Symbol |
|---|---|---|---|---|
| | **LENGTH** | | | |
| mm | millimetres | 0.039 | inches | in |
| m | metres | 3.28 | feet | ft |
| m | metres | 1.09 | yards | yd |
| km | kilometres | 0.621 | miles | mi |
| | **AREA** | | | |
| mm$^2$ | millimetres squared | 0.0016 | square inches | in$^2$ |
| m$^2$ | metres squared | 10.764 | square feet | ft$^2$ |
| km$^2$ | kilometres squared | 0.39 | square miles | mi$^2$ |
| ha | hectares (10 000 m$^2$) | 2.53 | acres | ac |
| | **MASS (weight)** | | | |
| g | grams | 0.0353 | ounces | oz |
| kg | kilograms | 2.205 | pounds | lb |
| Mg | megagrams (1 000 kg) | 1.103 | short tons | T |
| | **VOLUME** | | | |
| mL | millilitres | 0.034 | fluid ounces | fl oz |
| L | litres | 0.264 | gallons | gal |
| m$^3$ | metres cubed | 35.315 | cubic feet | ft$^3$ |
| m$^3$ | metres cubed | 1.308 | cubic yards | yd$^3$ |

### TEMPERATURE (exact)

| Symbol | When You Know | Multiply By | To Find | Symbol |
|---|---|---|---|---|
| °C | Celsius temperature | 9/5 (then add 32) | Fahrenheit temperature | °F |

```
°F    32        98.6          °F 212
-40   0 |40   80  120  160  200|
-40  -20   0   20  |40   60   80  100
°C                 37              °C
```
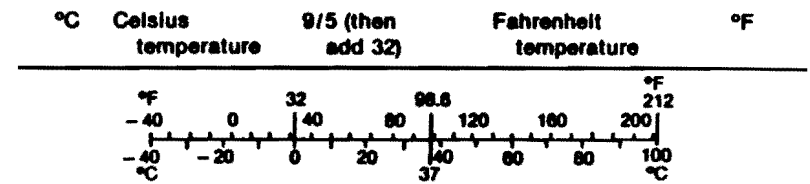
These factors conform to the requirement of FHWA Order 5190.1A.

* SI is the symbol for the International System of Measurements

iii

## ABSTRACT

This research report documents the development of optimization models for the control of signalized diamond interchanges during oversaturated traffic conditions. Oversaturated traffic conditions occur when the average traffic demand exceeds the capacity of the signal system. The dynamic optimization model proposed is the principal product of this research. The control objective of the dynamic model is to provide maximum system productivity as well as minimum delay for a selected roadway system. A special feature of this model is its ability to manage queue lengths on external approaches up to predetermined upper limits. The dynamic model was developed for conventional diamond interchanges and three-level diamond interchanges. The model takes the form of mixed integer linear programming. The effectiveness of the control strategies generated by the dynamic model was compared to those derived from conventional signal timing models, using the TRAF-NETSIM microscopic simulation model.

It was found that the dynamic models produced optimal signal timing plans for the oversaturated signalized interchanges. The dynamic model consistently outperformed the conventional models with respect to system productivity. This conclusion was drawn from the TRAF-NETSIM simulation. The dynamic model solutions significantly reduced total system delay for most test cases, while slightly increasing the delay for a few test cases.

Queue management on external approaches is a primary concern in the traffic control of congested signalized interchanges. The queue management capability is a critical feature in signal timing model for oversaturated environments. The dynamic model was found to be superior to the conventional models in queue management for the congested interchanges. The dynamic model controls queue lengths by efficient and timely changes of signal timing plans as demand changes. Traffic control strategies presented in this research were designed to minimize the transitional delay due to frequent changes of the timing plans.


KEY WORDS: Dynamic optimization model, signalized interchanges, TRAF-NETSIM, diamond interchange.

## IMPLEMENTATION

The optimization models proposed in this study can be used by traffic engineers for a variety of purposes. The models can be used to develop optimal signal timing plans for operation in pretimed signal systems. They can also be evaluate existing or proposed signalized interchanges during oversaturated traffic conditions. However, the models should be further enhanced to promote wide field applications. The findings should be helpful to traffic engineers who design and operate signal systems at signalized diamond interchanges.

## DISCLAIMER

The contents of this report reflect the views of the authors who are responsible for the opinions, findings, and conclusions presented herein. The contents do not necessarily reflect the official views or policies of the Federal Highway Administration or the Texas Department of Transportation. This report does not constitute a standard, specification, or regulation. Additionally, this report is not intended for construction, bidding or permit purposes. Dr. Carroll J. Messer, P.E. #31409, was the engineer in charge of the project.

# TABLE OF CONTENTS

TABLE OF CONTENTS
(Continued)

## LIST OF FIGURES

# LIST OF FIGURES
## (Continued)

## LIST OF TABLES

# 1. INTRODUCTION

## 1.1    PROBLEM STATEMENT

The signalized diamond interchange is a widely used form of freeway-to-street or freeway-to-freeway interchange.    Efficient movement of traffic through a signalized interchange is critical in maintaining an acceptable level of service in the freeway corridor. During high-volume and possibly saturated conditions, inappropriate traffic control may produce long queues and excessive delays.  Long queues can become a safety problem when the ramp (or frontage road) queues overflow onto the busy freeway mainline, or arterial queues spill back and block adjacent intersections, as demonstrated in Figure 1-1.
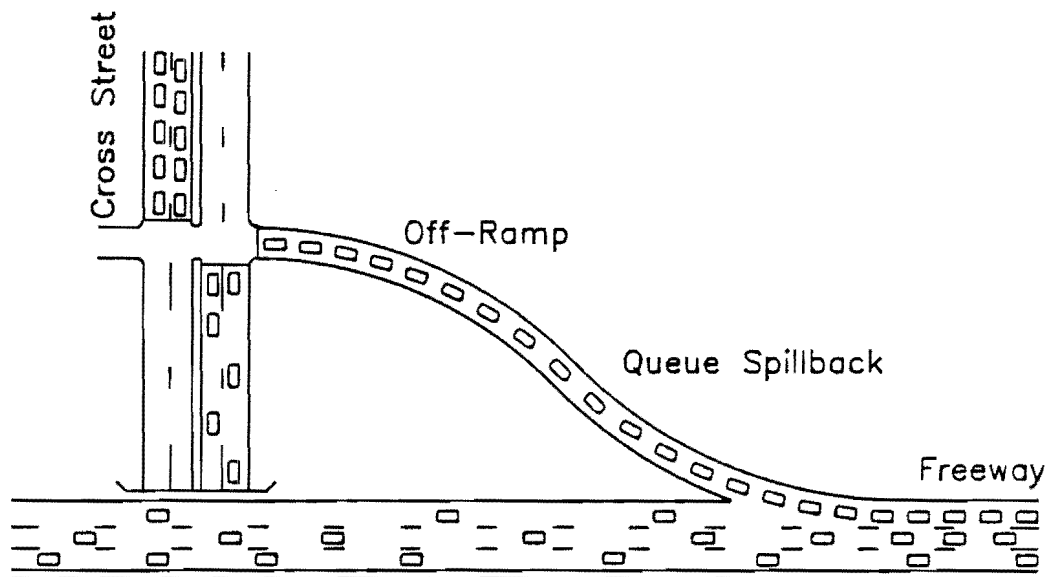


Figure 1-1.  Queue Spillback to Freeway Mainline

Pignataro et al. (*1*) defined *congestion* as a condition in which all waiting vehicles cannot pass through the intersection in one signal cycle.  They also defined *saturation* (or *oversaturation*) as the condition when vehicles are prevented from moving freely, either because of the presence of vehicles in the intersection itself or because of back-ups in any of the exit links of the intersection.  In signalized interchanges, oversaturation occurs when traffic demand exceeds interchange capacity.  Queues fill entire blocks or exit ramps and interfere with the performance of adjacent facilities when this heavy demand continues for a long time period.  Sometimes freeway exit ramps are blocked by the extended queues. Queue spillback to freeway mainlines may occur in the heavily loaded interchanges.  In oversaturated conditions, congestion is unavoidable, thus the control policy should be aimed

1

at postponing the onset and/or the severity of secondary congestion caused by the blockage of adjacent intersections or freeway off-ramps that are not the originators of the congestion.

Control strategies have been developed and applied successfully for the control of undersaturated signalized interchanges, but most of them appear to be ineffective or invalid when traffic volumes become excessively high. Traffic engineering models like PASSER III (2) and TRANSYT-7F (3) have been produced to assist traffic engineers in developing signal timing plans for signalized diamond interchanges. None of these are applicable to oversaturated environments. It would be almost impossible to modify these programs to produce an optimal control policy for oversaturated interchanges. There is an urgent need to develop optimal control strategies for oversaturated signalized interchanges found in Texas.


## 1.2    RESEARCH OBJECTIVES

The goal of this research was to develop an optimization model to provide optimal traffic signal control policies for oversaturated signalized interchanges. Generally the control objective of traffic signal timing has been to obtain maximum bandwidth and/or minimum delay. However, the control objective for oversaturated environments should be to maximize throughput in the system during the control period, i.e., the *productivity*. When demands are extremely high, the control policy should be such that queue lengths on all internal links of the roadway system do not exceed queue storage capacity, and simultaneously all available green times are utilized as fully as possible in order to obtain maximum system productivity. This control objective has been pursued for the control of freeway on-ramps (4, 5).

For the control of oversaturated interchanges, the optimization model should have the capability of controlling queue lengths on external approaches. When traffic demand exceeds interchange capacity, the queue formation on specific approaches depends on the magnitude and duration of the heavy demand. Consequently, the traffic engineering model should be dynamic to accommodate the variation in demand during the control period.

The specific objectives of this research were as follows:

1.    Develop a static optimization model for traffic signal control that maximizes system productivity for a system of two oversaturated intersections, and perform sensitivity analyses for investigating performance of this model;

2.    Develop dynamic optimization models which have a queue management capability for signalized interchanges; and

3.    Use the dynamic models to develop optimal control strategies for the oversaturated signalized interchanges and evaluate the control strategies.

2

## 1.3    RESEARCH METHODOLOGY

The optimization models presented in this research were designed to be effective for congested traffic environments. The models were developed for off-line signal timing tools. The stochastic nature of traffic demand was considered explicitly in the formulation of the models. Since real traffic data were not available for this study, artificial data representing congested conditions were generated and used for testing the models. TRAF-NETSIM (6), a microscopic simulation model developed for Federal Highway Administration, was used to evaluate the control strategies.

This report consists of eight chapters. Chapter 2 deals with background of the research. An extensive literature review was performed concerning traffic control of signalized interchanges and research efforts on oversaturated intersection control. In Chapter 3, a static optimization model is introduced for traffic signal control that maximizes system productivity for the two-intersection problem. This static optimization model becomes the basis for the dynamic optimization models. Chapter 4 describes sensitivity analysis to demonstrate the appropriateness of the hypotheses engaged in the static optimization model. Chapter 5 deals with the development of the dynamic optimization models for external queue management. The dynamic models, considered as the major product of this research, are developed for conventional diamond interchanges and three-level diamond interchanges. In Chapter 6, the performances of the dynamic models are evaluated by comparing them with conventional models. Chapter 7 deals with considerations on future implementations of control strategies produced using the dynamic models. In Chapter 8, conclusions and recommendations for further studies are described.

# 2. RESEARCH BACKGROUND

While extensive studies have been conducted on the design and traffic control of undersaturated signalized interchanges, few studies have been performed for oversaturated interchanges. Some theories have been developed on improved traffic signal control in congested traffic environments. However, there has been no reported work to apply these complex traffic control theories to congested urban diamond interchanges. This is a critical problem since increasing traffic demand is a likely occurrence in urban areas of Texas into the foreseeable future and congested traffic environments will be common.

This study on the control of congested signalized interchanges is timely. In this chapter, studies on the design and control of signalized interchanges and on traffic signal control for congested conditions are reviewed for three types of interchanges presently used in the United States. One type has not yet been constructed in Texas, however.

## 2.1 SIGNALIZED INTERCHANGES

Various types of signalized interchanges are currently available. Figure 2-1 shows typical signalized interchange configurations. From the viewpoint of traffic operations these interchanges are classified based on the number of signalized intersections incorporated in each interchange, as follows:

1. Single Point Urban Interchange (SPUI, one intersection),
2. Tight Urban Diamond Interchange (TUDI, two intersections), and
3. Three-Level Diamond Interchange (TLDI, four intersections).

Bonneson and Messer (7) performed a national survey of SPUI's. They presented design, operational, safety, structural, and economic issues about the SPUI. Figure 2-2 presents a SPUI without frontage roads located in Phoenix, Arizona and SPUI with frontage roads located in Largo, Florida. Currently, SPUI's do not exist in Texas.

The TUDI is a popular form of freeway-to-street interchange. A typical TUDI is shown in Figure 2-3. The design includes one-way frontage roads and U-turn bays, commonly found in Texas. This design is different from the urban arterial with two intersections in that left-turn bays on the internal links extend to the upstream links. The 4-phase-with-two-overlaps signalization strategy is commonly used with this design in the United States, although some three-phase arrangements are also sometimes used.

The TLDI is normally utilized for freeway-to-freeway interchange in urban environments. As shown in Figure 2-4-a, TLDI's consists of four signalized intersections and two pairs of one-way streets. Two TLDI's exist in Austin and one in Dallas. The TLDI shown in Figure 2-4-a,b is a three-level interchange at US 290 and IH 35 in Austin, Texas.
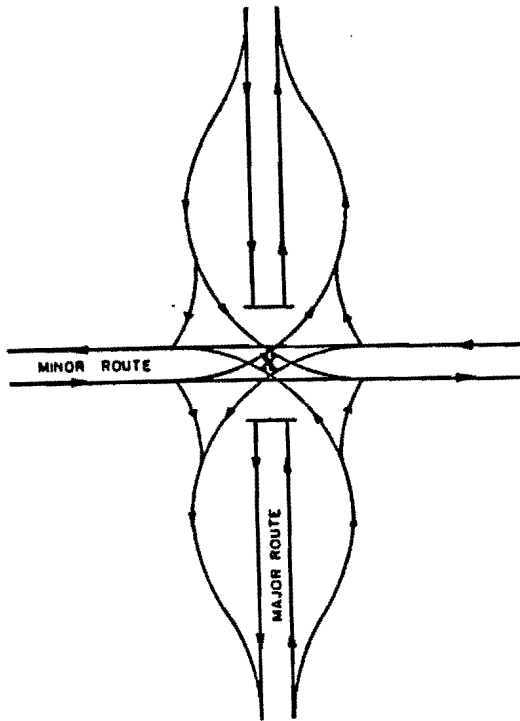
4

Single Point Urban Interchange

MINOR ROUTE

MAJOR ROUTE

MINOR ROUTE

Frontage Road

MAJOR ROUTE

Conventional Diamond Interchange

MAJOR ROUTE

MAJOR ROUTE
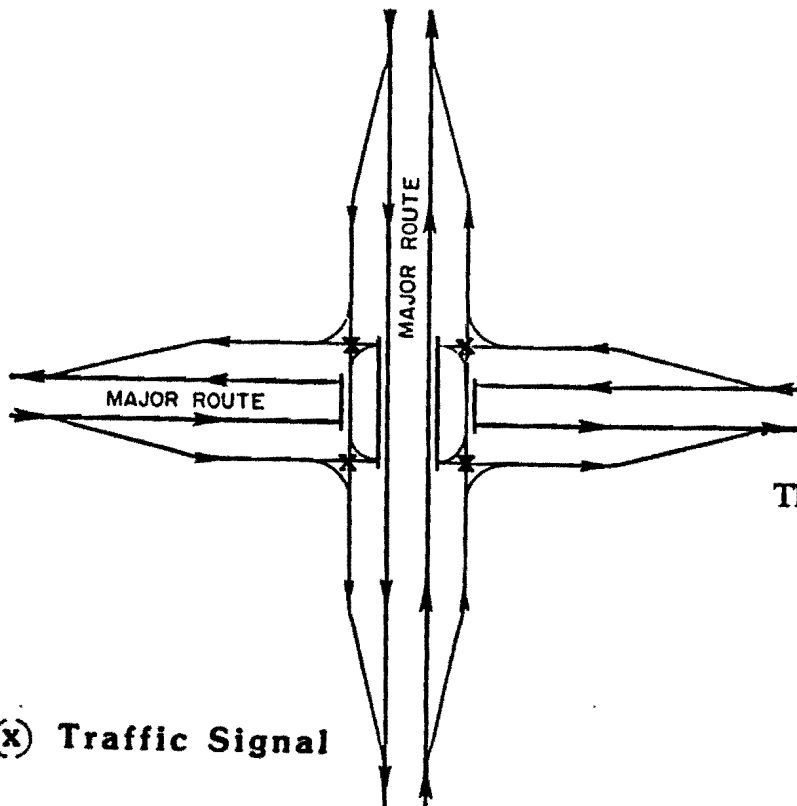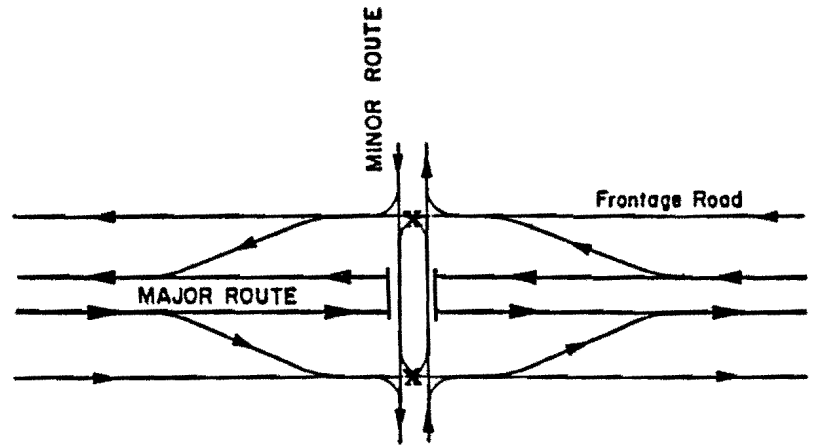
Three-Level Diamond Interchange

(X) Traffic Signal

Figure 2-1. Typical Signalized Interchange Configurations

5
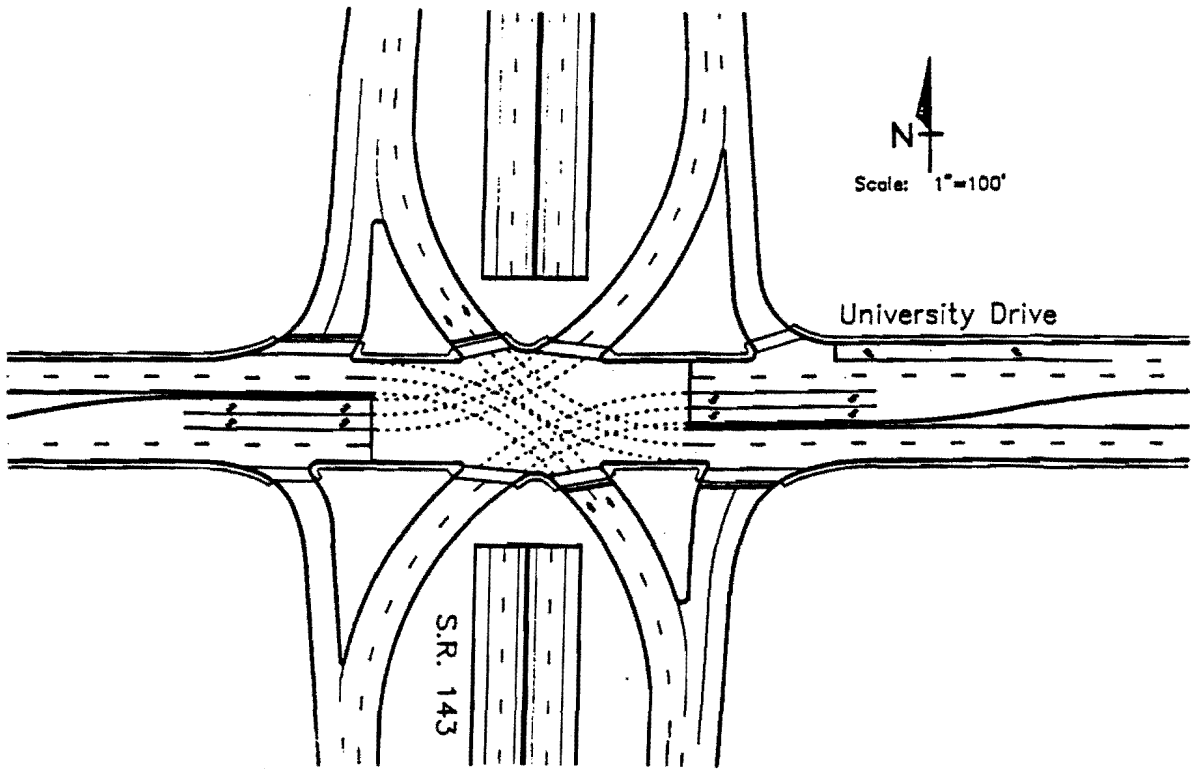
(a) SPUI without Frontage Road Located in Phoenix, Arizona
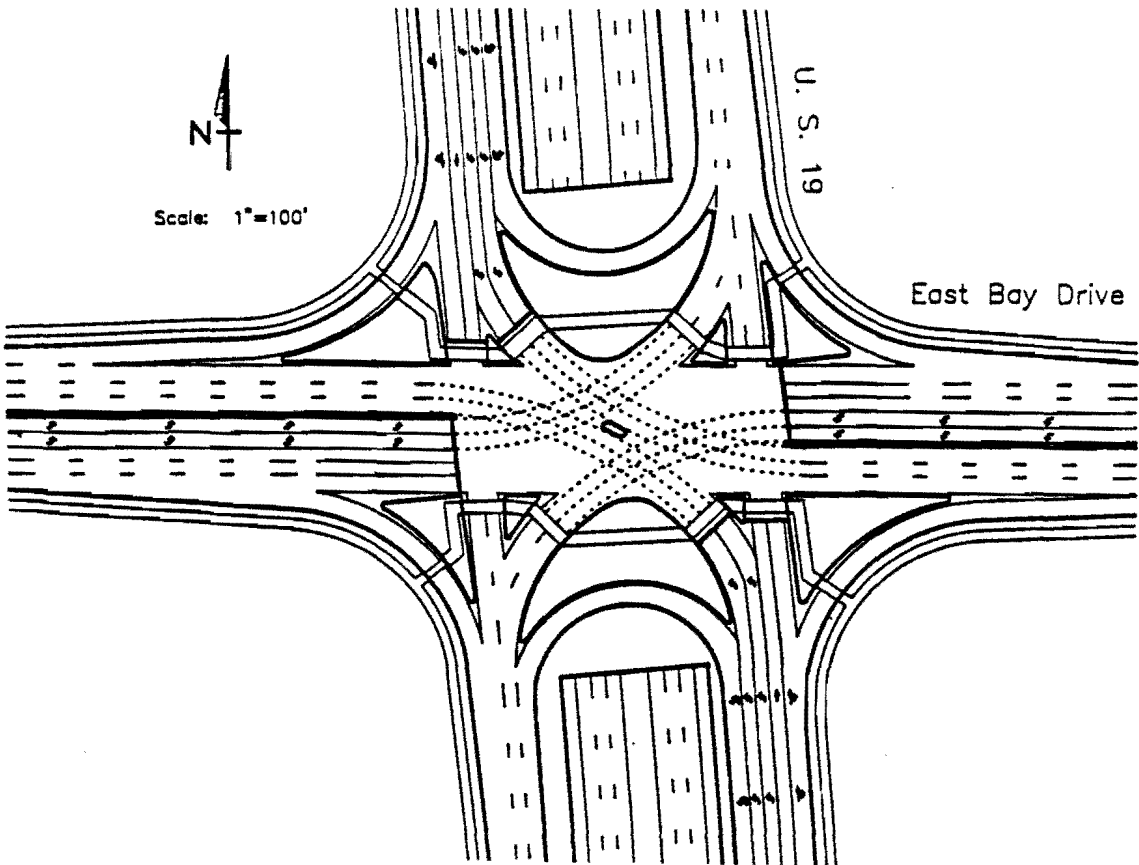


(b) SPUI with Frontage Road Located in Largo, Florida

Figure 2-2.   Single Point Urban Interchange
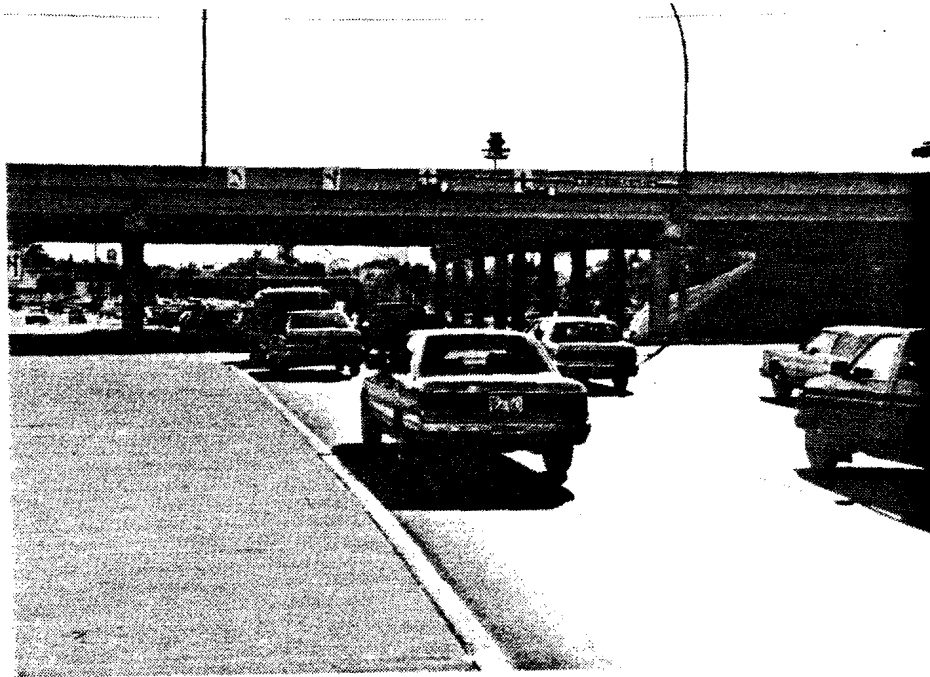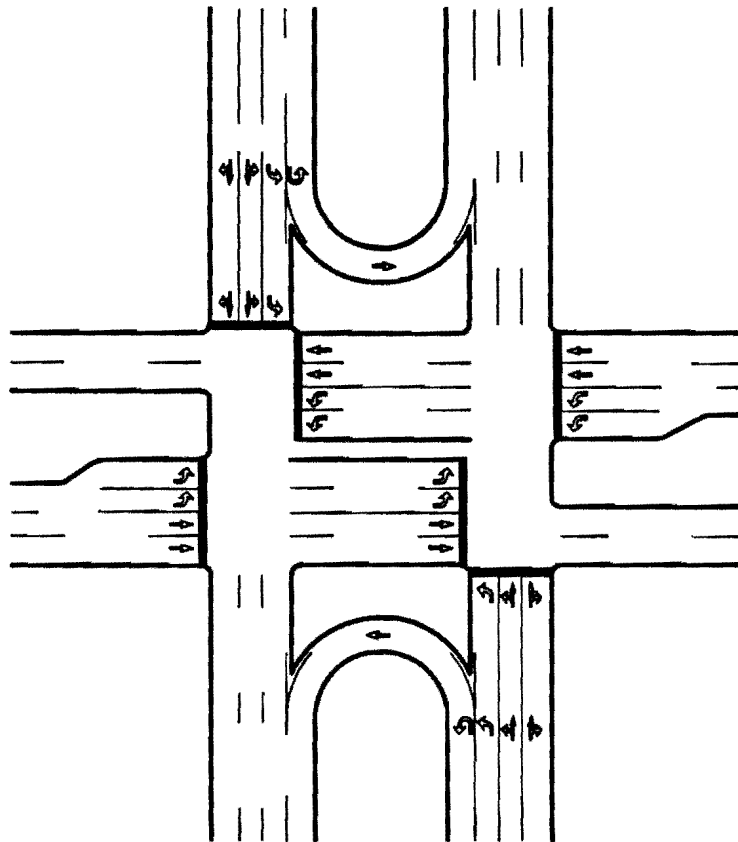
Figure 2-3. Typical Tight Urban Diamond Interchange
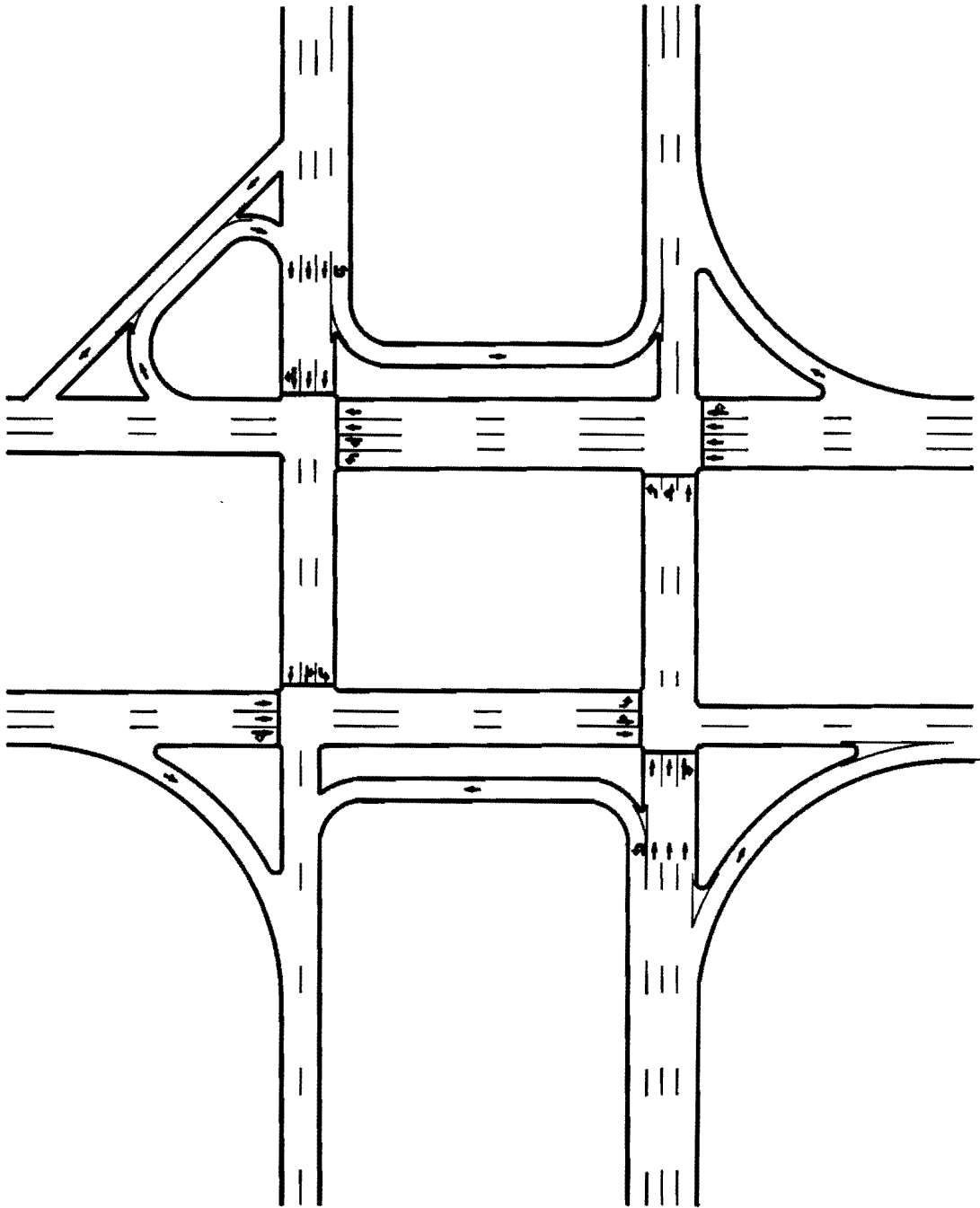
Part a.

Figure 2-4. Three-Level Diamond Interchange Located in Austin, Texas.
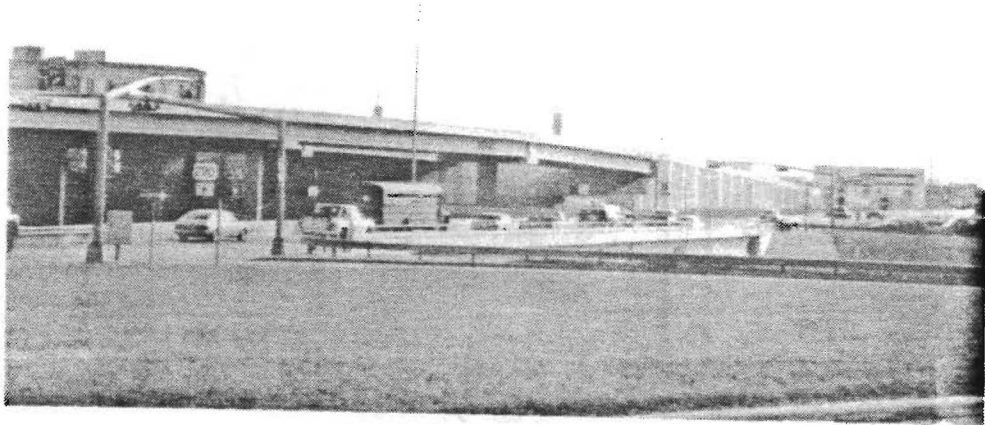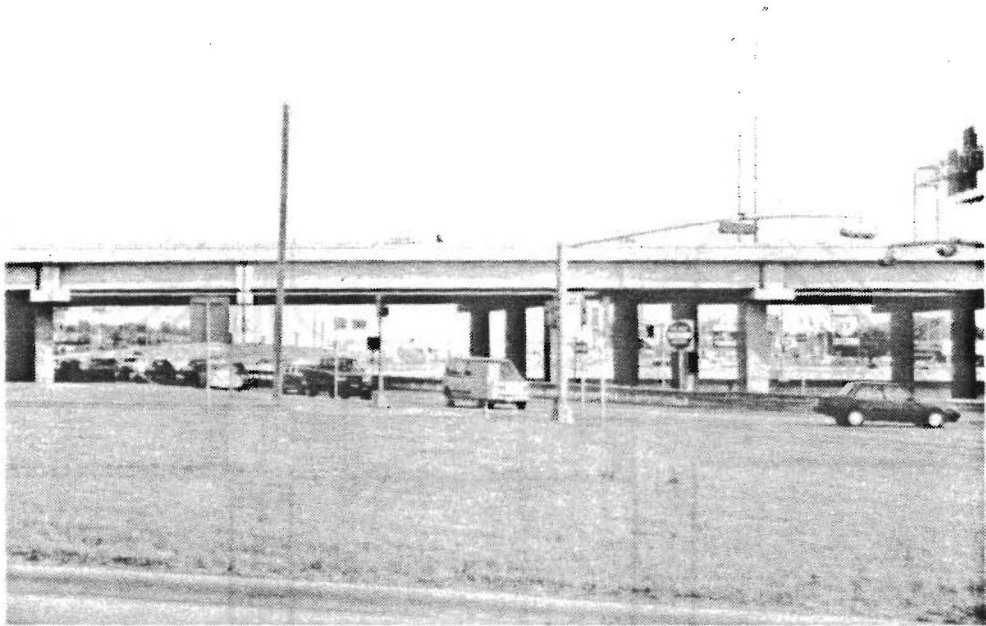
Figure 2-4.  (Continued)

9

## 2.2    STUDIES ON TRAFFIC SIGNAL CONTROL FOR CONGESTED CONDITIONS

Since Webster (8, 9) initiated studies on traffic signal timing in the late 1950s, much research on traffic signal control has been performed. Most of the research studies focused on undersaturated traffic conditions. A limited number of studies have addressed the area of traffic control for oversaturated environments. This section reviews the previous research on traffic control for congested traffic environments. The studies can be categorized into three classes: theoretical approaches, practical guidelines, and traffic models.

### 2.2.1    Theoretical Approaches

Theoretical studies have attempted to develop a control policy for oversaturated environments during the last thirty years. The problem of pretimed signal control during the peak hour was first considered by Gazis and Potts (10) who derived the optimality conditions for an oversaturated one-way no-turn intersection. In another paper, Gazis (11) extended the control policy for two oversaturated linked intersections with one-way operation. Singh and Tamura (12) formulated a dynamic optimization problem for oversaturated traffic networks as a linear quadratic problem based on Gazis's theories. Michalopoulos (13, 14, 15) proposed an optimal control policy for both pretimed and real time control. His control policy was to minimize total system delay, subject to queue length constraints.

Longley (16) and Gordon (17) have proposed algorithms for the real time control of isolated intersections. Their control philosophies were based on the fact that traffic signals cannot clear queues at the initial bottleneck locations of primary congestion. Their signal control objective was to maintain the growth of the queues in a predetermined ratio to available storage in order to postpone the onset of secondary congestion. Pignataro et al. (1) suggested queue actuated control as a highly responsive signal control strategy. This is a control policy that provides an approach with a green indication automatically when the queue on that approach becomes equal to, or greater than, the available storage length.

### 2.2.2    Practical Guidelines

Practical guidelines have been published to assist traffic engineers in understanding the cause and severity of traffic congestion and to provide control strategies associated with the congestion types. Pignataro et al. (1) presented guidelines for the treatment of traffic congestion on street networks. The guidelines provided both a tutorial and an illustrated reference on what techniques to consider and how to consider them systematically. OECD (18) provided policy-makers and traffic engineers with an up-to-date assessment of traffic congestion management. ITE (19) has published the proceedings of its 1987 national conference dealing with traffic congestion.

Shibata and Yamamoto (20) suggested on-line real-time control for isolated intersections with multi-phase operation. Rathi (21) and Lieberman (22) proposed queue management control, a form of internal metering, which is designed to manage queue length to reduce the probability of spillback. They showed that backward progression was optimal or near optimal for a street with long queues and slow discharge headways.

## 2.2.3 Traffic Engineering Models

A number of algorithms and computer models have been developed to aid the traffic engineer in designing signal timing plans. Off-line computer techniques that are well documented and have received considerable testing and application are TRANSYT-7F, PASSER II, PASSER III, SIGOP, TRAF-NETSIM, TEXAS, etc. Only TRANSYT-7F and TRAF-NETSIM have a feature to explicitly consider the effect of queue spillback.

The Traffic Network Study Tool (TRANSYT, 23) is one of the most widely used models in the United States and Europe for signal network timing design. It is a macroscopic and deterministic model used to simulate and optimize signal timing on coordinated arterials and grid networks. It determines optimum phase splits and offsets that minimize the performance index of a linear combination of stops and delays, using the hill-climb search method. TRANSYT-7F (4) is the Federal Highway Administration's version of TRANSYT-7, which uses North American nomenclature for input and output.

TRANSYT-7F Release 6 added a number of new modelling capabilities. One of them is an expansion of the optimization objective function to optionally include excess queue backup (spillover), and/or operating cost. The portion of queues spilling over to an upstream intersection is weighted in the objective function. The weighted queue overflow is added to the performance index. The green split and offset are adjusted in the optimization routine so as to avoid queue spillover. This new option would be useful in congested networks having short links. TRANSYT-7F cannot model time-varying queues since it is a deterministic model. Actually, in oversaturated approaches, queues are growing as time passes. Due to a lack of this capability, the option of excess queue weighting does not appear to be very effective for signal timing optimization during oversaturated conditions.

TRAF-NETSIM (6) is a microscopic and stochastic model that simulates individual vehicular behavior in response to various factors that cause traffic congestion. TRAF-NETSIM, formerly UTCS-1 and NETSIM, has been successfully validated and applied for simulating traffic control strategies on urban networks (24, 25, 26). TRAF-NETSIM has many features that are not available in other traffic programs. Simulating congested traffic conditions is a feature unique to TRAF-NETSIM. Labrum and Farr (27) analyzed the cost-effectiveness of traffic control alternatives for a congested diamond interchange using NETSIM for extended periods of time. They demonstrated that NETSIM could simulate congested traffic conditions.

11

Wong (28) explained how TRAF-NETSIM simulates oversaturated traffic conditions as follows:

"TRAF-NETSIM models saturated conditions and intersection overflow. If the receiving lanes are full, a vehicle discharging from the stop line may either wait or join the queue. If it is a left- or right-turning vehicle, it will always join the queue and block the intersection. If it is a through vehicle, the program assigns a probability (user specified or default) of joining the queue. (The default probability is 1.00 for their first through vehicle, 0.81 for the second, 0.69 for the third, and 0.40 for the fourth.) Vehicles waiting at the stop line will incur delay but will not affect cross street traffic. Vehicles blocking the intersection will affect cross-street traffic."

GTRAF (29) is an interactive computer graphics system which provides displays on a color monitor depicting the input data to, and the results generated by, the TRAF family of simulation models. The graphic animation of GTRAF visually demonstrates how TRAF-NETSIM simulates the condition where vehicles are prevented from moving freely either because of the presence of vehicles in the intersection itself or because of back-ups in any of the exit links of the intersection. Figure 2-5 illustrates the graphic animation display of GTRAF for a single intersection.

As TRANSYT-7F has limited capability, only TRAF-NETSIM is currently applicable to oversaturated traffic environments. TRAF-NETSIM does not have the capability of signal-timing optimization. There is a need to develop an optimization model that can handle oversaturated signalized intersections and interchanges.
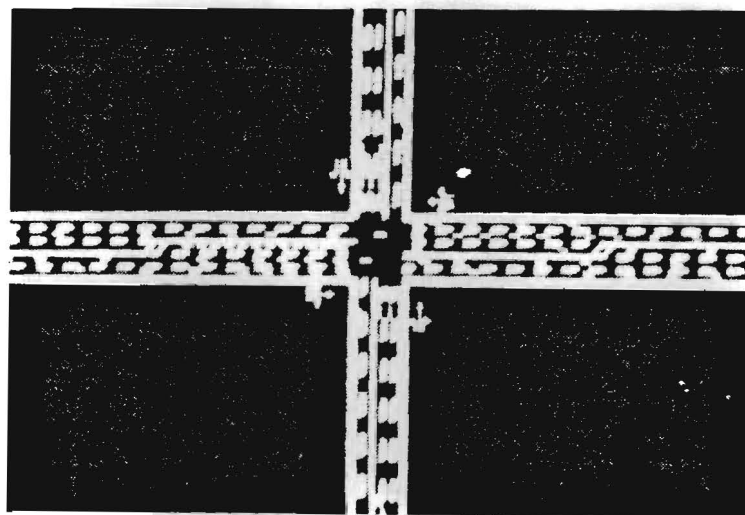


Figure 2-5. GTRAF Graphic Animation Display of Single Intersection

# 3. STATIC OPTIMIZATION MODEL

## 3.1 INTRODUCTION

Two types of the optimization models were developed in this research: a static model and a dynamic model. Conventional traffic engineering models such PASSER III (2) or TRANSYT-7F (3) can be regarded as static models. Once the control period is determined, the peak hourly volume (PHV) is selected for each movement. In the static models, this PHV is used to calculate traffic signal timing, and one signal timing plan is applied to the entire control period. Actually, traffic demands outside the peak hour are not considered in the design of the signal plan. A static model proposed in this chapter was designed to be applicable to the procedure using the PHV.

When the queue storage capacity on the cross streets (or external approaches) at arterials is limited, queue spillback to the intersections adjacent to the arterial could cause severe operational problems. Traffic signal timing should be flexible in order to control queue lengths on the external approaches. For effective queue control, the model should be dynamic so as to reflect time-varying demand during the control period. The dynamic optimization model will be described in Chapter 5.

Conventional traffic engineering models provide optimal signal timing to obtain maximum bandwidth and/or minimum delay at signalized intersections. In congested roadway systems, however, these are not the desirable control objectives; instead, signal control should produce maximum system productivity.

*System productivity* is defined as the total number of vehicles discharged from the roadway system under consideration during the control period. In other words, as many vehicles as possible should be serviced through the specified roadway system during a given time period. Wattleworth and Berry (4) theoretically proved the equivalency of maximizing system output rate and minimizing travel time in dynamic freeway on-ramp control. This strategy can be applied to the optimal traffic signal control of saturated surface streets.

This chapter describes the formulation of a "static" model for developing optimal signal timing plans for a system of two oversaturated intersections. The model maximizes system productivity based on the peak hour traffic demands as determined from three-hour control periods. The model produces a single pretimed plan for the entire three-hour control period. This model is not traffic responsive to short-term volume variations and serves primarily as a benchmark for comparing the performance of the more refined dynamic model to follow. In either case, the following control objectives should be attained to achieve maximum system productivity:

1. Full utilization of green indication times;
2. Maximization of outputs during the green indication time;

3.   Full utilization of queue storage capacity of internal links;
4.   Stabilization of queue lengths; and
5.   Prevention of queue spillback.

The optimization model uses mixed integer linear programming (MILP) to mathematically model the above requirements. MILP has been successfully used in formulating several signal timing optimization models (*30, 31, 32*). The MILP problem could be solved using software packages available for mathematical programming like MPCODE (*33*) and LINDO (*34*). The MILP problems in this research were solved using LINDO. LINDO (Linear, Interactive and Discrete Optimizer) is an interactive linear, quadratic, and integer programming system designed for use by a wide range of users.

## 3.2   FORMULATION

The formulation of the static model is initially described for a "Unit Problem" consisting of a single arterial and its two intersections, shown in Figure 3-1. One-way cross streets were used for simplicity. The model for the unit problem can be modified and extended for actual roadway systems having more than two intersections and/or two-way cross streets without difficulty. Here, approaches 1, 2, 3, and 4 are regarded as external approaches and movements 6, 7, 16, and 37 as internal movements.
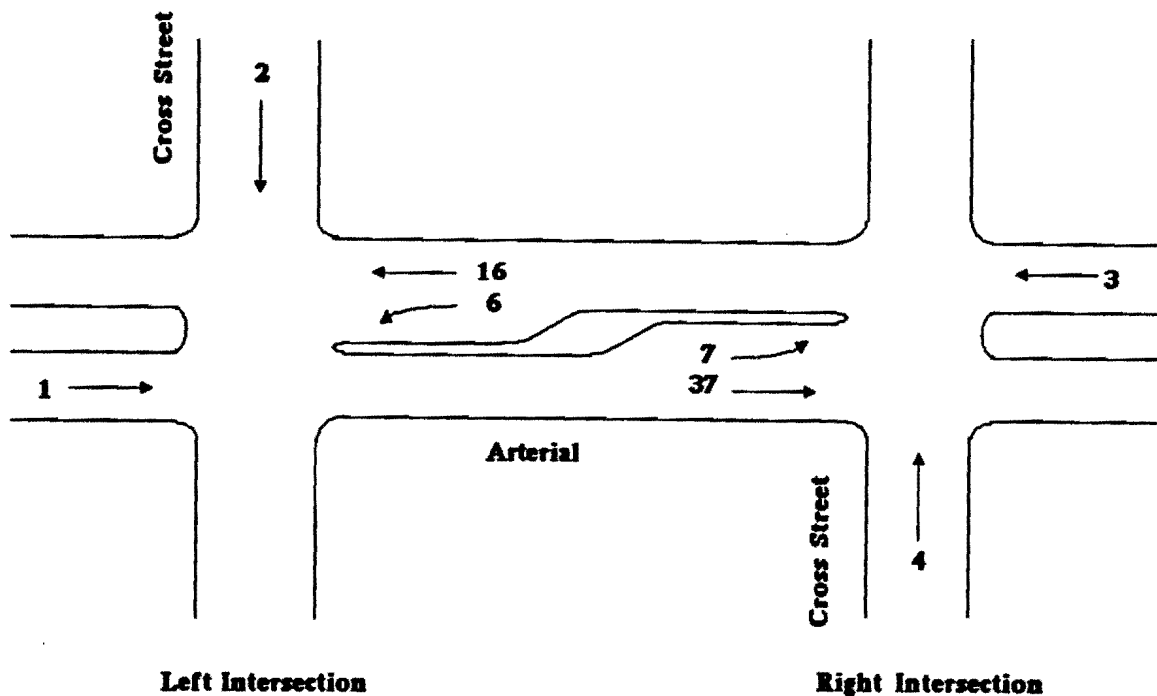


Figure 3-1.  Arterial with Two Intersections

**Left Intersection**      **Right Intersection**
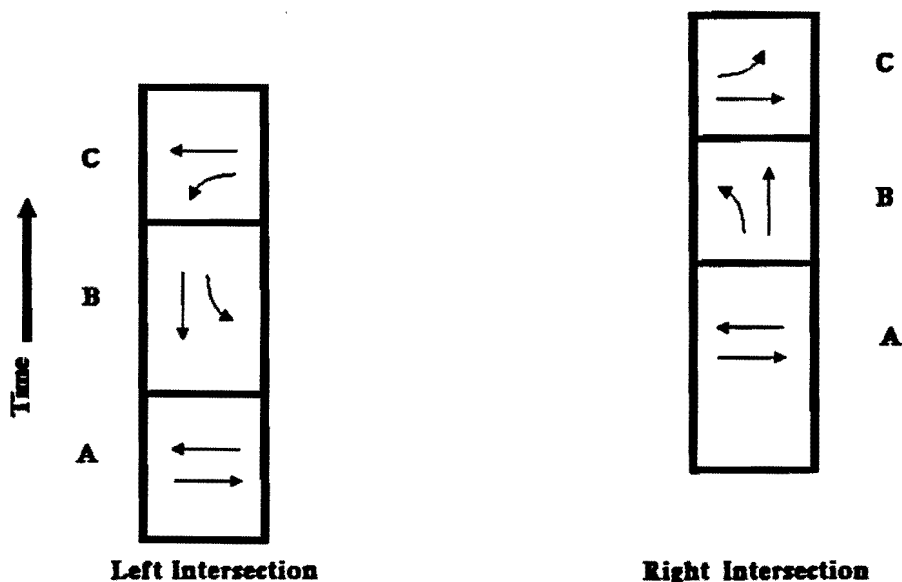
FIGURE 3-2. Three Basic Phases and Phase Sequence

At the intersection of a two-way arterial and a one-way cross street, there are usually three non-conflicting phases, as shown in Figure 3-2 (2). Phase A is dedicated to through and right-turning traffic on the arterial. Phase B provides exclusive right-of-way to all cross street movements. Phase C is necessary to clear traffic between intersections, particularly the outbound left-turn movement. Figure 3-2 illustrates a leading left turn sequence at both intersections. The following notations were used in the static model formulation:

$C$ = system cycle length, sec,

$G_i$ = effective green time for movement i, sec,

$S_i$ = saturation flow for movement i, veh/sec,

$V_i$ = average arrival rate for movement i, veh/sec,

$N_i$ = number of vehicles moving during green time for movement i, veh/cycle, which is the minimum of $\{S_iG_i, V_iC\}$,

$Z_i$ = 0 for oversaturation, that is, $N_i = S_iG_i$, 1 for undersaturation, that is, $N_i = V_iC$,

$M$ = very large positive value, called *Big-M*,

$l$ = lost time for individual phase, sec,

$Q_i$ = queue storage for internal movement i, veh,

$P_{ij}$ = proportion of turning movement shown in Figure 3-3,

$T_i$ = queue growing speed at external movement i, veh/sec,

$a$ = lane distribution factor for internal links, and

$b$ = lane distribution factor for external links.

15
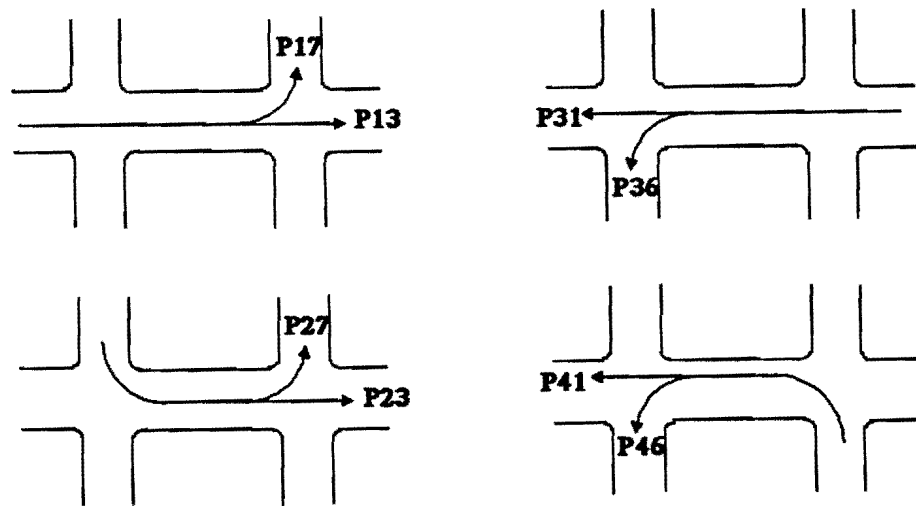
FIGURE 3-3. Notation for Turning Percentages.

### 3.2.1 Objective Function

Congestion on the internal links often adversely affects the performance of upstream intersections. In a system of short internal links, the queues generated at congested internal approaches sometimes extend into and consequently block upstream intersections. Under this condition, the vehicle discharge rate at the upstream intersection (or input rate to the system) becomes less than ideal. By eliminating this congestion, the upstream signal is able to service more vehicles. If all external approaches are full of vehicles waiting for service and the internal links are not congested, input and output of the roadway system would be balanced. Under such a situation, increasing system output (or system productivity) increases system input. The concept is similar to that of freeway on-ramp control (4).

The objective function of the static model is to maximize the input to the roadway system and constraints for preventing queue backup were incorporated into the MILP formulation. If an external approach is fully saturated, the number of vehicles discharged during one cycle is proportional to the phase duration associated with the external approach. The traffic signal cycle at each intersection consists of two external phases (A and B) and one internal phase (C), shown in Figure 3-2. Increasing the durations of Phases A and B can increase the number of vehicles entering the roadway system. Consequently, maximum productivity can be obtained by maximizing phase durations for the external approaches and minimizing phase durations for the internal approaches, subject to the constraints noted below. The objective function of the static model is:

$$\text{Maximize} \quad p = G_1 + G_2 + G_3 + G_4 - G_6 - G_7 \tag{1}$$

16

### 3.2.2 Constraints

System productivity can be increased by increasing the phase durations for external movements; however, there are upper limits on the external phase durations. The upper limits can be formulated using proper constraints. The phase duration can be interpreted as effective green time in the following discussions. The constraint sets satisfying the five objectives listed in the introduction of this section are described below.

*Set 1.* In a coordinated signal system, the sum of phase durations at each of the individual intersections shown in Figure 3-1 must be equal to the system cycle length:

$$G_1 + G_2 + G_6 + 3l = C \qquad (2a)$$
$$G_3 + G_4 + G_7 + 3l = C \qquad (2b)$$

*Set 2.* For the internal links, the input to the link must be less than or equal to the output in order to obtain the stability of queue lengths over many cycles (Objective 4). Thus, for the four internal links:

$$P_{17}N_1 + P_{27}N_2 \leq \alpha S_7 G_7 \qquad (3a)$$
$$P_{13}N_1 + P_{23}N_2 \leq \alpha S_{37}(G_3 + G_7) \qquad (3b)$$
$$P_{36}N_3 + P_{46}N_4 \leq \alpha S_6 G_6 \qquad (3c)$$
$$P_{31}N_3 + P_{41}N_4 \leq \alpha S_{16}(G_1 + G_6) \qquad (3d)$$

where $\alpha$ is a lane utilization factor for the green split, usually not greater than 1.

According to the above constraint set, oversaturation would never occur at the internal approaches. Due to the stochastic nature of vehicle arrival and discharge headways, the deterministic balance of the input and output might not be valid, resulting in unexpected oversaturation on the internal approaches. It is desirable to provide additional green indication times for the internal phases to reduce the possibility of unexpected oversaturation. A smaller value for $\alpha$ results in a larger internal phase duration. A default value of 1.0 was used for $\alpha$ in the following discussion, unless otherwise noted.

The left-hand side of the Constraint Set 2 represents the number of vehicles entering the internal links during one cycle. The right-hand side represents the capacity of individual movements on the internal links. With this constraint set, demand on the internal approaches never exceeds capacity. This constraint set determines the necessary proportions of all phase durations, ensuring stable queue lengths on the internal links from one cycle to the next. Theoretically, no vehicles stay at internal links for more than two cycles. Smallest possible phase durations should be provided for the internal phases through the objective function. The small phase durations force platoons to compress when they discharge at the internal phases. That is, vehicles are discharged at compressed headways, fully utilizing phase durations (Objective 1) and maximizing output during the phase duration (Objective 2).

17

*Set 3.* The maximum number of vehicles stored on internal link i must be less than its queue storage, $Q_i$:

$$P_{17}N_1 + P_{27}N_2 \leq \beta Q_7 \qquad (4a)$$
$$P_{13}N_1 + P_{23}N_2 \leq \beta Q_{37} \qquad (4b)$$
$$P_{36}N_3 + P_{46}N_4 \leq \beta Q_6 \qquad (4c)$$
$$P_{31}N_3 + P_{41}N_4 \leq \beta Q_{16} \qquad (4d)$$

where $\beta$ is an adjustment factor for queue storage, usually not greater than 1.

The left-hand side of Constraint Set 3 are identical to that of Constraint Set 2, which is the number of vehicles entering internal links during one cycle. The maximum queue lengths might be affected by the quality of traffic progression between intersections. The queue lengths expressed in these constraints are formulated in a conservative manner. Assuming that every vehicle stops when entering the internal links, the maximum queue length is identical to the number of vehicles entering the internal link.

It should be noted that Constraint Set 3 determines an optimal system cycle length. Constraint Set 2 plays a role in stabilizing queue lengths over time by adjusting green split; yet, it cannot control actual queue lengths. These queue lengths could be controlled by adjusting cycle lengths. A large cycle length gives a more effective green indication time to the intersection than does a small cycle length; however, the former increases the possibility of queue spillback into the upstream intersection. The relationship between system cycle length and system productivity has the form of a concave function, which will be demonstrated in Chapter IV, "Sensitivity Analysis." This constraint set provides the optimal cycle length, which fully utilizes queue storage (Objective 3) and prevents queue spillback (Objective 5).

The queue storage capacity of internal link i, $Q_i$, is the maximum queue length that traffic engineers want to maintain over the cycle. This storage capacity can be calculated as follows:

$$Q_i = \frac{(\text{link length, feet})}{(\text{average vehicle storage length, feet})} \times (\text{number of lanes})$$

According to the above constraints, queued vehicles never spillback to the upstream intersection. Yet, due to the stochastic nature of vehicle arrivals and lane utilization, actual queue lengths fluctuate around the average value, which might cause queue spillback. In determining the queue storage, $Q_i$, a storage buffer should be provided to absorb such natural fluctuations; the adjustment factor $\beta$ is used for this purpose. The smaller the adjustment factor $\beta$, the smaller the optimal cycle length. A value of one was used in the following discussion for convenience, unless otherwise noted.

*Set 4.* The number of vehicles entering the intersection during the green indication

time for movement i is expressed as:

$$N_i = \text{minimum } \{S_iG_i, V_iC\} \tag{5}$$

Mathematical expressions for the number of vehicles discharged ($N_i$) during the green time ($G_i$) depend on whether the corresponding approach is oversaturated or not. If the approach is oversaturated, then $N_i$ is equal to the product of saturation flow ($S_i$) and phase duration ($G_i$). That is, the productivity during the phase is proportional to the phase duration; therefore, increasing the external phase duration as much as possible given cycle length results in maximum productivity. If the approach is undersaturated, then $N_i$ becomes the product of demand (vehicles per second) and cycle length (seconds). The productivity would not depend on the phase duration, but on the approach demand and the cycle length. It should be noted that whether an approach is oversaturated or undersaturated cannot be predetermined. The reason is that the oversaturation of the approach depends on how much green time is assigned to the approach. The static model automatically determines the state of saturation during the optimization procedure.

Equation 5 cannot be solved directly using linear programming. This equation must be transformed into the following equivalent linear form:

$$N_i \leq S_iG_i$$
$$N_i \leq V_iC$$
$$S_iG_i - N_i \leq MZ_i$$
$$V_iC - N_i \leq M(1 - Z_i)$$

where $Z_i$ is an integer variable having binary values. For $Z_i = 0$ (oversaturated condition), $N_i$ is equal to $S_iG_i$; otherwise, $N_i$ becomes $V_iC$. Unfortunately, the static model now becomes a complex Mixed Integer Linear Programming (MILP) problem because of the integer variable, $Z_i$, in the above formulation.

*Set 5.* Maximum cycle length constraint:

$$C \leq C_{max} \tag{6}$$

For long internal links, the static model produces long cycle lengths as the optimum solution. The cycle lengths should be constrained by a practical upper limit considering.

*Set 6.* Minimum green constraints:

$$G_i \geq G_{i\,min} \tag{7}$$

where $G_{i\,min}$ is a minimum green indication time for phase i. The minimum green time can be determined from pedestrian or driver expectancy requirements. Additional constraints can be added the model to manipulate the green splits as described in the next section.

19

## 3.3   GREEN SPLIT FOR EXTERNAL PHASES

One feature of the static model is that phase durations for the external movements are adjustable by adding optional constraints to achieve prescribed objectives. The sum of phase durations of the external phases can be expressed as follows:

$$G_1 + G_2 + G_3 + G_4 + 4l = 2C - (G_6 + G_7 + 2l) \tag{8}$$

According to Equation 8, a two-intersection system can be analyzed as an isolated intersection with four-phase operation, as shown in Figure 3-4. Cycle length (C) and internal phases ($G_6$ and $G_7$) are calculated automatically in the MILP formulation, after weighting factors are applied to the external phases ($G_1$, $G_2$, $G_3$, and $G_4$). The generalized form of the optional constraint set of weighting factors is expressed as follows:

$$\frac{G_1}{w_1} = \frac{G_2}{w_2} = \frac{G_3}{w_3} = \frac{G_4}{w_4}$$

$$\tag{9}$$

where $w_i$ = weighting factor of approach i..0
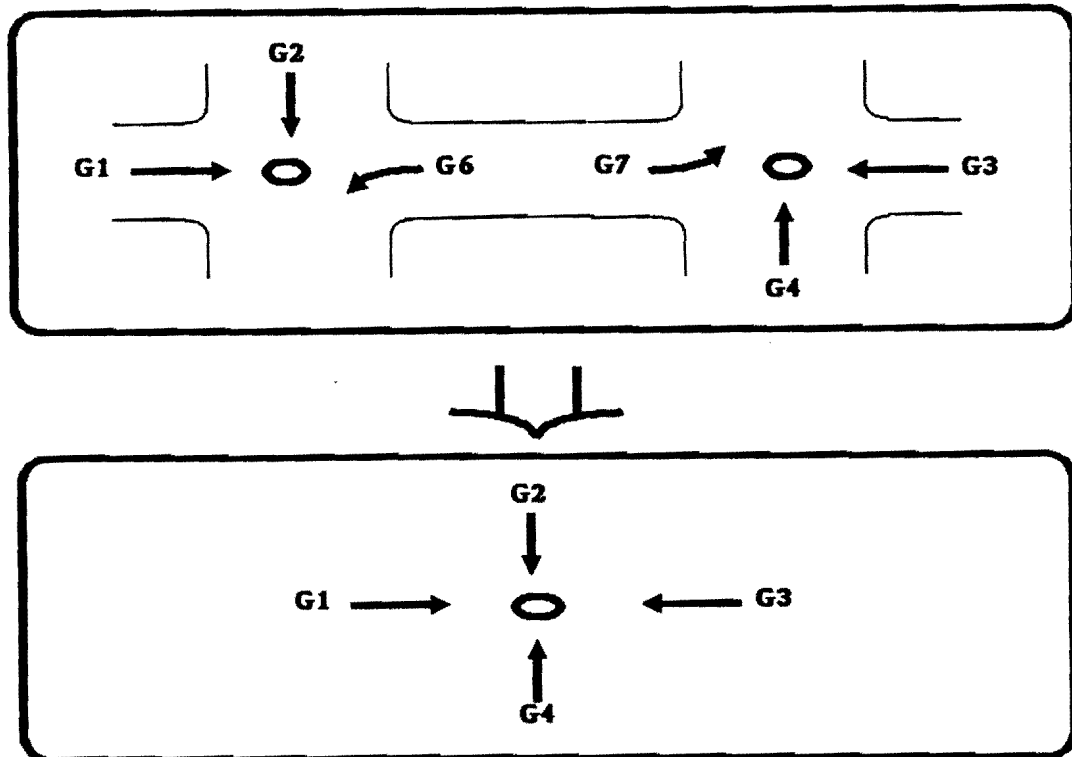


Figure 3-4.  Conversion of a Two-Intersection System into Single Intersection

20

The weighting factors, $w_i$, should be selected with care, based on geometric and traffic conditions. Larger $w_i$ factors for approach i result in larger $G_i$ for the approach. Examples are presented in the following sections.

### 3.3.1 Green Split Based on Demand

A conventional method of calculating green splits is to allocate green times according to approach traffic flow ratios. That is,

$$\frac{G_1}{y_1} = \frac{G_2}{y_2} = \frac{G_3}{y_3} = \frac{G_4}{y_4} \tag{10}$$

where $y_i = V_i/S_i$ is flow ratio for external movement i. This scheme is desirable when the arterial system is not saturated and/or when the resulting queue lengths on the external movements are not critical. The scheme also gives the least overall delay to external approaches (8).

### 3.3.2 Green Split Based on External Queue Lengths

When an arterial system is oversaturated and the queue-storage capacities for external approaches are insufficient, engineers may want to control external queue lengths so that they do not hurt the performance of the total system. Under this condition, the green split based on demand only is not appropriate for queue management. Longley's queue control policy (16) appears more desirable. When intersections are oversaturated, the queue lengths will continue to grow as long as demand volumes exceed intersection capacity. The control strategy should aim to postpone queue spillback to adjacent intersections as long as possible and hence reduce its severity.

The queue-growing speed per cycle ($T_i$) for external approach i is defined as the amount of demand exceeding capacity per cycle, which is expressed as follows:

$$T_i = V_i C - G_i S_i \tag{11}$$

The green split should be adjusted so that the four competing queues simultaneously fill up the queue storage of their associated links. This green split can prevent a queue on the shortest link from reaching its maximum earlier than the others; thus, queue spillback can be postponed as late as possible. The fill-up ratio for external link i is expressed as $T_i/L_i$. Thus, the optional constraint for the green split based on the queue lengths is expressed as follows:

$$\frac{T_1}{L_1} = \frac{T_2}{L_2} = \frac{T_3}{L_3} = \frac{T_4}{L_4} \tag{12}$$

21

where $L_i$ = queue storage capacity of external approach i. This constraint ensures that the queues for all approaches simultaneously reach their allowable maximums as long as demands are constant. This scheme is desirable for oversaturated systems with limited queue-storage capacity.

Usually traffic demand during the peak hour is not constant. Queue formation is sensitive to the time-varying demand. It is desirable to take into account this dynamic nature of traffic within the queue management model. The dynamic optimization model for queue management at oversaturated roadway systems will be described in Chapter 5, "Dynamic Optimization Model."


## 3.4    OFFSET

The static model produces an optimal cycle length and green splits, but not offsets. An important characteristic of the static model is that its optimal solution for maximum productivity is not sensitive to offset between intersections. To fully utilize the capacity during an internal phase, the optimal solution produced by this model is designed so that the vehicles entering from external links are forced to stop at the internal links. They are then released at saturation headways during the next cycle, which is accomplished by assigning the minimum green time required for undersaturation to internal clearance phases. In the static model, the adjustment of the internal offset may reduce average delay on the internal links, but not significantly affect the system productivity. The appropriateness of this assumption is demonstrated in the next chapter.

# 4. SENSITIVITY ANALYSIS

## 4.1    INTRODUCTION

An efficient method of evaluating mathematical models is to examine the sensitivity of the model predictions to small changes in major variables. Elements of traffic signal control are cycle length, green split, offset, and phase sequence. In developing the static model described in Chapter 3, three hypotheses about the traffic signal control elements were involved as follows:

1.    There exists an optimum cycle length which maximizes system productivity. System productivity would be lost due to lost time for cycle lengths less than the optimum, and due to queue spillback into upstream intersections for cycle lengths larger than the optimum. Refer to Figure 4-1(a).

2.    There exists an optimum green split which maximizes system productivity. System productivity would be lost due to increasing queue lengths on internal links for Phase-C duration (left-turn phase) less than the optimum, and due to unused green time for a duration greater than the optimum. Refer to Figure 4-1(b).

3.    Offset does not have a major effect on system productivity within a nominal range of offsets at the optimal cycle length and green split for the phase sequence.

The purpose of this sensitivity analysis is to demonstrate the appropriateness of the above hypotheses. This research investigated the relationships between the major signal timing elements and system productivity through sensitivity analysis. It also studied the effect of the timing elements on system delay.

Another objective is to examine the optimal solution produced by the static model to determine whether it optimizes productivity. The optimal solution of the static model is the signal timing that maximizes system productivity. The static model forms the basis for the dynamic model presented in the next chapter, "Dynamic Optimization Model." Therefore, this analysis also provides insight into the performance of the dynamic model.

## 4.2    STUDY APPROACH

### 4.2.1    Experimental Design

The test and evaluation procedure of the static model followed four steps:

Step 1.        Experimental plan,
Step 2.        Optimization using the static model,
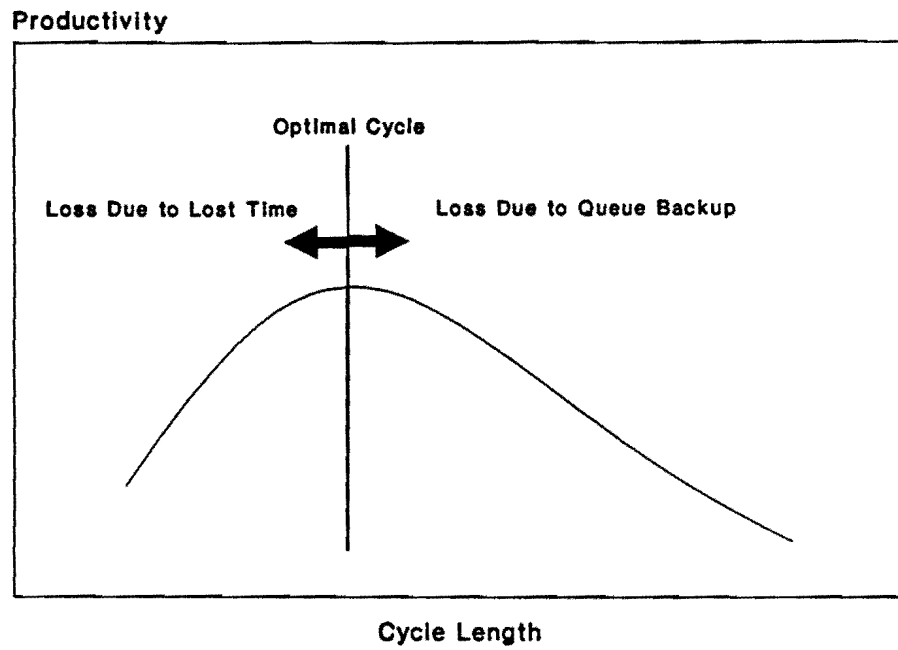
**Productivity**



(a) Cycle Length versus Productivity
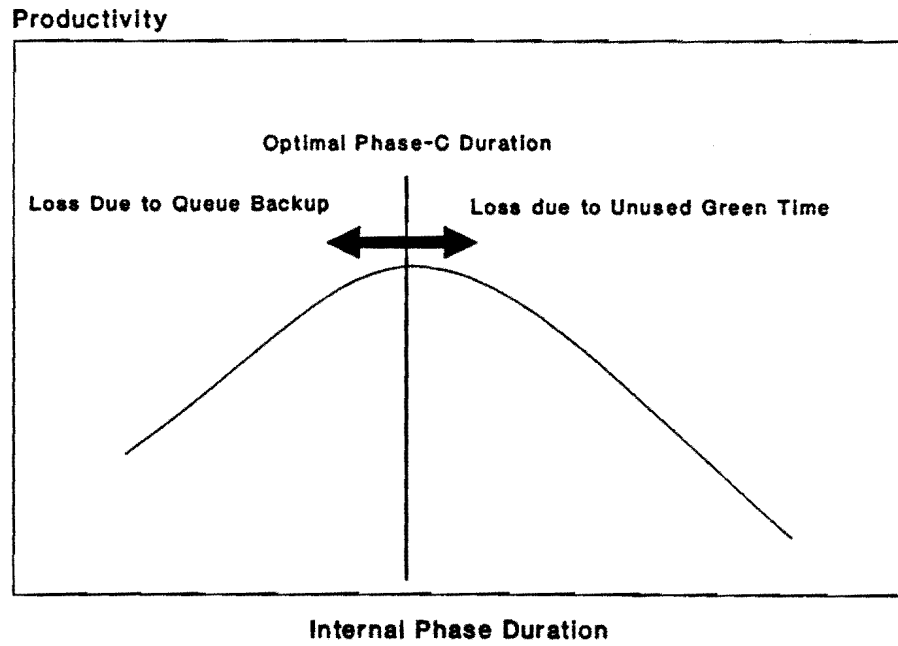
**Productivity**



(b) Internal Phase Duration versus Productivity

Figure 4-1. Relationships between Signal Timing Variables and Productivity

24

Step 3.    Simulation using TRAF-NETSIM, and

Step 4.    Analysis of results.

The input data for the base case were generated artificially. The input data represented oversaturated traffic conditions for an arterial with two signalized intersections. To investigate the effects of the input traffic and geometric data on the optimal solution, the base case was modified as follows:

1.    Lengths of internal links (200, 300, and 500 feet),
2.    Cycle lengths (5-second increments from 40 to 110 seconds),
3.    Turning percentages (three cases of origin-destination patterns), and
4.    Offsets (5-second increments from 0 up to the cycle length).

The static model was used to obtain the optimal signal timings for the above cases. Green splits were calculated based on approach demands in all the cases. These signal timing plans were then simulated by TRAF-NETSIM. Signal timings deviating from the optimal timings were also simulated, and their performances were compared to those of the optimal timing. Signal timing optimality could be demonstrated by comparing the performance between the optimal timing and the other timings deviating from the optimal timing.

TRAF-NETSIM was used to evaluate the signal timing plans. Due to its inherent variability in generating traffic volumes, a simulation trial for each signal timing plan was replicated four times, using different random number seeds. A 15-minute simulation time of control was used for every simulation trial.

## 4.2.2    Description of Base Case

As illustrated in Figure 4-2, the roadway for the base case is an arterial with two lanes in each direction. The two intersections are spaced 300 feet apart. Left-turn traffic on the arterial has a left-turn bay with an exclusive phase. Cross streets are one-way facilities with two moving lanes. Traffic volumes and turning percentages are shown in Figure 4-3. Assuming a vehicle discharge headway of two seconds per vehicle, the intersections are oversaturated having the traffic volumes and patterns depicted in Figure 4-3. The volume-to-capacity ratio of the arterial is 1.3 when the ratio is calculated using the signal timings obtained from the static model. A zero offset was used for the base case signal timing plan.

## 4.2.3    Measures of Effectiveness

TRAF-NETSIM provides various measures of effectiveness (MOE's) for traffic operations produced by given signal control strategies. In this research, the objective of
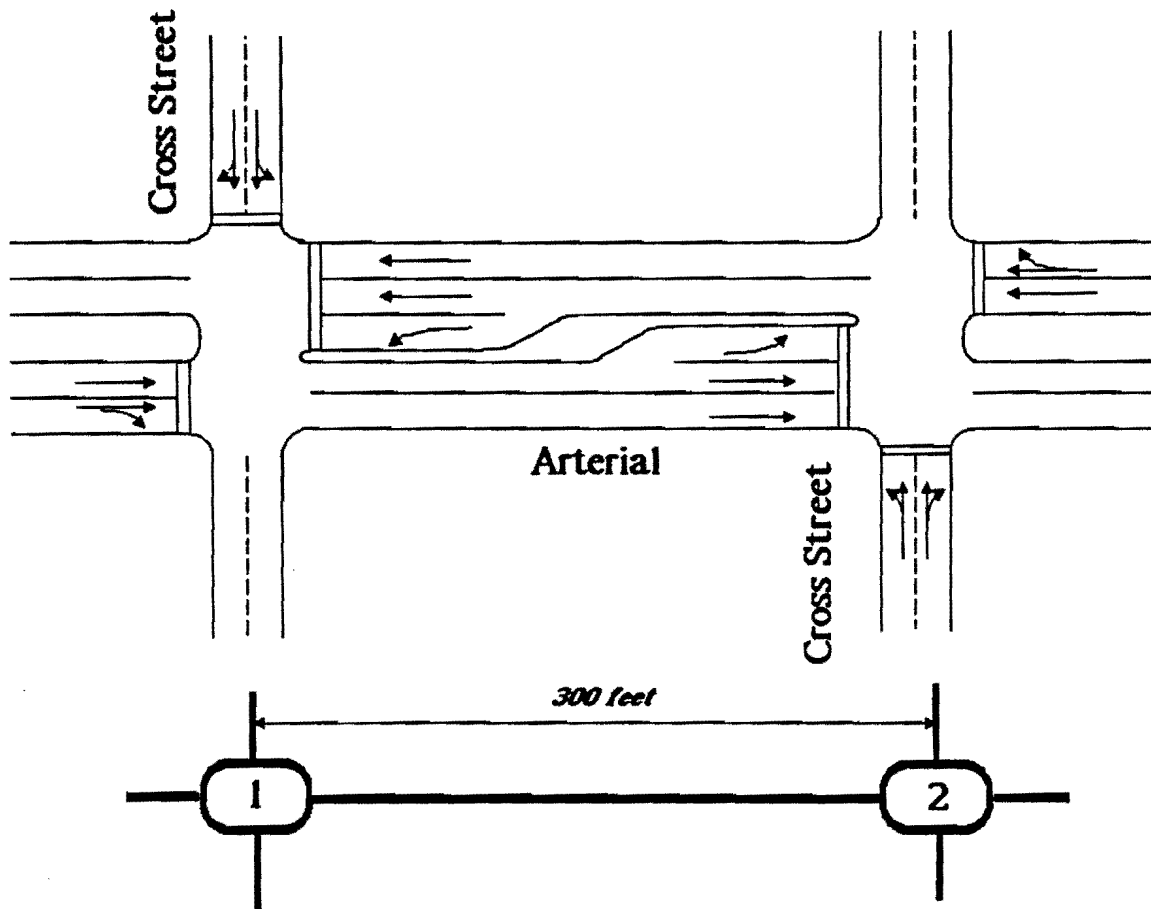
Figure 4-2. Roadway System for Base Case

traffic signal control was to maximize system productivity during congested periods. The total number of *vehicles discharged* during the simulation period appeared to be the most appropriate of all MOE's because the number of vehicles discharged indicated the system productivity for a given signal timing. The number of vehicles discharged is seldom used in a normal traffic study while *average delay* is widely used in traffic engineering.

The average delay was also investigated to test the performance of signal timing. TRAF-NETSIM gives four MOE's in seconds per vehicle: total time, delay time, queue time, and stop time. The *queue time* is comparable to the average queue delay of other deterministic models; so the average delay used in this research is the queue time provided in the TRAF-NETSIM output.

26
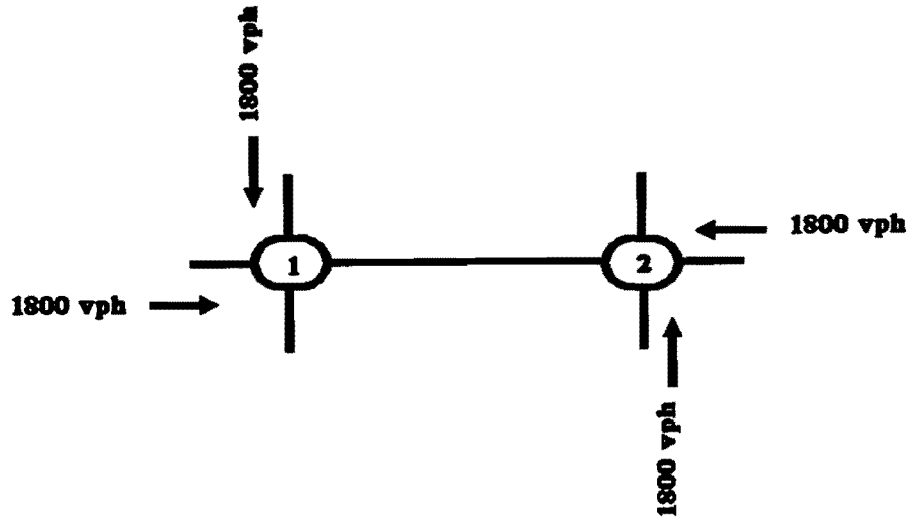
(a) Input Volume
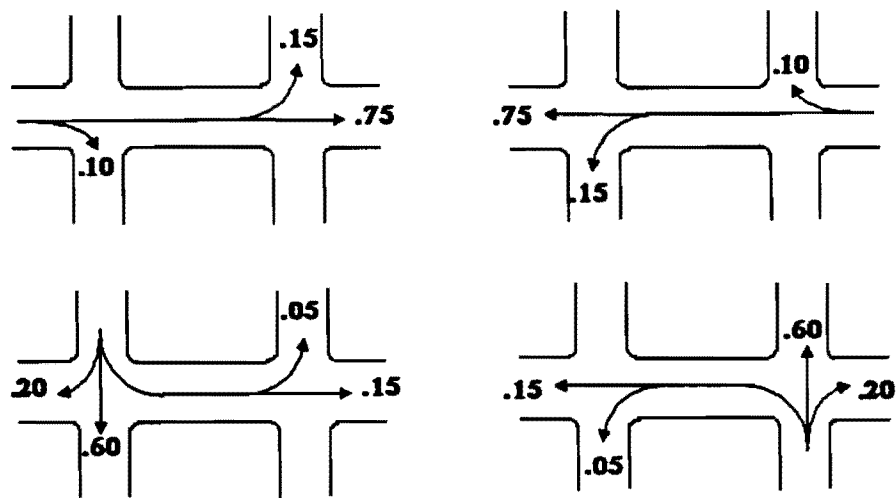


(b) Turning Percentage

Figure 4-3. Traffic Characteristics for Base Case

## 4.3   RESULTS

### 4.3.1   Cycle Length

According to Pignataro et al. (*1*), one of the most prevalent and erroneous beliefs in the traffic engineering community is that the capacity of an intersection increases substantially as the cycle length increases. His concern was that cycle lengths should be determined from lengths of feeding links in order to avoid excessively long queues. Intersection capacity, the sum of critical lane volumes ($\Sigma V$), is a function of cycle length. The formula that expresses this relationship is:

$$\Sigma V = \frac{3600}{h} (1 - \frac{\Sigma l}{C}) \tag{13}$$

where C is the cycle length in seconds, $\Sigma l$ is the total lost time in seconds, and h is the saturation headway in seconds per vehicle. For h = 2.0 sec, as C approaches infinity, $\Sigma V$ converges to 1,800 vph per lane. When traffic demand is near or over this value, increasing the cycle length beyond a certain point has little effect on an oversaturation problem. Unnecessarily long cycle lengths tend to create excessive queue lengths, which often cause serious operational problems at upstream intersections as a result of queue spillback.

A plot of cycle length versus vehicles discharged over a range of link lengths is presented in Figure 4-4. Optimal green splits for the analysis period were as developed from the static MILP model. The data points in this figure were obtained from the TRAF-NETSIM simulation. The ideal case was simulated using TRAF-NETSIM to show ideal system productivity. The ideal case provides an infinite length for the internal links on an arterial. On an arterial with limited intersection spacing, the vehicles discharging at the upstream intersection are often impeded by vehicles stalled in the receiving link. In the ideal case, vehicles can be discharged freely at the stop line without being impeded by the stalled vehicles. As shown in Figure 4-4, vehicle discharge increased continuously as cycle length increased. Long cycle lengths reduce the loss of system productivity due to lost time. As the cycle length is longer, the curve for the ideal case becomes flatter.

Arterials having three different link lengths were also simulated to show actual system productivity (Figure 4-4). A plot for a link length of 300 feet showed a typical concave curve. Vehicle discharge increased continuously up to an optimal cycle length (around 75 sec) and decreased beyond this point. This trend was an expected result, as depicted in Figure 4-1(a). System productivity was lost due to lost time for cycle lengths less than the optimum and due to queue spillback to the upstream intersection for cycle lengths larger than the optimum. A plot for a 200-foot link showed a shape similar to the 300-foot link. Maximum productivity was found at a 50-second cycle. For the 500-foot link case, vehicle discharge increased continuously to a 75-second cycle and then flattened for cycle lengths between 75 and 100 seconds. The curve slightly decreased beyond the 100-second cycle.
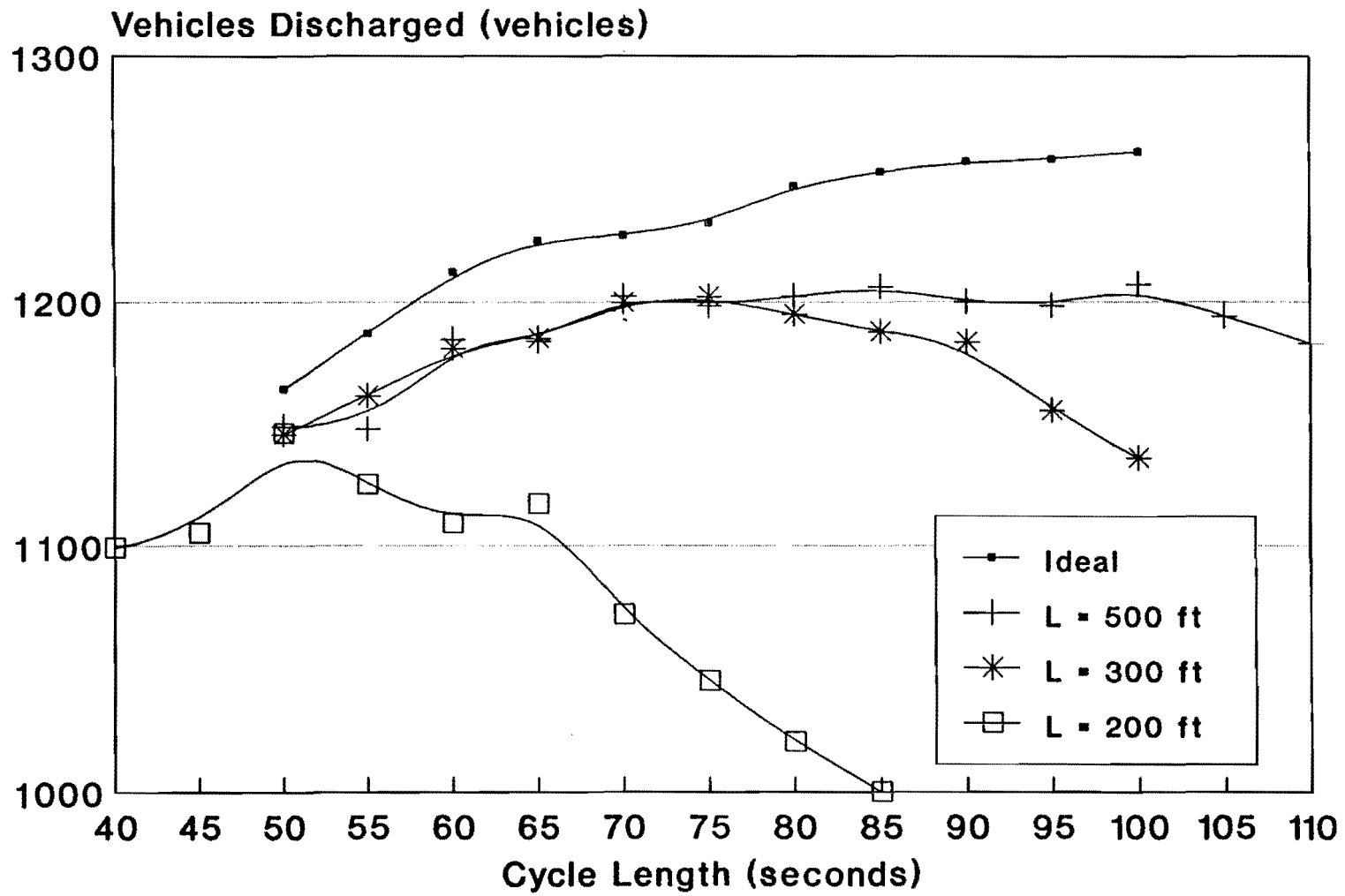
Figure 4-4. Plot of Cycle Length versus Vehicles Discharged
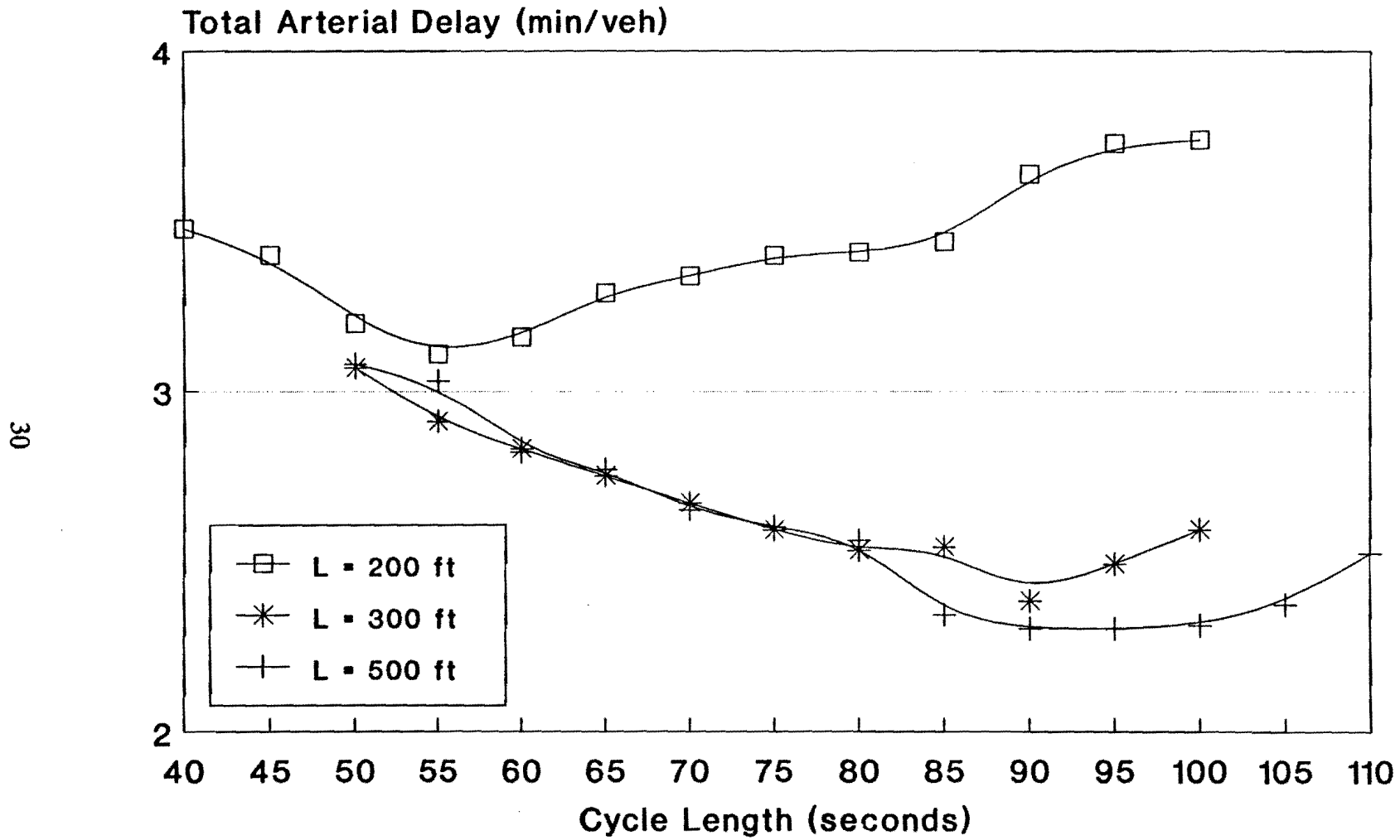
Figure 4-5. Plot of Cycle Length versus Total Arterial Delay

Figure 4-5 shows the relationship between cycle length and total arterial delay produced from the TRAF-NETSIM simulation. The curves in this figure have the form of convex functions. The minimum delay cycle lengths were 55 seconds for the 200-foot link and 90 seconds for the 300-foot link, respectively. For the 500-foot link, the curve is relatively flat for cycle lengths between 90 and 100 seconds. Delay increases beyond the 100-second cycle. Figure 4-6 shows the relationship between link length and optimum cycle length. This figure demonstrates that optimal cycle length is related to link length. The optimum cycle length increases as link lengths become longer.
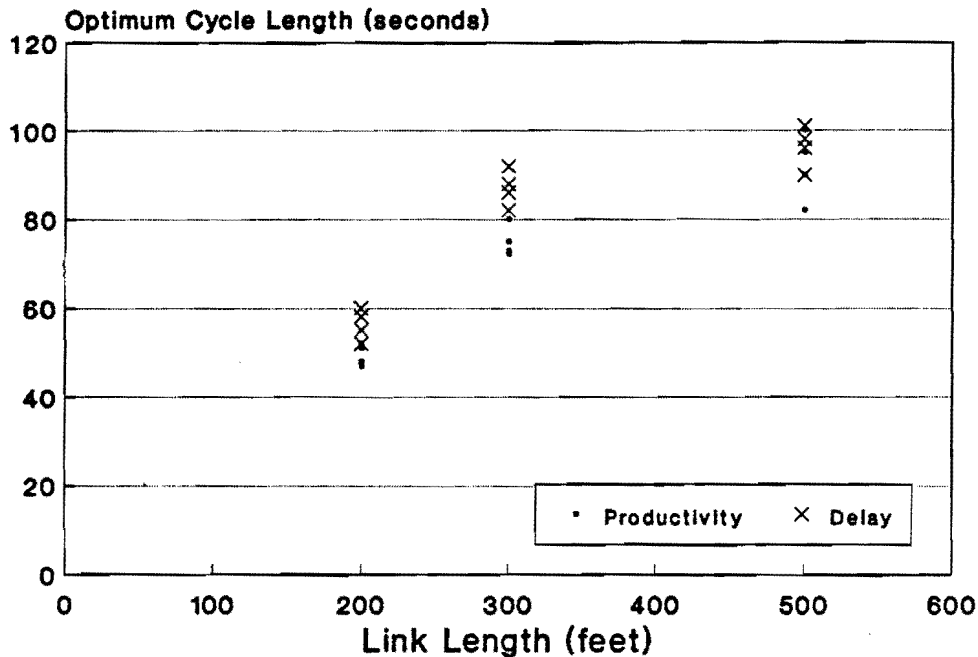


Figure 4-6. Plot of Link Length versus Optimal Cycle Length

The static model, as a deterministic model, optimizes signal timing based on average queue lengths over many cycles. In the real situation, queue lengths fluctuate around the average values due to their stochastic nature. Even at the optimal cycle length, there is a chance of queue spillback. The side effect of queue spillback is potentially serious. In selecting a system cycle length, it is safer to choose the cycle length slightly less than the optimal in order to reduce the queue-spillback probability. The static model produced optimal cycle lengths of 54, 76, and 105 seconds for link lengths of 200, 300, and 500 feet, respectively, when the average vehicle storage length was assumed to be 25 feet per vehicle.

## 4.3.2   Green Split

This research studied the effect of green split on system productivity to demonstrate the appropriateness of the green split hypothesis (Hypothesis 2). Whether the optimal green

31
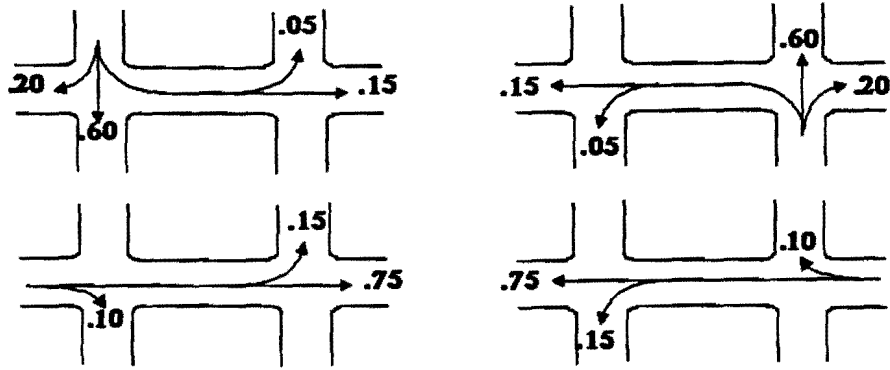
(a) Case 1 - Base Case
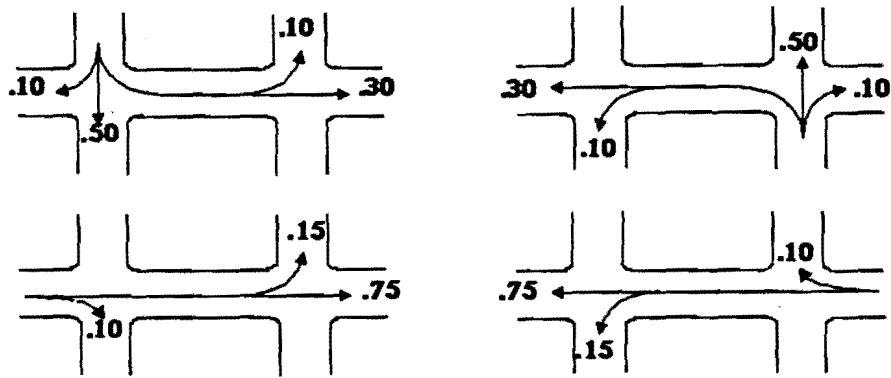


(b) Case 2 - Heavy Turn-In Traffic from Cross Street
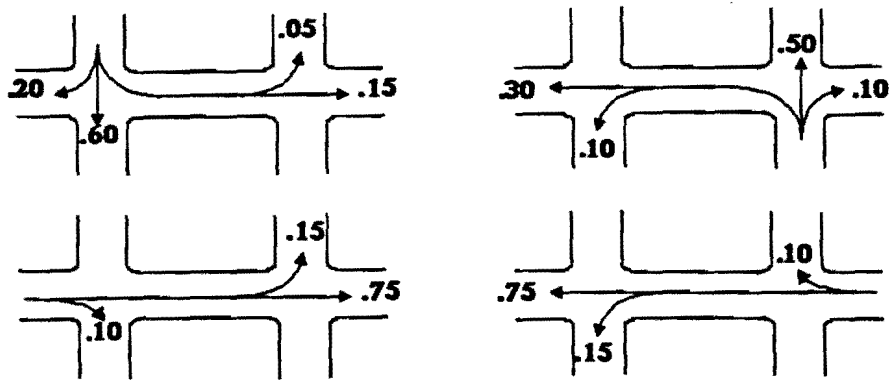


(c) Case 3 - Asymmetric Turn Percentages

Figure 4-7. Three Cases of Turning Percentages

32
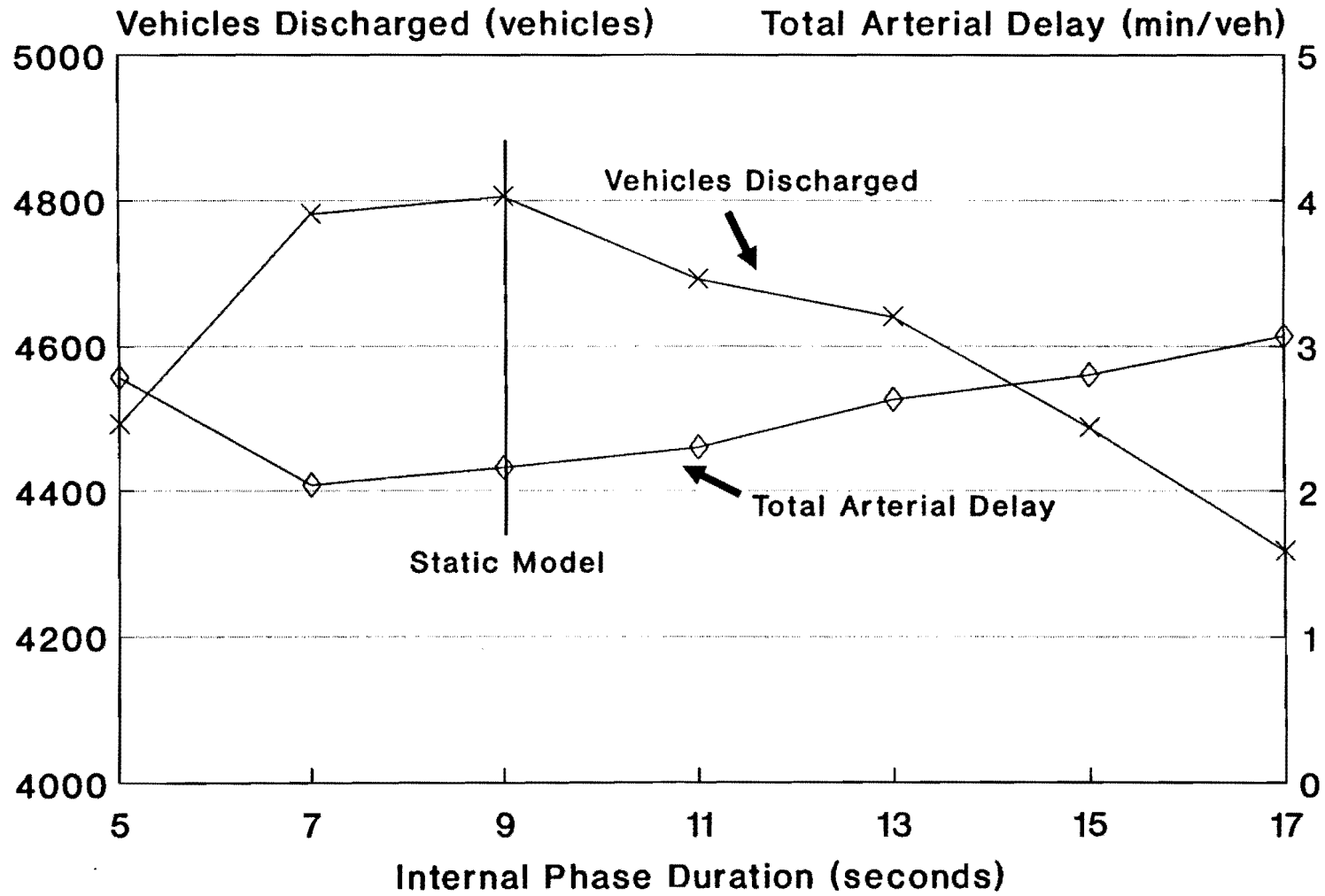
Figure 4-8. Effects of Green Split on Vehicle Discharge and Total Arterial Delay (Case 1)

**Vehicles Discharged (vehicles)**     **Total Arterial Delay (min/veh)**
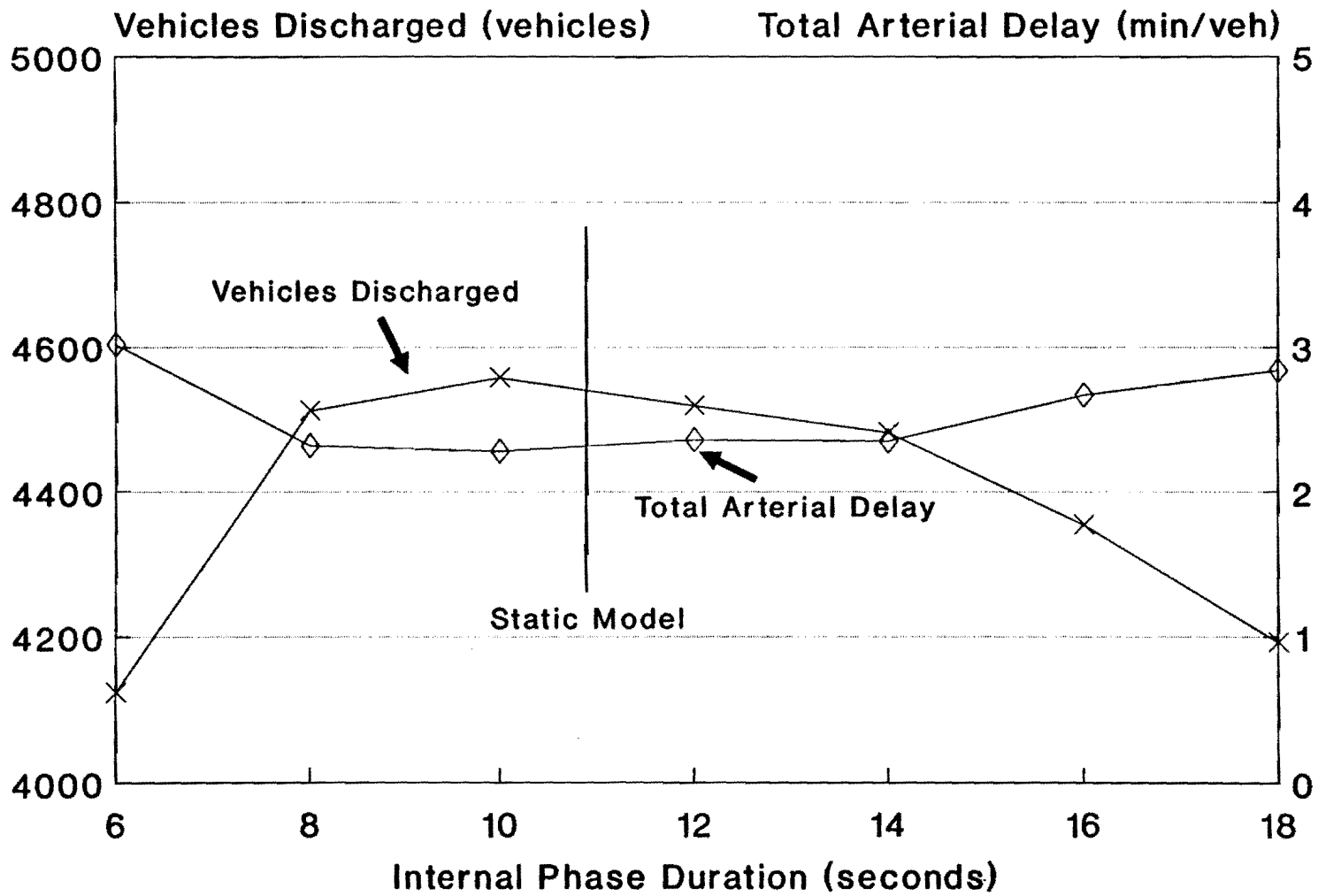
Figure 4-9. Effects of Green Split on Vehicle Discharge and Total Arterial Delay (Case 2)

34
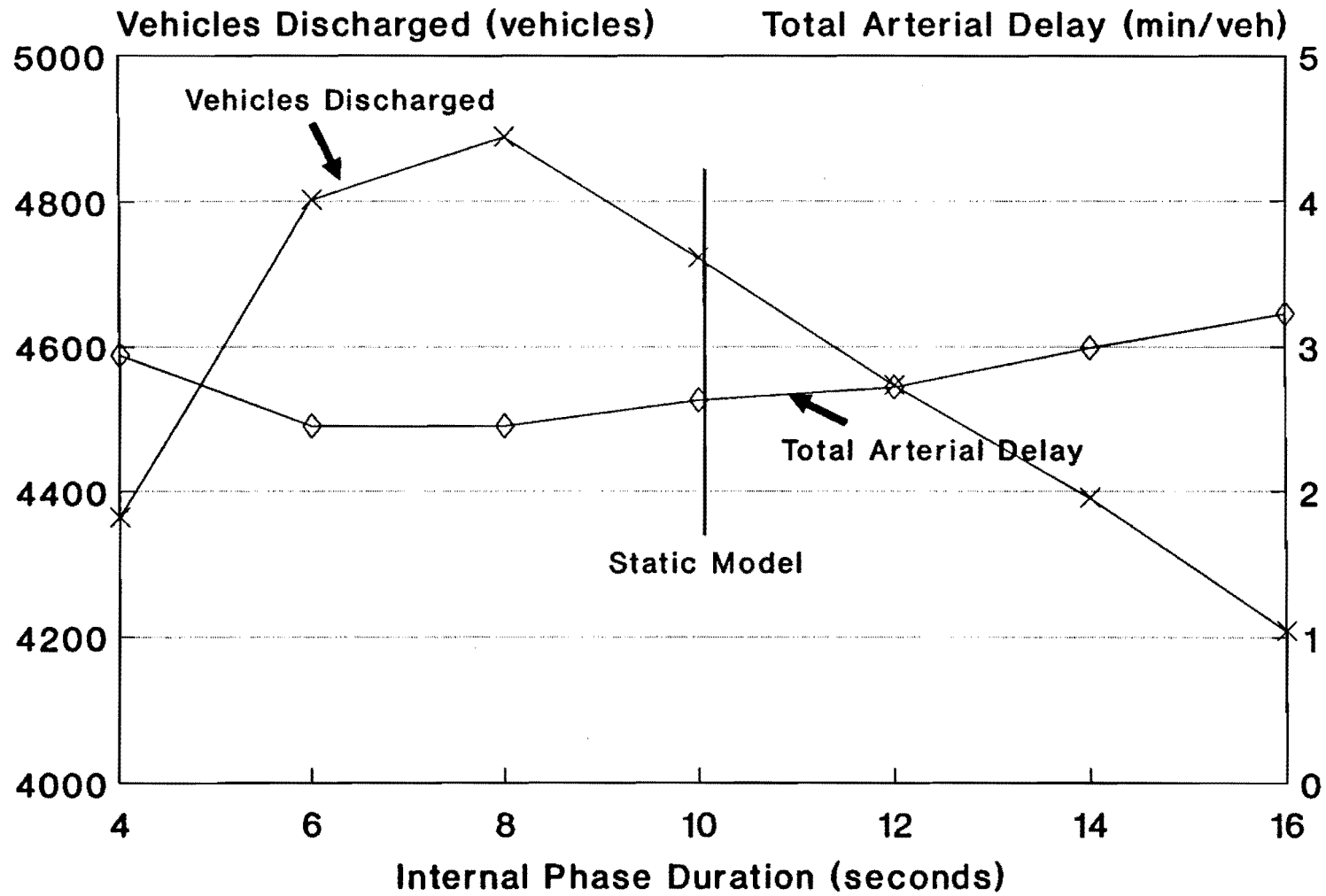
Figure 4-10. Effects of Green Split on Vehicle Discharge and Total Arterial Delay (Case 3)

split produced by the static model was really optimal was also tested through TRAF-NETSIM simulation. Three cases of turning percentages were prepared, as shown in Figure 4-7. Case 1 has turning percentages identical to the base case. In Case 2, traffic entering from the cross streets onto the arterial is double that of Case 1. In Case 3, the right intersection has turning percentages identical to Case 1 and the left intersection is identical to Case 2. Cases 1 and 2 have a symmetric traffic patterns, while Case 3 has an asymmetric pattern.

Figures 4-8, 4-9, and 4-10 show the effect of green split on system productivity and total arterial delay. In Figure 4-8, the green time for internal clearance phase (Phase C) was progressively increased by two seconds starting at five seconds. Green times for external phases (Phases A and B) were simultaneously reduced by one second, while keeping the cycle length constant. The green time did not include intersection clearance time. A curve showing the relationship between internal phase duration and system productivity became a concave function. The vehicle discharge increased to the internal phase duration of nine seconds, then decreased continuously for durations above nine seconds. This result agrees with the hypothesis made in the development of the static model for green splits in Figure 4-1(b). System productivity was lost due to increasing queue length on the internal link for the internal phase durations less than the optimum and unused green time for the internal phase durations greater than the optimum. A curve for total arterial delay was convex, as expected.

The relationship between the internal phase duration, vehicle discharge, and total arterial delay for Cases 2 and 3 (Figures 4-9 and 4-10) showed a pattern similar to Case 1. Vehicle discharge had concave functions while the total arterial delay had convex functions. The three cases, however, gave different optimal internal phase durations. This result means turning percentage is a major factor in determining green splits. When the signal timings for the three cases were developed using the static model, it produced optimal internal phase durations of 9, 11, and 10 seconds for Cases 1, 2, and 3, respectively. These optimal durations are slightly larger that those predicted by the sensitivity analysis using the TRAF-NETSIM simulation.

### 4.3.3  Offset

According to current practice in signal timing design, the best offsets are selected based on maximum bandwidth (PASSER II (3), MAXBAND (31)) or minimum delay and stops (TRANSYT-7F (4)). While a number of studies have been conducted to determine the effects of offset on arterial progression, average delay, and stops, none have considered system productivity. The objective of this section is to examine the effect of offset on system productivity and average delay.

Given the roadway and traffic characteristics of the base case (Figure 4-3), optimal cycle lengths and green splits were generated by the static model. It should be noted that

the offset reference points are the starting point of Phase A of both intersections, as demonstrated in Figure 4-11. Two cycle lengths were simulated using TRAF-NETSIM. One was the optimal cycle length (75 seconds), and the other was a cycle length below optimal (60 seconds). Green splits were fixed for the two cycle lengths.
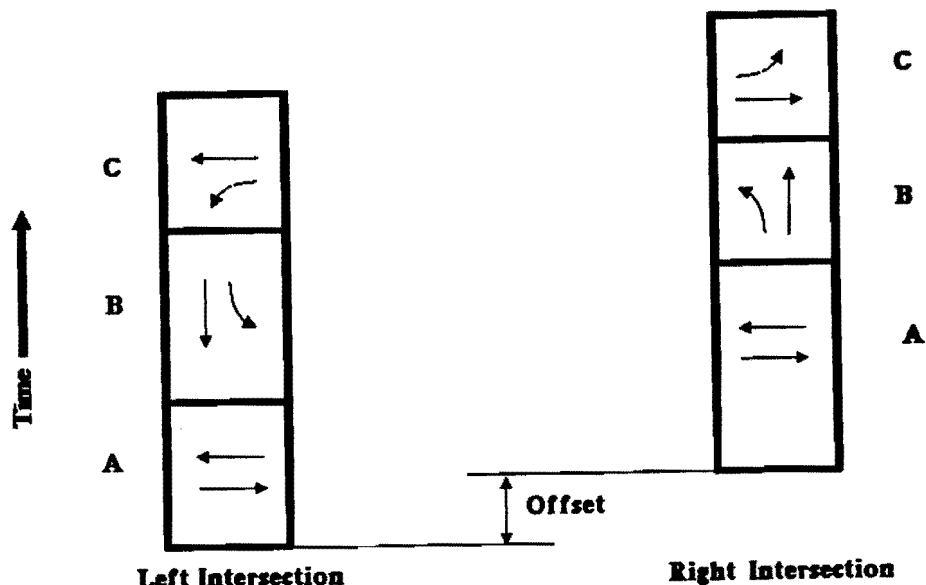


Figure 4-11. Definition of Offset

Figure 4-12 shows the effect of offset on the average delay for the internal links. For both cycle lengths, minimum internal delay is observed at the offset value of half the cycle length (alternate offset), and maximum delay is observed around the zero offset (simultaneous offset). The percent differences between minimum and maximum delay are approximately 100 percent for the 60-second cycle and 75 percent for the 75-second cycle. These results, indicate that average delay on the internal links is sensitive to offset.

Figure 4-13 shows the effect of offset on total interchange delay at 60- and 75-second cycle lengths. The curves in these figures have a different trend to that of offset versus internal delay (Figure 4-12). The curves are almost flat for the entire range of offsets.

Figure 4-14 shows the effect of offset on total vehicle discharge for the interchange system. Maximum vehicle discharge was obtained near simultaneous offset (zero offset) for both cycle lengths. However, percent differences between the minimum and maximum are only one percent for the 60-second cycle and four percent for the 75-second cycle. These differences appear relatively trivial compared to internal delay. From these results, it can be concluded that neither arterial delay nor system productivity is very sensitive to offset.

37
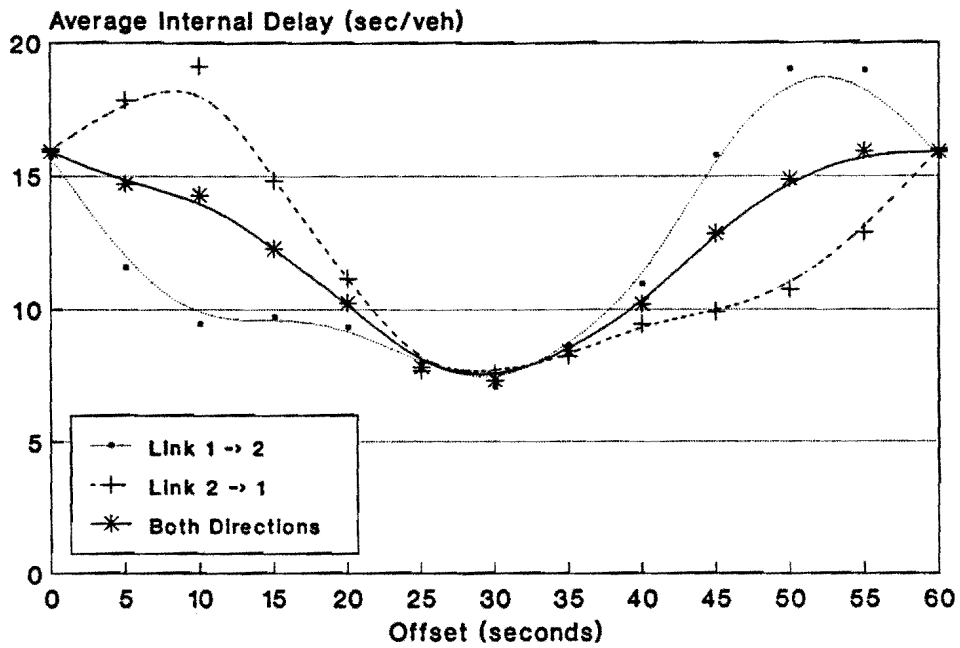
(a) Cycle Length = 60 seconds
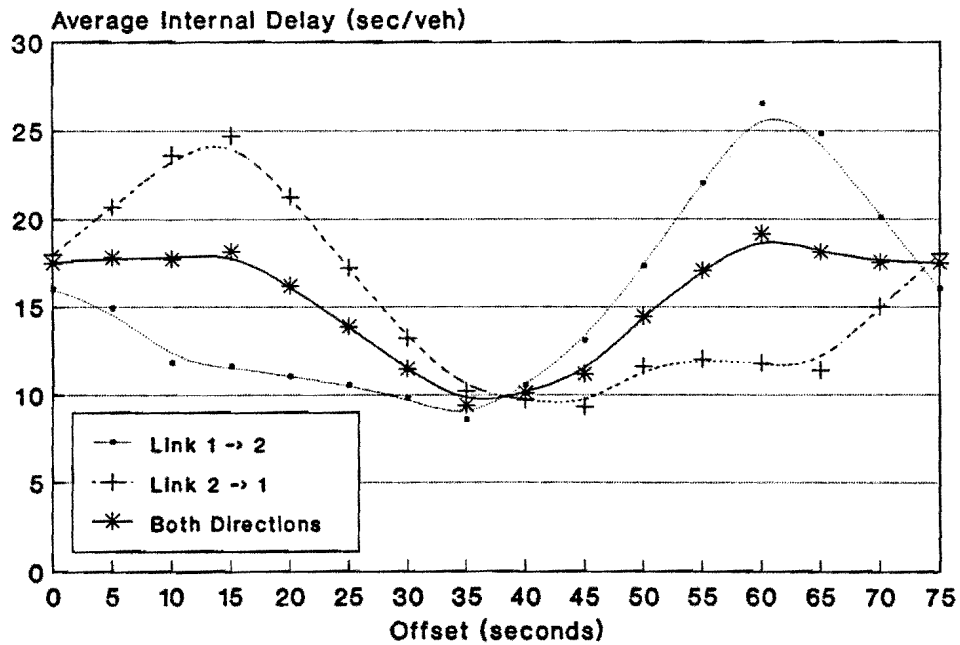


(b) Cycle Length = 75 seconds

Figure 4-12. Plot of Offset versus Average Internal Delay

**Total Interchange Delay (min/veh)**

(a) Cycle Length = 60 sec.
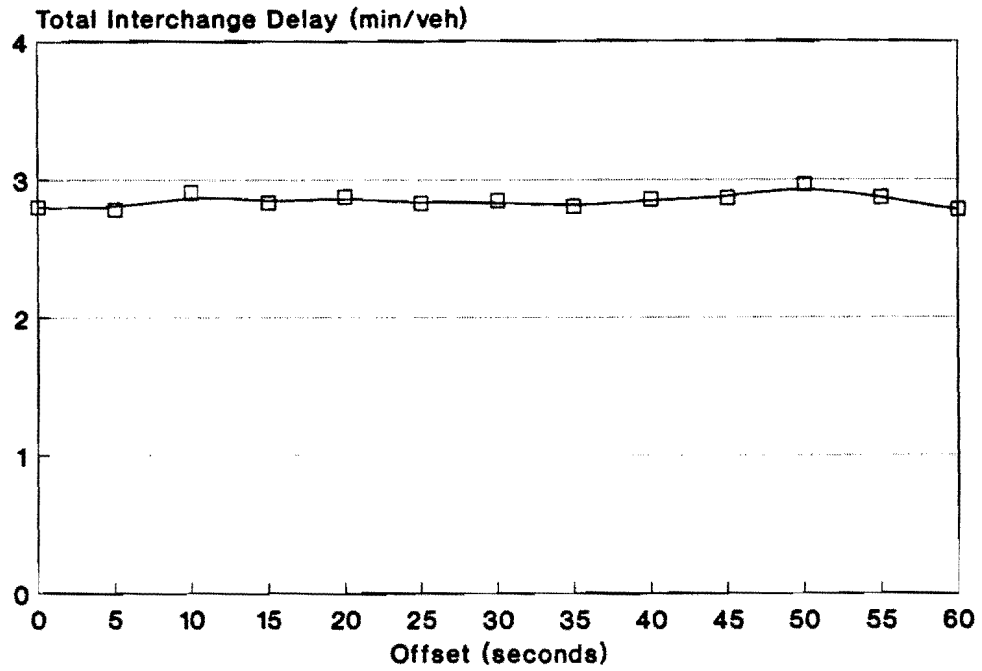
**Total Interchange Delay (min/veh)**
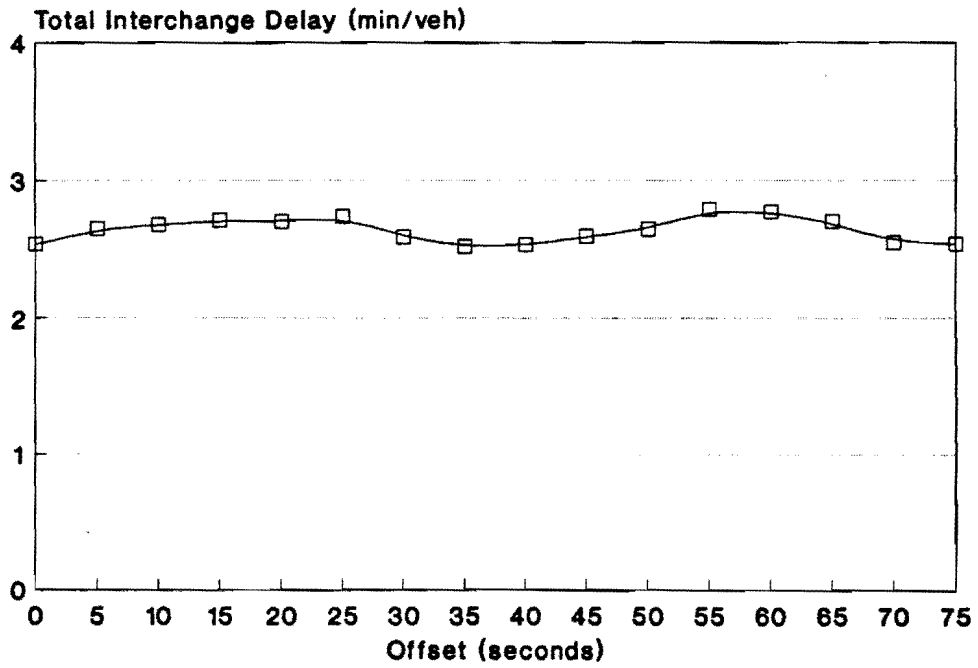
(b) Cycle Length = 75 sec.

Figure 4-13. Plot of Offset versus Total Interchange Delay

39
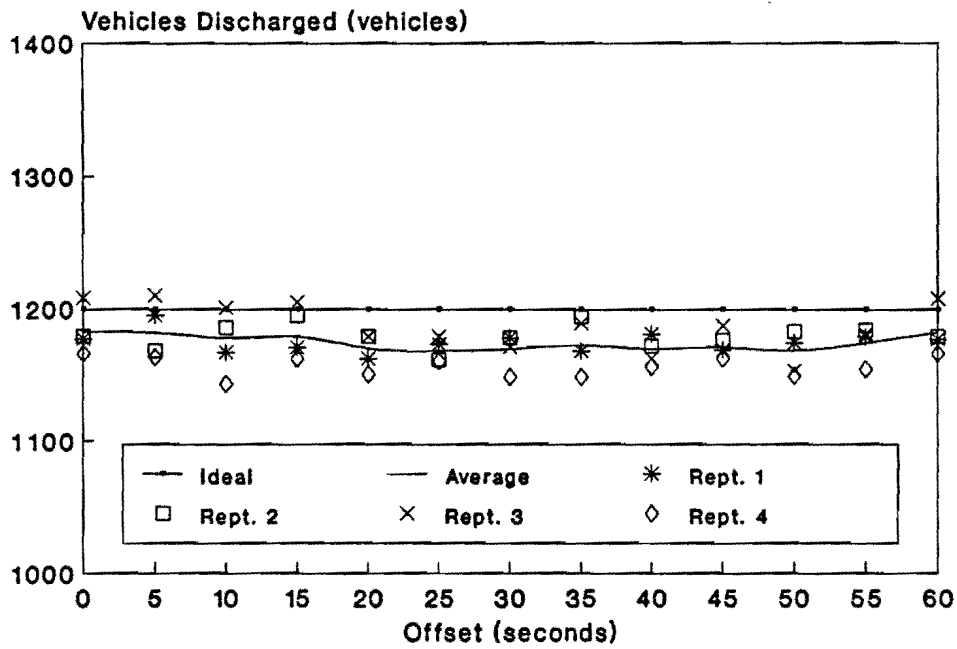
(a) Cycle Length = 60 seconds
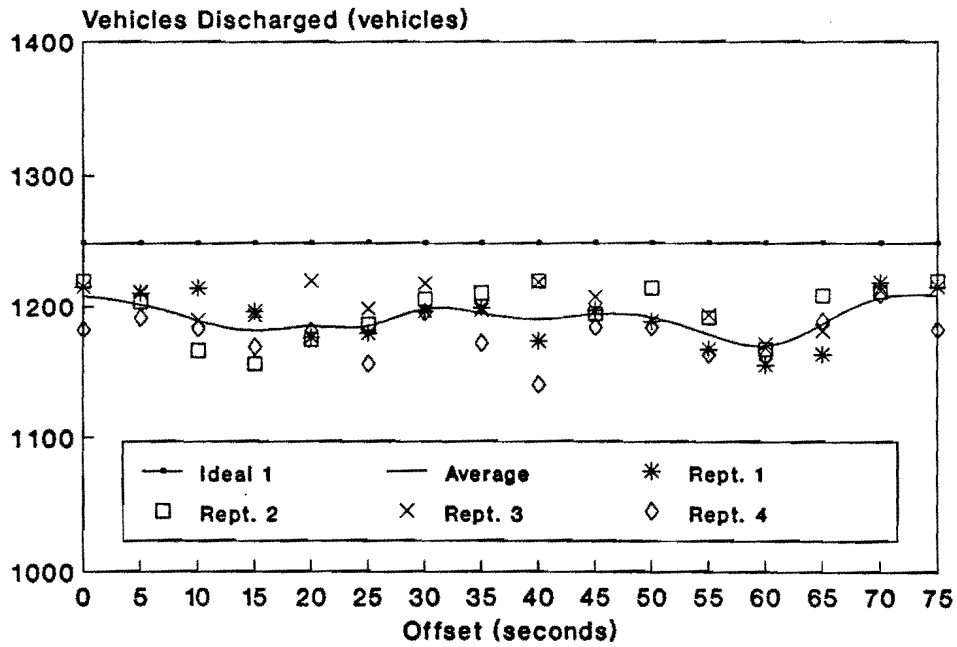


(b) Cycle Length = 75 seconds

Figure 4-14. Plot of Offset versus Vehicles Discharged

# 5. DYNAMIC OPTIMIZATION MODEL

## 5.1  INTRODUCTION

Suppose the queue storage capacities on the external approaches to a signalized interchange are limited and the queue spillback to the intersections or freeway mainlanes adjacent to the interchange can cause severe operational problems. As the main objective of traffic signal control during oversaturated conditions is to obtain maximum system productivity, this control objective can not be accomplished without considering potential queue spillback on the external approaches. This spillback may cause serious operational problems on the interchange, including the adjacent intersections or transportation facilities.

The two-fold control objectives proposed by Michalopoulos (*13*) appear reasonable to address this condition. First, the queues developing on external approaches must be restricted so that adjacent upstream intersections are not blocked. Second, total system delay during the entire control period should be minimized. It is believed that control strategies satisfying these objectives would also maximize total system productivity.

It is evident that queue formation depends largely on the magnitude and duration of the heavy demand. Conventional static models like PASSER III (*3*) and TRANSYT-7F (*4*) that use one set of demand data during the entire control period are not appropriate for dynamic queue management. These static models consider only the average magnitude of heavy demand in signal timing optimization, not its duration. The optimization model for queue management should accommodate dynamic variation in traffic demand. The static model developed in Chapter 3 was extended into a dynamic optimization model for queue management, the main product of this research.

The following assumptions were used in the mathematical formulation of the dynamic model:

1. The control period is divided into multiple time slices of 15 minutes each;
2. The variable traffic demands are known for all the time slices; and
3. The traffic demand occurring during each time slice is uniform.

The dynamic model was formulated to obtain minimum delay subject to queue length constraints. The core of the dynamic model consists of the static model. The static model for maximum productivity was used for the formulation of individual time slices. The dynamic model also includes formulas to define relationships of queue carryover between time slices. The model has two groups of constraints; one for individual time slices and the other for the control of queue lengths. The constraints adjust green indication times between time slices and approaches so that maximum queue length does not exceed the allowable storage capacity. In the dynamic model, signal timing plans, usually the green splits, change with every time slice. Green splits are adjusted toward minimizing delay and

41

permitting queues to build to a predetermined upper bound.  Mixed integer linear programming (MILP) is also used in the mathematical formulation of the dynamic model.

The signalized interchange is classified by the number of intersections included within it, as follows:

1. Single Point Urban Interchange (SPUI, one intersection),
2. Tight Urban Diamond Interchange (TUDI, two intersections), and
3. Three-Level Diamond Interchange (TLDI, four intersections).

In this chapter, the dynamic models for the TUDI and the TUDI are described.  The model for the SPUI is excluded in this report because the SPUI currently does not exist in Texas.  The model for the SPUI can be formulated with ease because it is simply a single intersection problem.

One special feature of the dynamic model is that the signal timing plan changes for every time slice, usually every 15 minutes in response to changing traffic patterns.  Since average traffic flows vary with time, it is desirable to change signal timing accordingly.  Such frequent changes in a fixed-time signal system, however, may sometimes cause serious operational problems.  To change from one timing plan to the next, phase durations may need to be either lengthened, shortened or possibly even omitted.  During this process, excessive delay or unexpected intersection blockage can be caused by the loss of green time on some approaches and the loss of coordination for the entire network.  Efficient methods for changing plans can minimize this transient delay.  An effort to reduce these transition problems is addressed in the following sections.

## 5.2    TIGHT URBAN DIAMOND INTERCHANGE

The Tight Urban Diamond Interchange (TUDI) is the most widely used form of freeway-to-arterial interchange in Texas.  A typical conventional diamond interchange and its node-link diagram for the TRAF-NETSIM coding are shown in Figure 5-1.  The design includes one-way frontage roads and U-turn bays, commonly found in Texas.  If the U-turn bays exist at the diamond interchange, frontage-road U-turn traffic has little effect on signal operation.  This design is different from the urban arterial with two intersections in that the left-turn bays on the internal links extend to the upstream links.

### 5.2.1   Control Strategy

The 4-phase overlap signalization strategy (35) has an advantage over three-phase strategies for geometric design shown in Figure 5-1.  A major advantage of the 4-phase strategy is that it generally does not produce queues on the internal links, particularly if no frontage road (or exit ramp) U-turns occur.  That is, the 4-phase strategy results in nearly
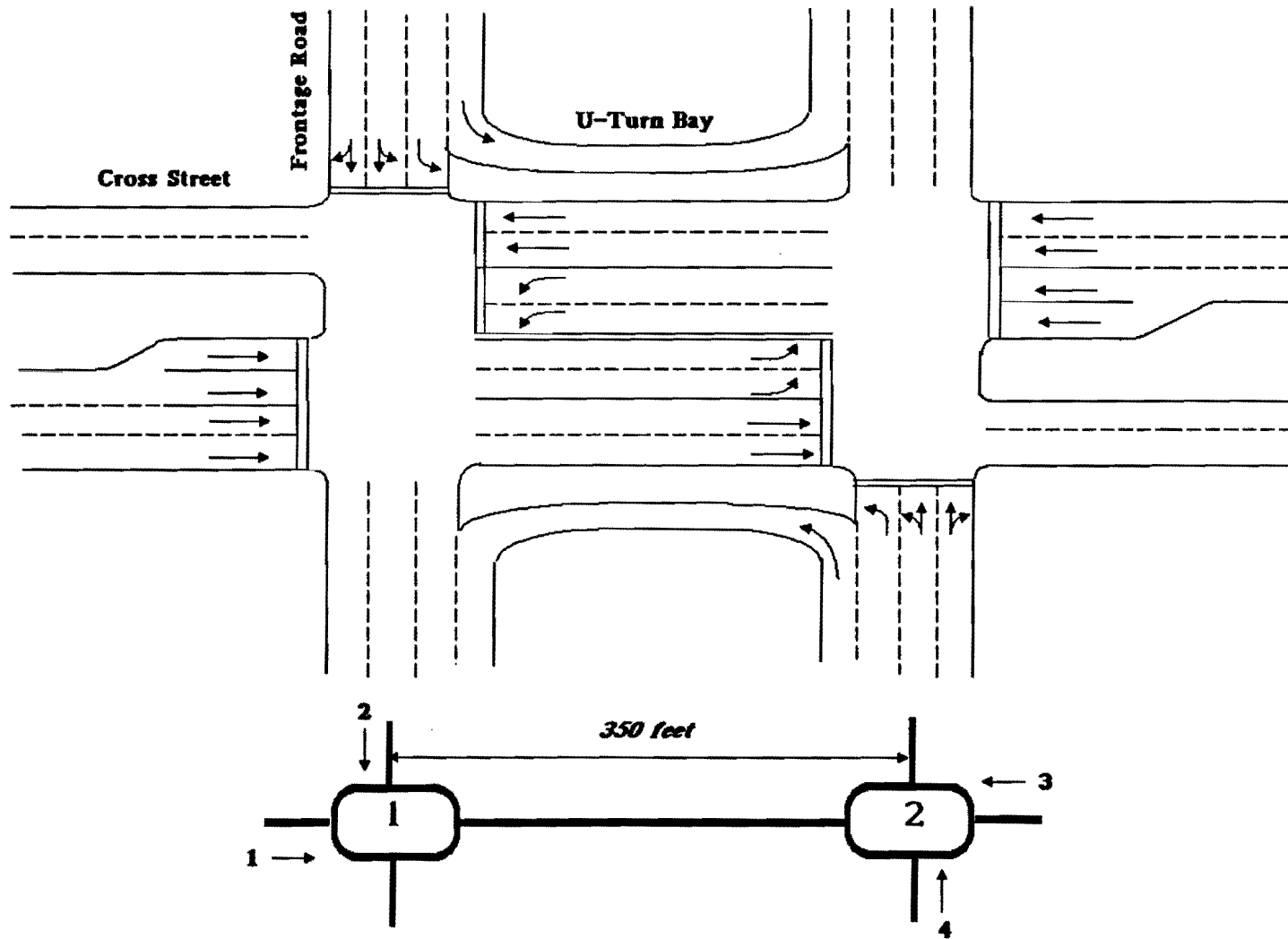
Figure 5-1.  Tight Urban Diamond Interchange
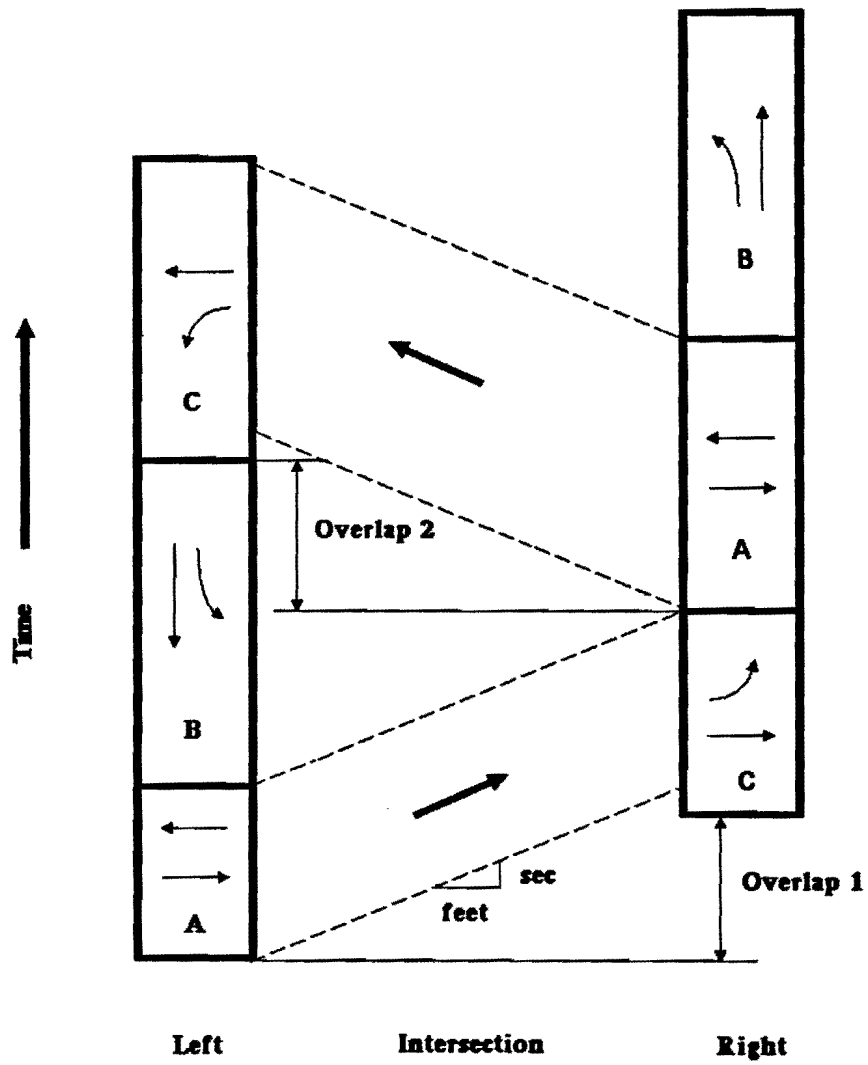
Figure 5-2. Four-Phase with Overlap at TUDI

perfect progression between two closely spaced signalized intersections within the interchange, as shown in Figure 5-2.

An effort to reduce the signal timing transition problem is addressed in this section. In the dynamic model, green splits change every time slice, usually at 15-minute intervals. TRAF-NETSIM allows users to input a series of timing plans during a simulation period for fixed-time controllers. TRAF-NETSIM also provides three signal transition options: immediate, two-cycle, and three-cycle transitions.

Because frequent changes of the green times may cause operational problems at conventional diamond interchanges, a special coding scheme of the 4-phase overlap strategy in TRAF-NETSIM was prepared to minimize the problem, as shown in Figure 5-3. The phase sequence of 4-phase overlap strategy is ABC:ABC. Phases of the left intersection are normally coded as a sequence of ABC. Signal timing at the right intersection starts with Phase B of the duration identical to the overlap phase. Phases C and A are coded in intervals 2 and 3, respectively. Phase B is coded in interval 4 with the duration of Phase-B duration minus overlap, therefore, the sum of intervals 1 and 4 is the Phase-B duration. The
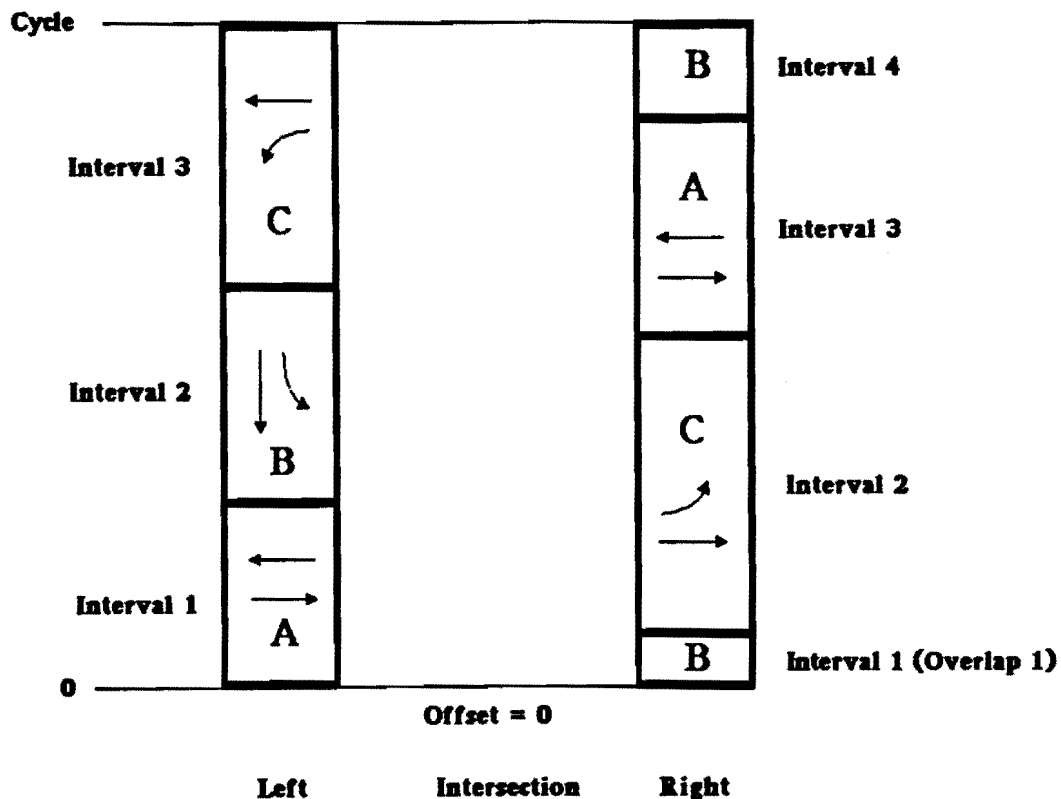


Figure 5-3. NETSIM Coding of 4-Phase-Overlap

**PLAN 1**

| | A | B | C |
|---|---|---|---|
| Left | 20 | 30 | 40 |

Intersection

| | A | B | C |
|---|---|---|---|
| Right | 42 | 20 | 28 |

Offset = 51 sec

**PLAN 2**

| | A | B | C |
|---|---|---|---|
| | 35 | 27 | 28 |

| | A | B | C |
|---|---|---|---|
| | 15 | 35 | 40 |

Offset = 39 sec
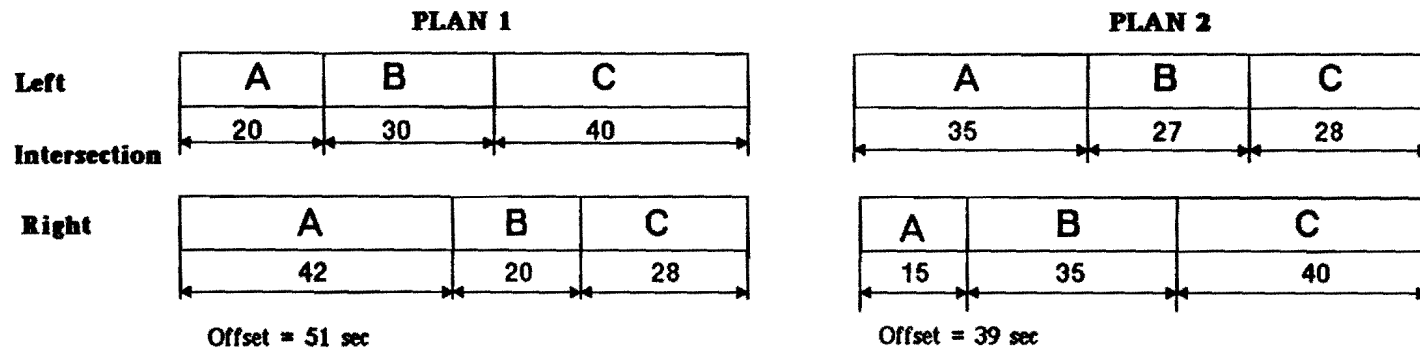
**(a) Two Timing Plans (C = 90 sec)**

Time (sec.)
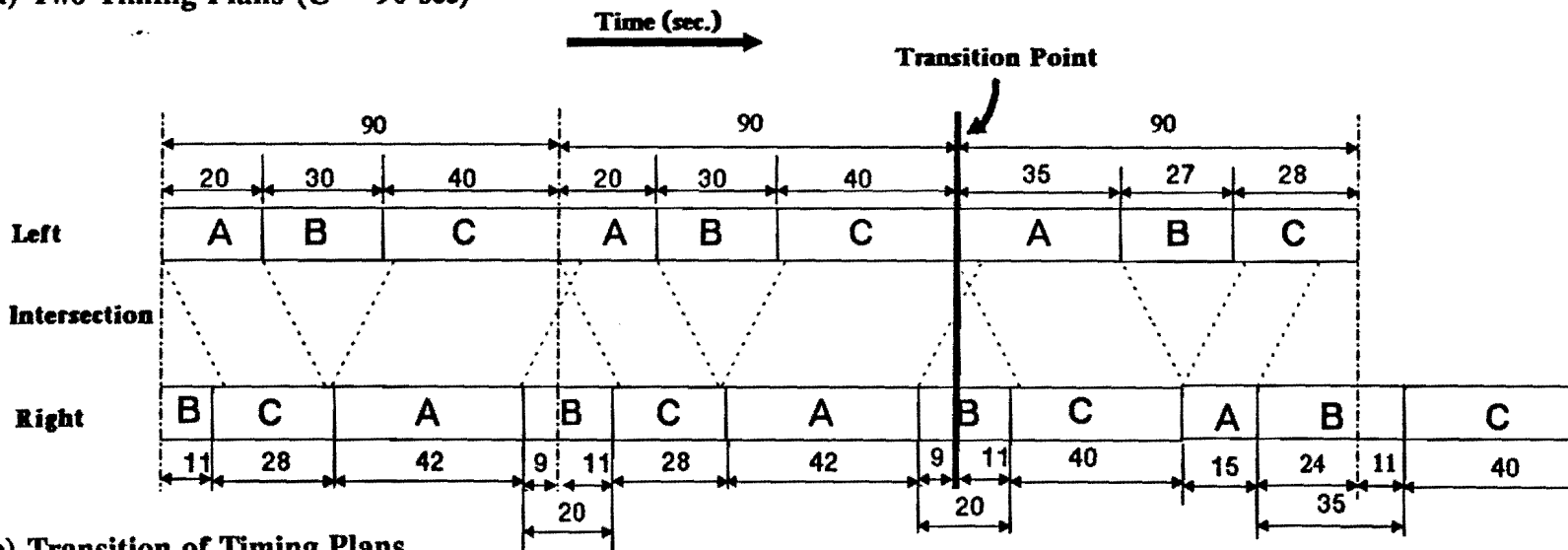
Transition Point

**(b) Transition of Timing Plans**

Figure 5-4. Transition of 4-Phase-Overlap

46

offset between the first interval of the two intersections must be zero so as to insure perfect progression.

Immediate transition should be applied in TRAF-NETSIM for the coding scheme to be effective in reducing the transition delay. Figure 5-4 illustrates how the coding scheme works during the transition period. Time Slice 1 is followed by Time Slice 2. Figure 5-4(a) shows two timing plans obtained from the 4-phase overlap strategy. Signal plans change suddenly at the end of Time Slice 1. Plan 1 changes into Plan 2 without losses of green time and progression, as shown in Figure 5-4(b). This coding scheme minimizes transient delay.

## 5.2.2  Formulation

The numbering scheme of movements and the signal phase scheme in the dynamic model are identical to those of the static model shown in Figures 3-1 and 3-2. The following notation is used in the formulation:

| | |
|---|---|
| $i$ | = signal phase and/or movement, $i = 1,2,3,4,6,7$, |
| $j$ | = time slice of duration $\Delta T$, |
| $C$ | = system cycle length, sec, |
| $l$ | = lost time per phase, sec, |
| $G_{ij}$ | = effective green time of phase $i$ at time slice $j$, sec, |
| $g_{ij}$ | = $G_{ij}/C$, green ratio normalized to cycle length, |
| $\phi$ | = one-direction overlap, sec, |
| $V_{ij}$ | = average input volume on approach $i$ at time slice $j$, vps, |
| $S_i$ | = saturation flow of approach $i$, vpsg, |
| $P_{ikj}$ | = proportion of turning movement, as shown in Figure 3-3, |
| $L_{ij}$ | = queue length of external phase $i$ at the end of time slice $j$, veh, |
| $N_j$ | = queue storage capacity of external phase $j$, veh, |
| $D_i$ | = delay for external approach $i$, veh-min, |
| TD | = total external delay, veh-min, |
| $Z_{ij}$ | = $\begin{cases} 0 & \text{when approach is undersaturated, and} \\ 1 & \text{when approach is oversaturated.} \end{cases}$ |

## Objective Function

The control objective of the dynamic model is to minimize total external delay. Total external delay is the sum of delays on all external approaches. Delay on individual approach $i$, $D_i$, is equivalent to the area formed by the x-axis and queue length line, as shown in Figure 5-5. Namely:

$$D_i = (1/2) \{(L_{i0} + L_{i1}) + (L_{i1} + L_{i2}) + \dots + (L_{i\,n-1} + L_{in})\} \Delta T$$
$$= (1/2) (L_{i0} + 2L_{i1} + 2L_{i2} + \dots + 2L_{i\,n-1} + L_{in}) \Delta T \tag{14}$$

47
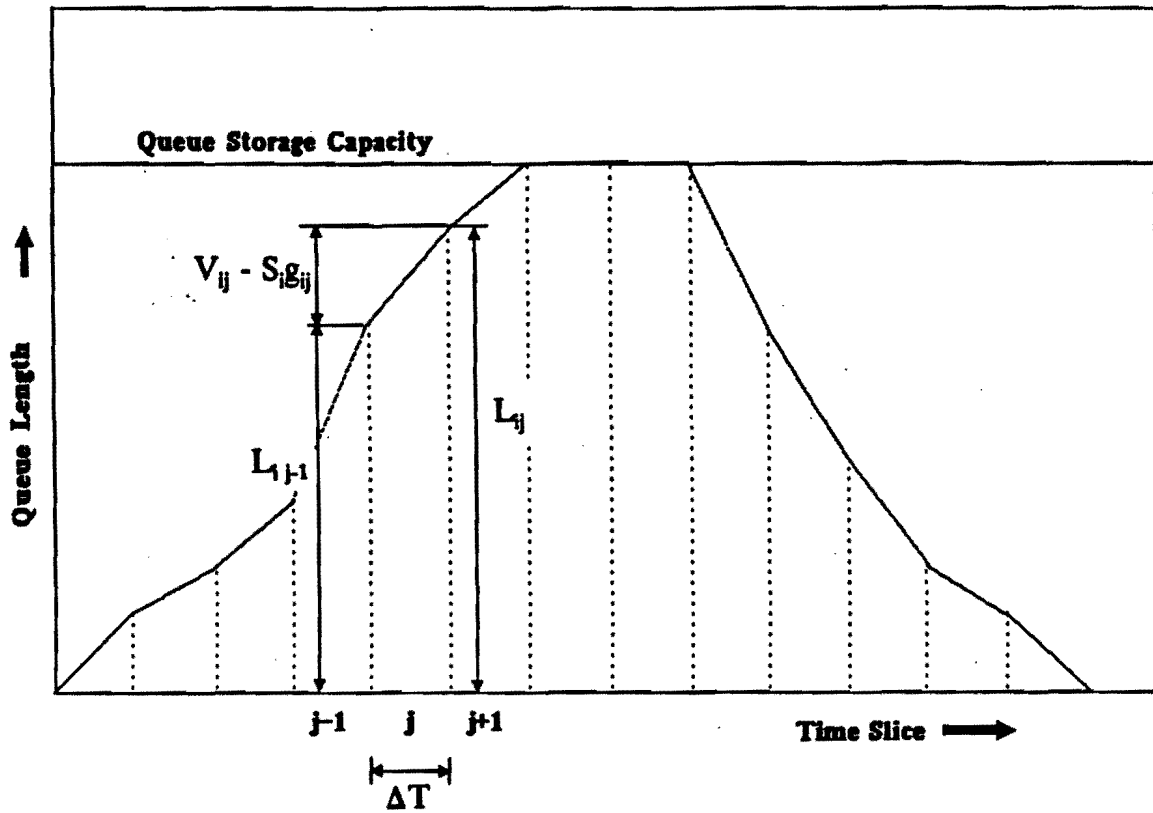
Figure 5-5. Queue Profile on Approach "i"

where n is the number of time slices. If an undersaturated traffic condition before the initiation and after the termination of the control period is assumed, then:

$$L_0 = L_n = 0$$

and,

$$D_i = \Delta T \sum_{j=1}^{n} L_{ij} \qquad \text{for all } i \qquad (15)$$

Because the duration of the time slice is a fixed $\Delta T$, the product of the duration of the time slice and the sum of the queue lengths over all time slices is equivalent to total delay on the individual approach. Therefore, the objective function to minimize total external delay, TD, is:

48

## Constraints

$$\text{Minimize} \quad TD = \Delta T \sum_{\text{all } i} \sum_j L_{ij} \tag{16}$$

*Set 1.* In coordinated signal systems, the sum of phase durations at the individual intersections must be equal to the system cycle length, C. For three-phase signals, this requirement leads to:

$$G_{1j} + G_{2j} + G_{6j} + 3l = C \qquad\qquad \text{for all } j \quad (17a)$$
$$G_{3j} + G_{4j} + G_{7j} + 3l = C \qquad\qquad \text{for all } j \quad (17b)$$

or, dividing by C to normalize the green splits:

$$g_{1j} + g_{2j} + g_{6j} = 1 - 3l/C \qquad\qquad \text{for all } j \quad (18a)$$
$$g_{3j} + g_{4j} + g_{7j} = 1 - 3l/C \qquad\qquad \text{for all } j \quad (18b)$$

*Set 2.* For the internal links, the input to the system must not be greater than the output in order to stabilize queue lengths over many cycles:

$$S_1 P_{17j} g_{1j} + S_1 P_{27j} g_{2j} \le \alpha S_7 g_{7j} \qquad\qquad \text{for all } j \quad (19a)$$
$$S_1 P_{13j} g_{1j} + S_2 P_{23j} g_{2j} \le \alpha S_{37}(g_{3j} + g_{7j} + 1/C) \qquad \text{for all } j \quad (19b)$$
$$S_3 P_{36j} g_{3j} + S_4 P_{46j} g_{4j} \le \alpha S_6 g_{6j} \qquad\qquad \text{for all } j \quad (19c)$$
$$S_3 P_{31j} g_{3j} + S_4 P_{41j} g_{4j} \le \alpha S_{16}(g_{1j} + g_{6j} + 1/C) \qquad \text{for all } j \quad (19d)$$

where $\alpha$ is an adjustment factor of saturation flow, usually not greater than 1.

Due to the complex lane configurations sometimes found on internal links and the stochastic nature of lane utilization, vehicles sometimes cannot fully utilize the available lanes. In this situation, it is desirable to adjust saturation flows using an $\alpha$ factor of less than 1. In most cases, however, the $\alpha$ factor should be 1. Smaller factor values give larger green times for internal phases, resulting in smaller green times for external phases.

*Set 3.* The 4-phase-overlap signalization strategy widely used in Texas was adopted for traffic control of the oversaturated CDI in this research:

$$G_{6j} + G_{7j} + 2l = C - 2\phi \qquad\qquad \text{for all } j \quad (19)$$

or,

$$g_{6j} + g_{7j} = \frac{(C - 2\phi - 2l)}{C} \qquad\qquad \text{for all } j \quad (20)$$

*Set 4.* The queue lengths occurring at the end of each time slice must be non-negative. The non-negativity is achieved by letting:

49

$$L_{ij} = \text{Max} \{ 0, L_{i\,j-1} + (V_{ij} - S_i g_{ij})\Delta T \} \qquad \text{for all } i, j \qquad (20)$$

which is equivalent to:

$$L_{ij} \geq 0 \qquad\qquad\qquad \text{for all } i, j$$
$$L_{ij} \geq L_{i\,j-1} + (V_{ij} - S_i g_{ij})\Delta T \qquad\qquad \text{for all } i, j$$
$$L_{ij} \leq M Z_{ij} \qquad\qquad\qquad \text{for all } i, j$$
$$L_{ij} - \{L_{i\,j-1} + (V_{ij} - S_i g_{ij})\Delta T\} \leq M(1-Z_{ij}) \qquad \text{for all } i, j$$

where $M > 0$ is sufficiently large such that $L_{ij} \leq M Z_{ij}$ is redundant with respect to any active constraint. $Z_{ij}$ is an integer variable having binary values.

As demonstrated in Figure 5-5, queue length on external approach i at the end of time slice j, $L_{ij}$, is the sum of any queues transferred from the previous time slice and the difference between input and output at the current time slice; namely:

$$L_{ij} = L_{i\,j-1} + (V_{ij} - S_i g_{ij})\Delta T \qquad\qquad\qquad (21)$$

The queue length estimation of Equation 21 is based on the Input-Output Analysis methodology. If $V_{ij} \geq S_i g_{ij}$, the queue length increases; otherwise, the queue length decreases. When an approach becomes undersaturated, the right-hand side of Equation 21 can have a negative value, as illustrated in Figure 5-6. Suppose the queue dissipates at time slice j and then grows again at time slice j+1. The actual profile of the queue length follows line ABCDE in Figure 5-6. Without the non-negativity constraints on $L_{ij}$, the dynamic model predicts an erroneous queue profile along line ABGHI. This prediction causes some false estimation of the queue length starting from time slice j+1.

This problem is solved by adding non-negativity constraints to the calculation of queue lengths in the dynamic model. The non-negativity constraints make the model estimate the queue profile along line ACDE. The queue length starting from time slice j+1 is estimated reasonably by adding the non-negativity constraints to the MILP formulation. Actual delay at time slice j is the area of AFB, whereas the dynamic model slightly overestimated the delay as the area of AFC. The overestimation has little effect on the optimal solution because the overestimated delay is usually minor compared to the total delay. Integer variables, $Z_{ij}$ were introduced for modelling the non-negativity of the queue lengths; thus, the dynamic model contains more features of Mixed Integer Linear Programming (MILP) than does the static model.

*Set 5.* The queue lengths at the end of each time slice must not exceed available queue storage capacity of their respective external links:

$$L_{ij} \leq \beta N_i \qquad\qquad\qquad \text{for all } i, j \qquad (22)$$

where $\beta$ is the adjustment factor for queue storage, usually not greater than 1. The
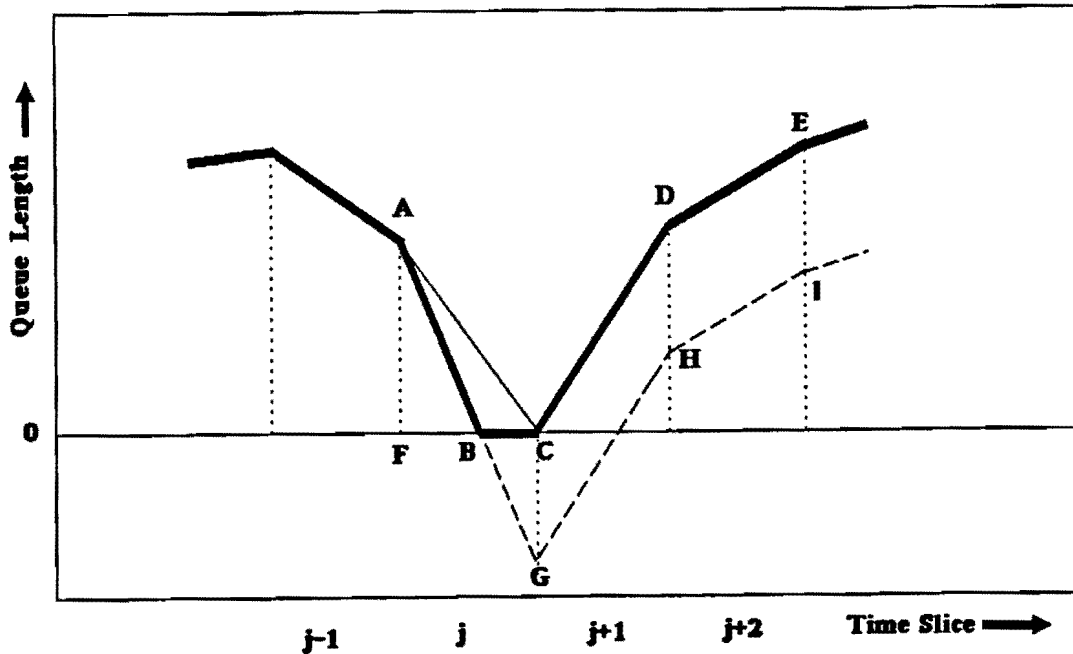
Figure 5-6. Role of Non-Negativity Constraints

adjustment factor, $\beta$, makes the queue storage capacity smaller than it actually is so as to provide a storage buffer to absorb some natural fluctuations in demand. The queue storage capacity of external link, $N_i$ is an upper limit for queue length on approach i. This storage capacity is calculated using the following equation:

$$N_i = \frac{(\text{Link Length, feet}) \times (\text{Number of Lanes})}{(\text{Vehicle Storage Length, feet})} \tag{23}$$

*Set 6.* The green time must be greater than the minimum green time:

$$g_{ij} \geq g_{i\,min} \qquad\qquad \text{for all i, j} \tag{24}$$

where $g_{i\,min}$ is minimum green ratio for phase i. The minimum green ratio can be determined from pedestrian crossing requirements or driver expectancy considerations.

## 5.3 THREE-LEVEL DIAMOND INTERCHANGE

The three-level diamond interchange is normally utilized for freeway-to-freeway interchanges in urban environments. The three-level diamond interchange includes four signalized intersections and two pairs of one-way streets. Figure 5-7 shows an example of
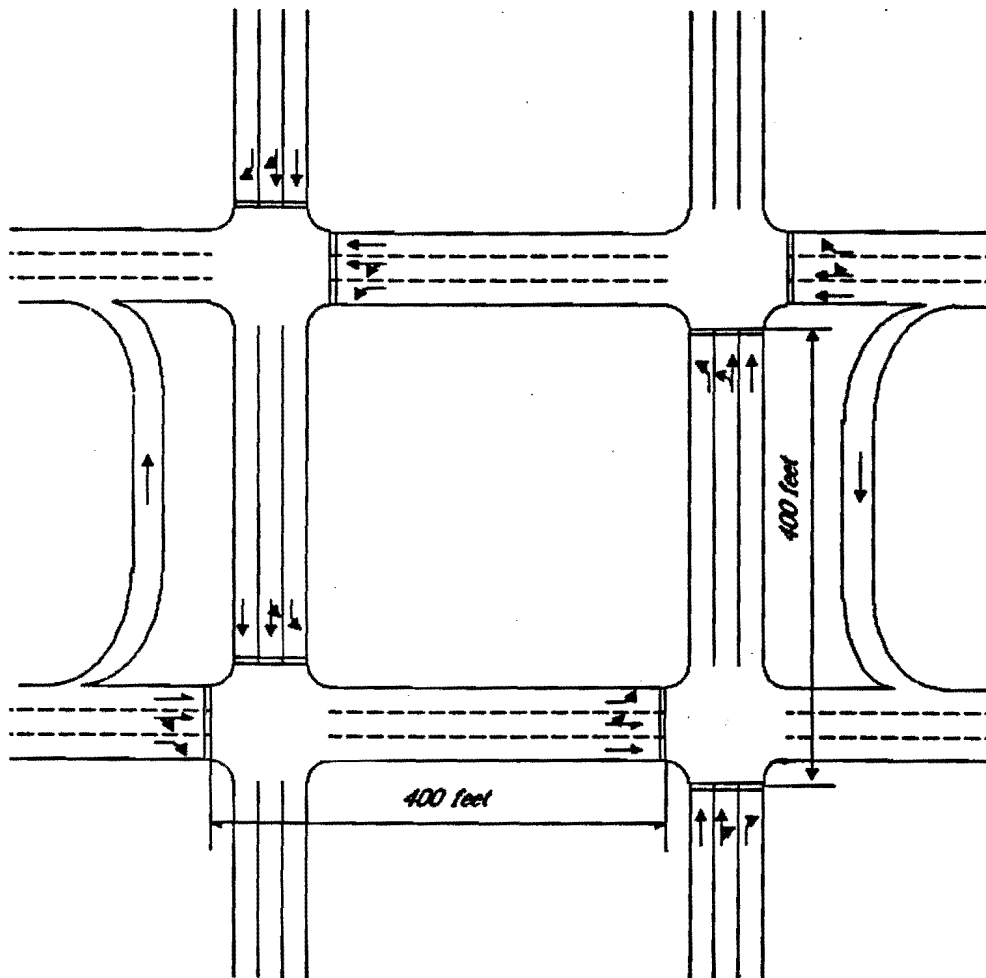
Figure 5-7. Three-Level Diamond Interchange

a three-level diamond interchange, adopted from the interchange of US 290 and IH 35 in Austin, Texas. Figure 5-8 also presents a link-node diagram of the three-level diamond interchange including four external links and four internal links.
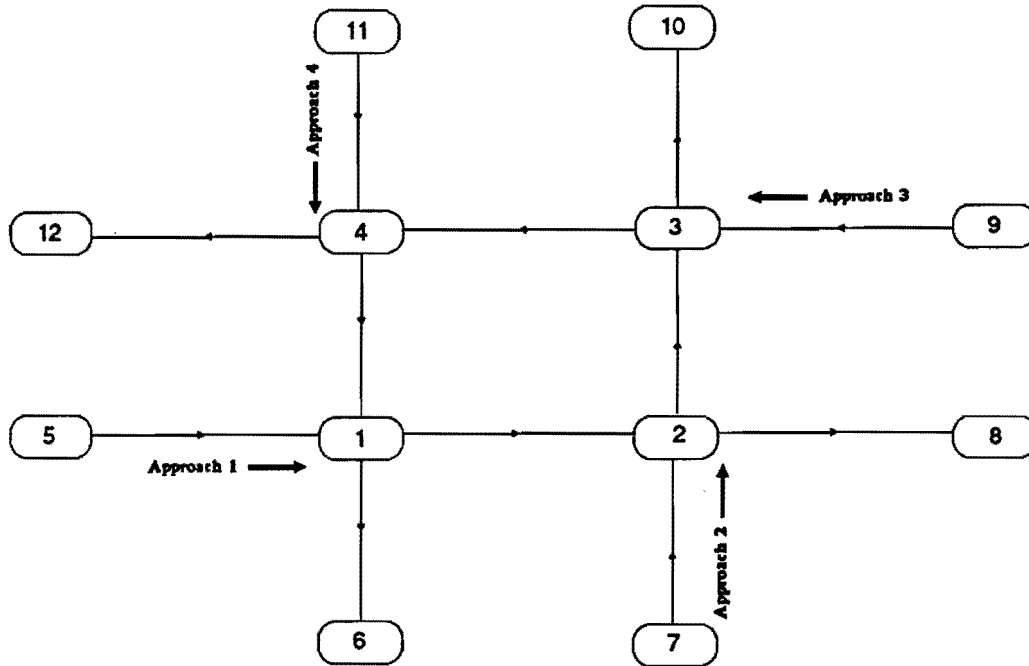


Figure 5-8. Link-Node Diagram of TDI in TRAF-NETSIM

While the three-level diamond interchange looks like a small grid network consisting of two pairs of one-way streets, traffic characteristics of this three-level diamond interchange are totally different from that of the grid network. In the three-level diamond interchange, most of the vehicles entering the signalized portion of the interchange make left turns at the next downstream intersection. For instance, the traffic loaded in link 1-2 is approximately the sum of the thru traffic from link 5-1 and link 11-4. That is, an internal link of the three-level diamond interchange should accommodate almost twice as much traffic as the urban grid network, assuming there are identical demands on the external links. Consequently, special care should be taken in designing the signal control strategy for the three-level diamond interchange.

## 5.3.1 Control Strategy

A limited number of studies have been done in the area of signal timing at three-level diamond interchanges (36). A 4-phase, 4-overlap strategy shown in Figure 5-9 is efficient and popular in the signal control of the three-level diamond interchange (37).
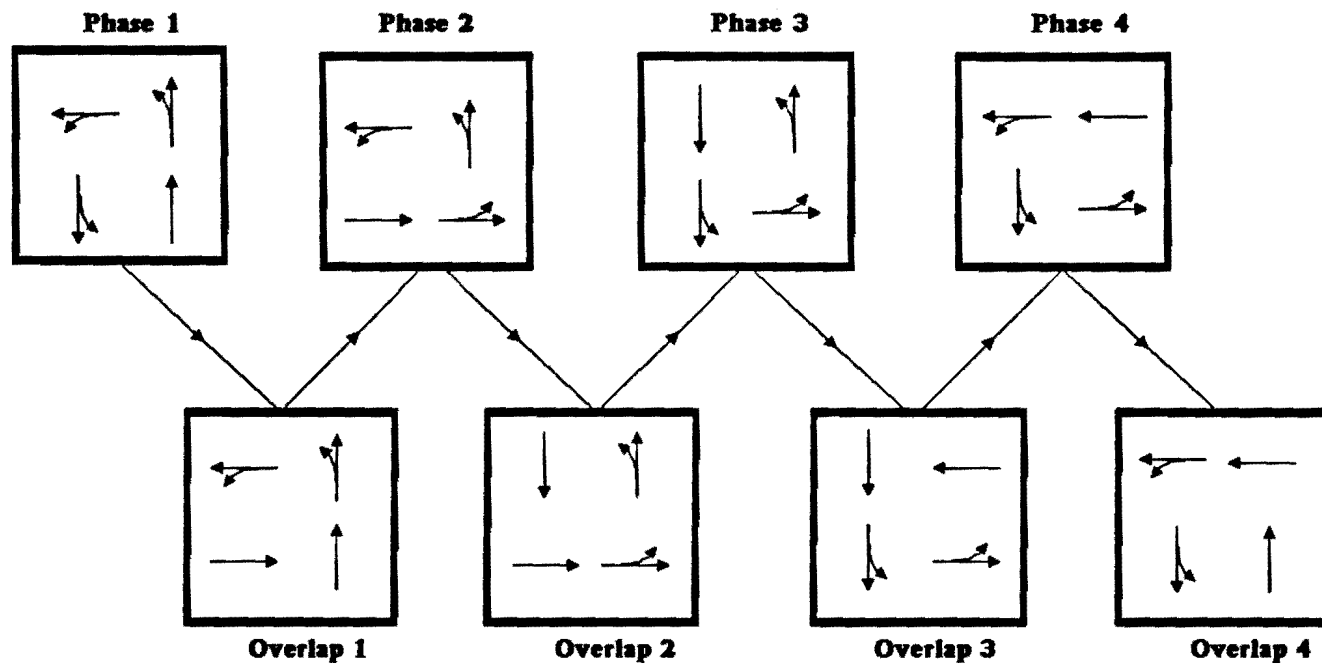
Figure 5-9. Four-Phase with Four Overlaps at TLDI

A major feature of this strategy is that it generally does not produce any queues on the internal links. Once vehicles enter the internal links, they can make left turns without stopping until they leave the interchange. When traffic demand is very high, however, the strategy tends to give needlessly large portions of green time to the internal phases. In other words, it provides an unbalanced Level of Service (LOS) between the internal and external links, usually good for the internal links and poor for the external links causing queue spillback.

To increase system productivity, there was a need to improve the LOS on the external links at the expense of decreasing LOS on the internal links. In this strategy, care should also be taken to prevent queue spillback in the internal links. If the green split is designed without any consideration of queue spillback, then upstream intersections are blocked by excessive queue lengths, resulting in the deterioration of system productivity.

Another disadvantage associated with the 4-phase 4-overlap strategy is the problem of signal-plan transition. The dynamic model was designed so that the signal plan changed for every 15-minute time slice. With this strategy, the starting time of the green indication at the four intersections are interrelated, thus frequent change of the signal plans causes a loss of green time on some approaches and a loss of coordination in the network. It is undesirable to utilize the same strategy in the dynamic model. The phasing scheme applied in the dynamic model should be offset-free. That is, the phasing scheme should be such that frequent changes of timing plans do not deteriorate system performance.

Based on these considerations, this study proposed a two-phase clearance strategy, as shown in Figure 5-10. During Phase 1, traffic on external approaches at Intersections 1 and 3 move together. During Clearance 1, the controller provides more green for a critical external approach out of the two, and changes phase indications for the internal movement of the other intersections. Phase 2 and Clearance 2 operate in a similar manner for Intersections 2 and 4. Generally the two-phase clearance strategy gives more green indication time for the external phases than does the 4-phase, 4-overlap strategy. In addition, the clearance phases of the two-phase scheme plays a role in preventing internal queue spillback.

The dynamic model was proposed for conventional diamond interchanges with multi-phase controllers in Section 5.2.2. The three-level diamond interchange has four intersections, and each intersection is a junction of two one-way streets. The controller at the individual intersection has two phases since there are only two conflicting movements. A large portion of the dynamic model for the conventional diamond interchange needed to be modified to model the three-level diamond interchange.

## 5.3.2 Formulation

|  Phase 1 | Clearance 1 | Phase 2 | Clearance 2 |
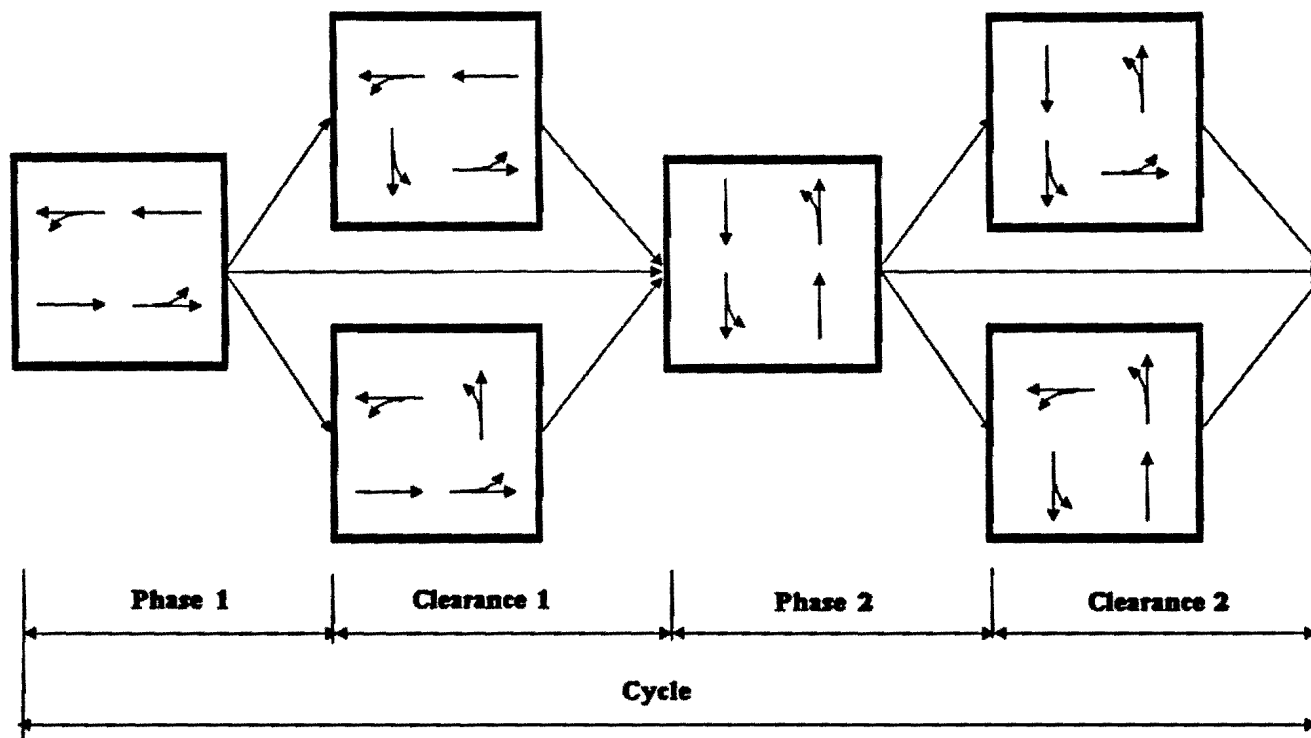
Cycle

Figure 5-10. Two-Phase with Two Clearances at TLDI

The numbering scheme shown in Figure 5-8 was used in this formulation and the notation is as follows:

$i$ = intersection, $i = 1,2,3,4$,

$j$ = time slice of duration $\Delta T$, 15 min, $j = 1,2,...,12$,

$C$ = signal cycle length, sec,

$l$ = lost time per phase, sec,

$g_{ij}$ = effective green time for external phase of intersection i at time slice j,

$r_{ij}$ = effective green time for internal phase of intersection i at time slice j,

$V_{ij}$ = average arrival volume on approach i at time slice j, vps,

$S_{E\,i}$ = saturation flow of external approach at intersection i, vpsg,

$S_{N\,i}$ = saturation flow of internal approach at intersection i, vpsg,

$P_{ikj}$ = proportion of traffic entering intersection i and exiting intersection k at time slice j,

$L_{ij}$ = queue length of external approach i at the end of time slice j, veh,

$N_i$ = queue storage capacity of external approach of intersection i, veh,

$TD$ = total delay on all external approaches, veh-min,

$Z_{ij}$ = 0 when approach i is undersaturated, and
1 when approach i is oversaturated.

## Objective Function

The sum of the queue lengths over all the time slices and approaches is equivalent to total external delay, TD. Therefore, the objective function to minimize total delay is:

$$\text{Minimize} \quad TD = \sum_i \sum_j L_{ij}\, \Delta T \qquad (25)$$

## Constraints

*Set 1.* The sum of green times for two-phase signals at the individual intersections must be equal to the system cycle length, C. For two-phase signals:

$$g_{ij} + r_{ij} = 1 - 2l/C \qquad \text{for all i, j} \quad (26)$$

*Set 2.* In the two-phase clearance strategy, the sum of green times for the critical external phases at the three-level diamond interchange must be equal to the system cycle length, C, as shown in Figure 5-10:

$$\text{Max}\{g_{1j}, g_{3j}\} + \text{Max}\{g_{2j}, g_{4j}\} = 1 - 2l/C \qquad \text{for all j} \quad (27)$$

The above equation can be converted into a series of linear equations using integer variables.

*Set 3.* For the internal links, the input must be less than or equal to the output in order to stabilize the queue lengths:

$$S_{E\,3}P_{3\,1\,j}g_{3j} + S_{E\,4}P_{4\,2\,j}g_{4j} \leq \alpha S_{N\,1}r_{1j} \qquad \text{for all } j \qquad (28a)$$

$$S_{E\,4}P_{4\,2\,j}g_{4j} + S_{E\,1}P_{1\,3\,j}g_{1j} \leq \alpha S_{N\,2}r_{2j} \qquad \text{for all } j \qquad (28b)$$

$$S_{E\,1}P_{1\,3\,j}g_{1j} + S_{E\,2}P_{2\,4\,j}g_{2j} \leq \alpha S_{N\,3}r_{3j} \qquad \text{for all } j \qquad (28c)$$

$$S_{E\,2}P_{2\,4\,j}g_{2j} + S_{E\,3}P_{3\,1\,j}g_{3j} \leq \alpha S_{N\,4}r_{4j} \qquad \text{for all } j \qquad (28c)$$

where $\alpha$ is a factor for saturation flow reduction, usually less than 1. The factor a would need to be carefully determined for each of the four intersections at a three-level diamond.

Due to complex lane configurations usually found on internal links and the stochastic nature of lane utilization, vehicles sometimes cannot fully utilize the available lanes. In this case, actual discharge headways at internal approaches would be less than the input value. In other words, the actual number of vehicles discharged during an internal phase would be less than the number predicted by the basic capacity model. Subsequently, the input-output balance would not be attained, and unexpected oversaturation would occur on the internal links. It is necessary to reduce the saturation flows at the internal approaches using the adjustment factor $\alpha$. Smaller values of $\alpha$ result in larger green times for internal phases and reduce the queue-spillback probability. Values that are too small will result in an unnecessarily long green time for the internal phases.

*Set 4.* The queue lengths at the end of each time slice must be non-negative:

$$L_{ij} = \text{Max} \{ 0, L_{i\,j-1} + (V_{ij} - S_{E\,i}g_{ij})\Delta T \} \qquad \text{for all } i, j \qquad (29)$$

*Set 5.* The queue lengths at the end of each time slice must be less than or equal to the available queue storage capacity:

$$L_{ij} \leq N_i \qquad \text{for all } i, j \qquad (30)$$

*Set 6.* The green time must be greater than the selected minimum green time:

$$g_{ij} \geq g_{i\,min} \qquad \text{for all } i, j \qquad (31)$$

Constraint Sets 1 through 3 replace Constraint Sets 1 and 2 of the original formulas in order to model the unique features of the three-level diamond interchange. The objective function and Constraint Sets 4 through 6 are identical to the original formulation.

## 5.4 DISCUSSION

The dynamic model was designed to produce optimal signal timing plans for oversaturated traffic conditions. The model evaluates the operations for all expected traffic demands on all movements over all time slices of the control period and provides a complete optimal timing plan for all time slices in one formal solution output. As presently formulated, however, this model may generate an undesirable solution for undersaturated conditions. Even if the rush hour is selected as the control period, traffic conditions may be undersaturated during some time slices. The dynamic model solution for these time slices may not be desirable because it sometimes assigns only minimum green time to an approach and excessive green times to the other approaches. The signal timing may result in unbalanced levels of service between the approaches. One can find the undersaturated time slices by analyzing the optimal solution of the dynamic model which is solved using LINDO and then proceeding as follows.

The integer variable $Z_{ij}$ indicates the traffic condition on the associated approaches. If $Z_{ij}$ is equal to zero for all approaches i at time slice j, then the time slice j is an undersaturated time slice. It is desirable to adjust the solution of the LINDO output for the undersaturated time slices. The dynamic model solution for these time slices should be replaced by a green split based on flow ratio. This green split can be calculated using the static model.

When heavy traffic demand lasts for a long period of time and queue storage capacity is limited, the dynamic model has an advantage over conventional static models due to its queue-control capability. Users may want to constrain the queues of all competing approaches to predetermined upper limits. The dynamic model, however, may not always produce a feasible solution if the queues on all external approaches are bounded such that the maximum total queue buildup exceeds the total queue storage capacity.

If heavy demand lasts for a long time period, the dynamic model attempts to assign green times to competing approaches and critical time slices to reduce queue lengths. When available green times are exhausted, all queue storage capacities are full of stopped vehicles, but demand for service still remains. The dynamic model cannot provide a feasible solution for this situation, due to its physical queue constraints. In this case, users must increase the queue constraint limits until the model produces a feasible solution. The dynamic model always produces a feasible solution if the queue length of at least one approach is unbounded.

59

# 6. EVALUATION OF DYNAMIC MODEL

The dynamic optimization models were proposed for traffic control of two signalized interchange types in the previous chapter: Tight Urban Diamond Interchange (TUDI) and Three-level Diamond Interchange (TLDI). Optimal control strategies were generated using the dynamic models for the two interchange types. The performances of these strategies were evaluated by comparing them with current signal timing models.

## 6.1 STUDY APPROACH

### 6.1.1 Experimental Design

The dynamic models were evaluated by comparing the performances of signal control strategies generated by the models to those of conventional models. Control strategies were generated twice for each interchange type; once using the conventional models and once using the newly developed dynamic models. Three different test cases were generated for each type of roadway system. Case 1 was designed as a base case. It was prepared so that its demand level was slightly over the capacity calculated by the conventional models. Cases 2 and 3 were designed by increasing the demand level and providing different time-varying demand profiles and/or origin-destination traffic patterns. Each interchange has slightly different test cases due to the different traffic and geometric characteristics of each system. The test cases for the individual roadway systems are described in detail in the following sections. Three-hour control periods divided into fifteen-minute time-slices were selected in designing the signal timing plans. The TRAF-NETSIM simulation of each control strategy was replicated five times using different random seed numbers.

PASSER III (2) was selected as the conventional model for conventional diamond interchanges. PASSER III is a deterministic optimization model designed exclusively for the signal timing of conventional diamond interchanges. A Webster's green split method using four-phase with four overlaps (37) was selected as the conventional model for the three-level diamond interchange.

The computer used in this research was a IBM PC/AT-compatible having a math coprocessor 80287. The computer time required to solve the MILP problems using LINDO ranged from 30 minutes to two hours. The three-level diamond problem took the longest time to solve. The MILP formulation for the three-level diamond interchange problem consists of 492 constraints, 144 general variables, and 72 integer variables.

TRAF-NETSIM required a great deal of time to simulate the oversaturated networks. It took approximately six hours to simulate each case. The simulation period was three hours, covering the entire control period of twelve 15-minute time slices. Usually, the computing time of TRAF-NETSIM is related to the number of vehicles in the roadway

60

system. Simulation time increases as the number of vehicles in the system increases. As oversaturated networks contain a large number of vehicles, simulation times were quite long. Computer running time of approximately 360 hours was spent on the 60 simulation runs in this study. The 60 simulation runs were the product of two roadway types, three test cases, two models, and five replications. Appendix A presents examples of the GTRAF graphic displays for all three types of highway interchange facilities.

## 6.1.2 Measures of Effectiveness

TRAF-NETSIM provides various measures of effectiveness (MOE's). Among them the following measures were used for evaluation purposes:

1.  Total travel (vehicle-miles) - the total distance traveled by all the vehicles released within the roadway system during the pre-determined control period,

2.  Vehicles discharged (vehicles) - the number of vehicles exiting the roadway system during the control period,

3.  Queue length (feet) - the distance occupied by stopped vehicles,

4.  Average delay (seconds/vehicle) - the time lost per vehicle while traffic is impeded by traffic control devices, and

5.  Stops per trip - the average number of stops experienced by vehicles released into the system.

Maximizing system productivity was a major control objective of the models proposed in this research. Total travel and vehicle discharge were the MOE's representing system productivity; thus, they were selected as major MOE's. The dynamic model's queue management capability was evaluated by examining queue lengths on external approaches. Average delay and stops, widely accepted MOE's, were also used to evaluate the performance of specific links.

## 6.1.3 Test Method

Statistical analyses were performed to test the superiority of the proposed model. A number of tests are available to test two samples. Nonparametric tests are appropriate when sample sizes are small and the normality assumption is not valid. In this research, five replications were conducted in simulating each signal control strategy. The same random seed numbers were used for the paired simulation trial of the conventional model with the dynamic model.

Hays (*38*) stated that the Mann-Whitney and Wilcoxon tests are generally regarded as the best of the order tests for two samples of all nonparametric tests. The Mann-Whitney test for two independent samples was not suitable since the samples in this research were paired. Consequently, the Wilcoxon rank-sum test for paired observations was selected for testing the simulation results.

The null hypothesis of the statistical tests was that the dynamic model did not improve system performance as compared to the selected conventional models typically used by traffic engineers. The research hypothesis was that the dynamic model improved the system performance. Improved system performance resulted in increased total travel and vehicle discharge, but reduced delay, stops, and queue backup.

## 6.2    RESULTS

### 6.2.1    Conventional Diamond Interchange

The performance of the dynamic model modified for conventional diamond interchanges was evaluated by comparing it with results generated by PASSER III. Three cases were prepared for the evaluation as follows:

Case 1. v/c = 1.07, Simultaneous peak time, Heavy cross-street left-turn,
Case 2. v/c = 1.13, Alternate peak time, Moderate cross-street left-turn, and
Case 3. v/c = 1.13, Random Demand, Moderate cross-street left-turn.

Demand in Case 1 was slightly higher than interchange capacity. Peak hour volume (PHV) was raised for Cases 2 and 3. Simultaneous peak time in Case 1 means that the peak demands on the four external approaches occurred at almost the same time. Alternate peak time of Case 2 means that peak demands on the external approaches did not occur simultaneously. The PHV of Approaches 1 and 2 occurred between Time Slices 1 and 4; PHV of Approaches 3 and 4 occurred between Time Slices 6 and 9. Random Demand in Case 3 means that demand profiles for the approaches were uneven and irregular. When compared with the other test cases, left-turn traffic from the cross street to the frontage road was heavy in Case 1. Approximately 60 percent of total traffic at internal approach of the right intersection turned left. The left-turn traffic for Cases 2 and 3 was reduced to 40 percent. Appendix B includes an example of the MILP formulation of Case 1. Appendix C contains detailed information on the three test cases, including time slice traffic volumes and turning percentages. Appendix D presents the optimal signal timing plan generated by the dynamic model.

Cycle length is an important signal timing variable. Messer (*35*) found that shorter cycle lengths produced larger interchange capacity in unconstrained diamond interchanges when the 4-phase overlap strategy was applied and total overlap was longer than total lost time. In this research an 11-second overlap and a 4-second phase lost time were used for

each direction. Total overlap for both directions is 22 seconds and total lost time for the four external phases is 16 seconds. Because the total overlap is longer than the total lost time, short cycle lengths can increase interchange capacity for the 4-phase overlap strategy according to Messer's finding. A short cycle length, however, can create an oversaturation problem at the internal left-turn phase, as illustrated in Table 6-1.

## TABLE 6-1  SIGNAL TIMING GENERATED BY PASSER III FOR CASE 2

| | | Left-Side Intersection | | | Right-Side Intersection | | |
|---|---|---|---|---|---|---|---|
| | | Phase Duration (second) | | | | | |
| Cycle Length | v/c Ratio | A | B | C | A | B | C |
| 55 sec | 1.09 | 15.6 | 20.6 | 18.8 | 25.6 | 15.2 | 14.2 |
| 90 sec | 1.14 | 22.1 | 30.2 | 37.7 | 38.0 | 21.7 | 30.3 |

Table 6-1 illustrates signal timing plans generated by PASSER III for Case 2 using the 4-phase overlap strategy. PASSER III produced the minimum delay cycle length of 55 seconds for Case 2. PASSER III chooses the minimum delay cycle by examining a range of feasible cycle lengths. In the 55-second cycle length, Phase A of the right-side intersection is much longer than Phase C of the left-side intersection. This signal timing causes oversaturation at the internal left-turn phase (Phase C) of the left-side intersection when Phase A of the right-side intersection is fully utilized. By increasing the cycle length up to 90 seconds, this problem was eliminated, as shown in Table 6-1. The 90-second cycle length was used for Cases 1 and 2 for this reason. In Case 3, a 75-second cycle length could eliminate the oversaturation problem and was used for the PASSER III run. For the dynamic model, a 90-second cycle length was used for all cases.

Table 6-2 summarizes the results of simulation using TRAF-NETSIM. It can be seen that total travel and vehicle discharge with the dynamic model are consistently larger than those obtained using PASSER III. The dynamic model increased delay by two percent in Case 1, while it decreased delay by 13 percent in Case 2, and by 14 percent in Case 3. As expected, this result means the dynamic model is more favorable when peak demands do not occur simultaneously among the approaches.

The dynamic model assigns large green times to an approach in peak traffic when the peak demands for the competing approaches occur alternately. In the next time slice, the large green time is assigned in a timely manner to other approaches experiencing heavy demand. If the peak demands occur at the same time, the dynamic assignment of the green times produces limited effectiveness when compared to the conventional static model. The

63

TABLE 6-2  COMPARISON OF PERFORMANCES BETWEEN PASSER III AND DYNAMIC MODEL USING TRAF-NETSIM

| | Total Travel (veh-mile) | Vehicles Discharged | Delay (min/veh) | Stops per Trip | Queue Backup(sec) |
|---|---|---|---|---|---|
| Case 1. V/C = 1.07, Simultaneous Peak Time, Heavy Cross-Street Left-Turn | | | | | |
| PASSER III | 8,542 | 16,483 | 2.73 | 1.5 | 0 |
| DYNAMIC MODEL | 8,560 | 16,521 | 2.79 | 1.5 | 0 |
| % DIFFERENCE | + 0.2 | + 0.2 | + 2 | 0 | |
| Improve ?[1] | yes | yes | no | no | |
| Case 2. V/C = 1.13, Alternate Peak Time, Moderate Cross-Street Left-Turn | | | | | |
| PASSER III | 9,008 | 17,559 | 3.51 | 1.5 | 0 |
| DYNAMIC MODEL | 9,171 | 17,791 | 3.04 | 1.5 | 0 |
| % DIFFERENCE | + 1.8 | + 1.3 | - 13 | 0 | |
| Improve ? | yes | yes | yes | no | |
| Case 3. V/C = 1.13, Random Demand, Moderate Cross-Street Left-Turn | | | | | |
| PASSER III | 8,814 | 17,391 | 2.08 | 1.3 | 0 |
| DYNAMIC MODEL | 8,876 | 17,521 | 1.78 | 1.3 | 0 |
| % DIFFERENCE | + 0.7 | + 0.7 | - 14 | 0 | |
| Improve ? | yes | yes | yes | no | |

1) Results of Wilcoxon rank-sum test
    Research Hypothesis:  Dynamic Model improved system performance.
    Significance Level = 0.05
    Sample Size = 5

dynamic model attempts to minimize total delay and to constrain maximum queue lengths. A model simply minimizing total delay without controlling queues would produce less delay than a model minimizing total delay as well as constraining queue lengths. The dynamic model can control queue lengths, but cannot reduce total delay for the case of simultaneous peak traffic demands.

Figure 6-1 shows the cumulative average delay for the total interchange, as estimated by TRAF-NETSIM. In Case 1, delay obtained using the dynamic model increases faster than that obtained using PASSER III. In Case 2, delay produced using the dynamic model is consistently smaller than that produced using PASSER III during the entire control period. No differences were observed in the number of stops. No queue spillback was estimated for either model since its elimination is a major advantage of the 4-phase overlap strategy.

Figure 6-2 shows queues on the external approaches as estimated from the Input-Output model in Case 1. In this figure, the queue length data points for the dynamic model were derived from the solution of the dynamic model. The dynamic model estimates queue lengths using the Input-Output model. Input is the time-slice demand and output is the number of vehicles discharged at the stop line. The difference between input and output is the queue length estimated by the dynamic model. The queue lengths for PASSER III were also estimated using the Input-Output model because PASSER III cannot estimate timing based on varying queue lengths on the external approaches.

From Figure 6-2, the PASSER III timing plan produced very long queues on Approach 3, exceeding the queue storage capacity. The dynamic model reduced this queue to the storage capacity and thereby produced slightly longer queues on the other approaches than those produced using PASSER III. Even if some portion of the queues on the critical approaches transfer to noncritical approaches, the overall queues were reduced by using the dynamic model due to its responsive green split capability.

Queues estimated by TRAF-NETSIM in Case 1 are shown in Figure 6-3. Queue profiles by TRAF-NETSIM have trends similar to that of the Input-Output model, but they are not the same. In Approach 3, PASSER III queues do not exceed 60 vehicles while the PASSER III queues reach 90 vehicles from the Input-Output model. The reason for this difference is that 1,200 feet was coded as the external link length for TRAF-NETSIM. TRAF-NETSIM produced an error message of out-of-memory for any link longer than this length. If too many vehicles stay in a link, the memory space for the vehicles in the source code of TRAF-NETSIM appears to be exhausted, resulting in an out-of-memory error. Queue profiles for the other cases are found in Appendix E.

Figure 6-4 shows comparisons of queue estimations between the Input-Output model and TRAF-NETSIM. Regression analysis was conducted to estimate the best fit line. The slopes of the regression lines are less than 1. This result means that Input-Output Analysis underestimates queue lengths compared to TRAF-NETSIM. The reason for this difference
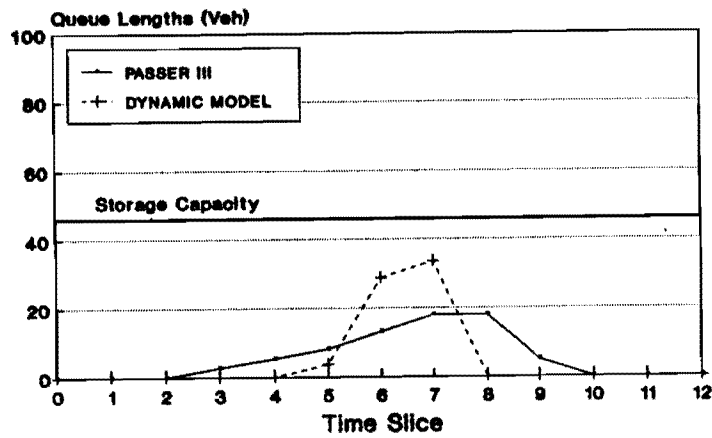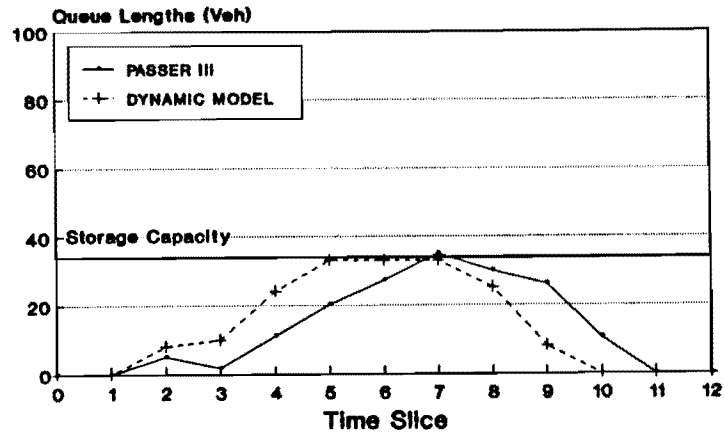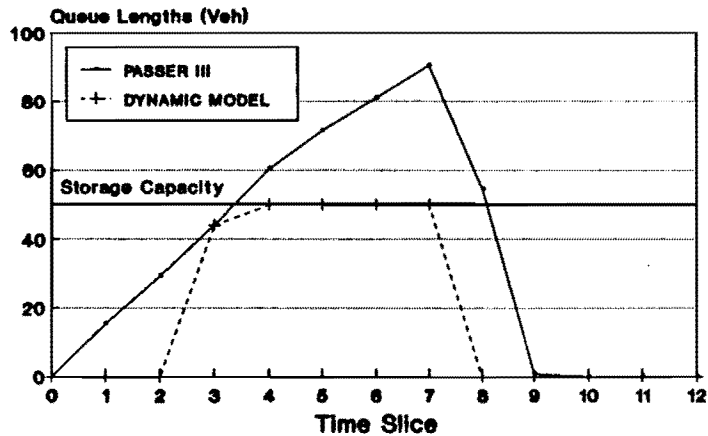
65
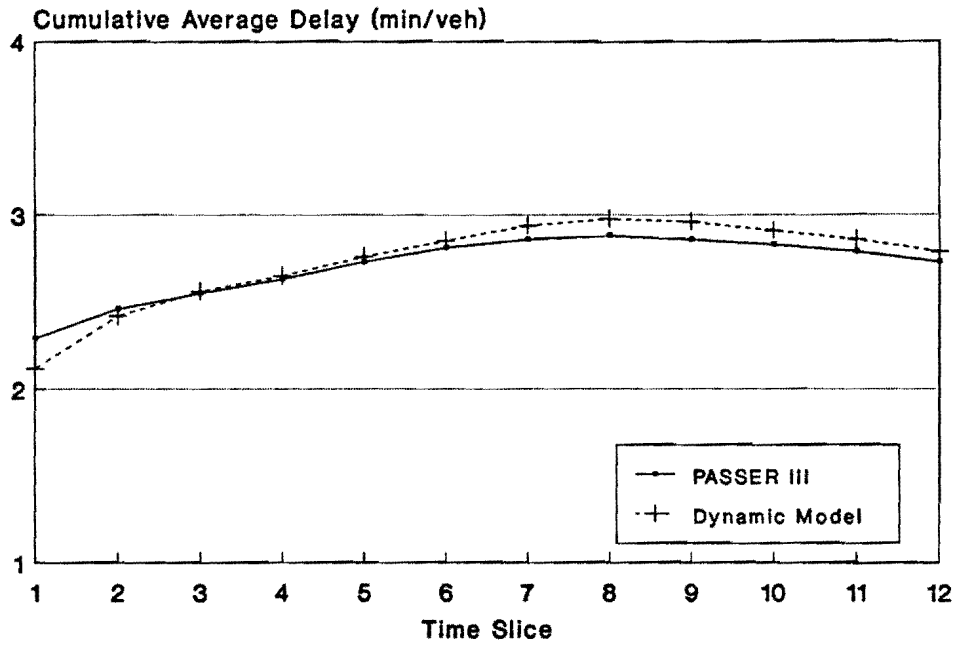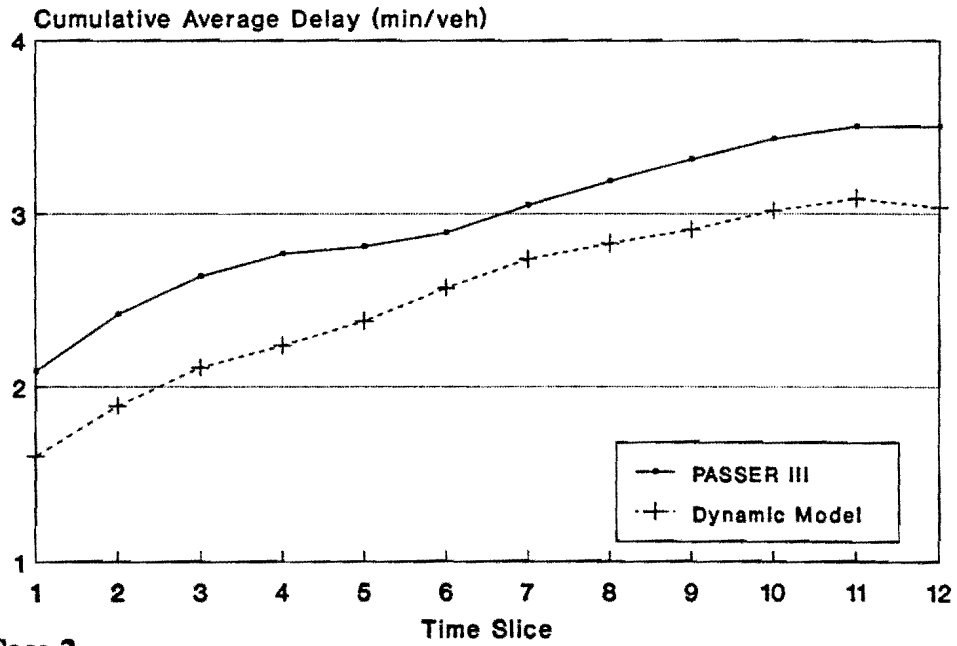
(a) Case 1



(b) Case 2

Figure 6-1. Cumulative Delay at TUDI (Cases 1 and 2)

66

(a) Approach 1

(b) Approach 2
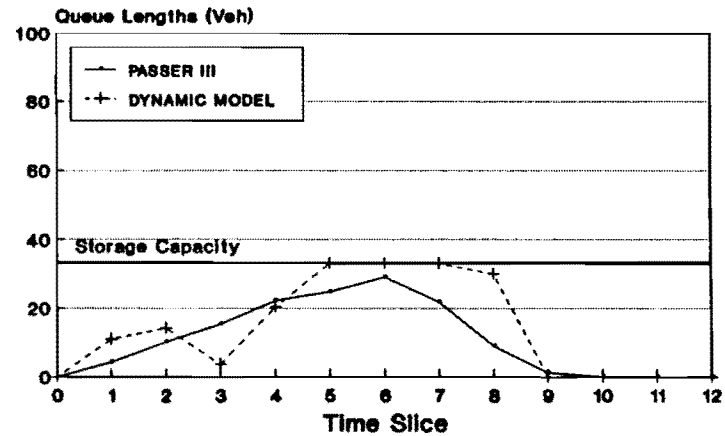
(c) Approach 3

(d) Approach 4

Figure 6-2.  Queues by Input-Output Analysis at TUDI (Case 1)

**Queue Lengths (Veh)**

- PASSER III
- DYNAMIC MODEL

Time Slice

(a) Approach 1

**Queue Lengths (Veh)**

- PASSER III
- DYNAMIC MODEL

Time Slice

(b) Approach 2

**Queue Lengths (Veh)**

PASSER III  DYNAMIC MODEL

Time Slice

(c) Approach 3

**Queue Lengths (Veh)**

PASSER III  DYNAMIC MODEL

Time Slice
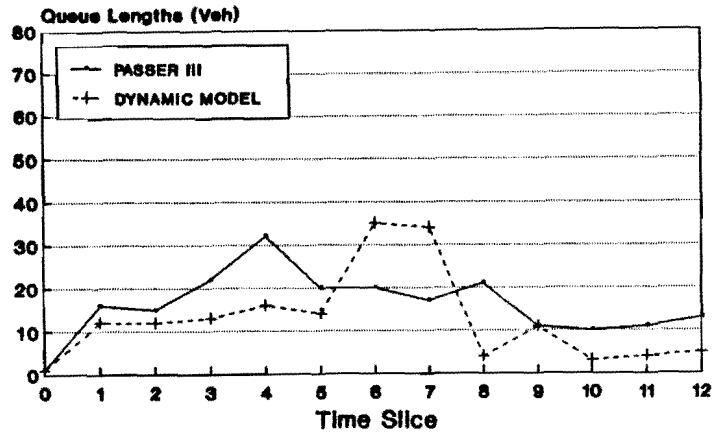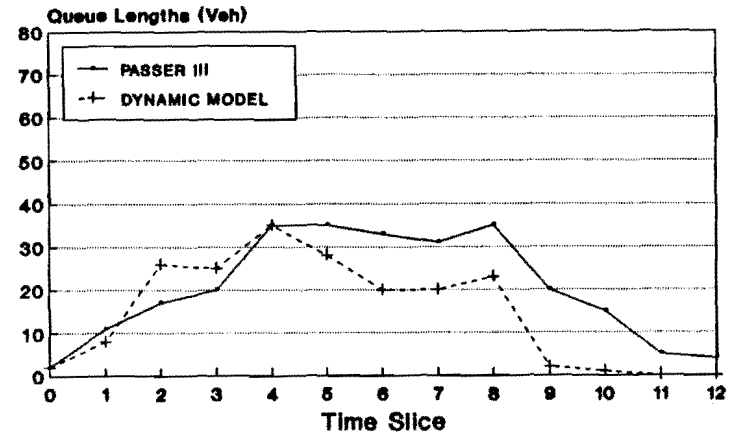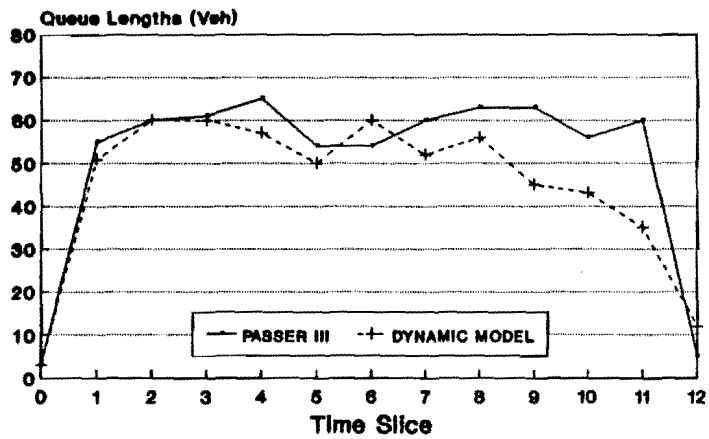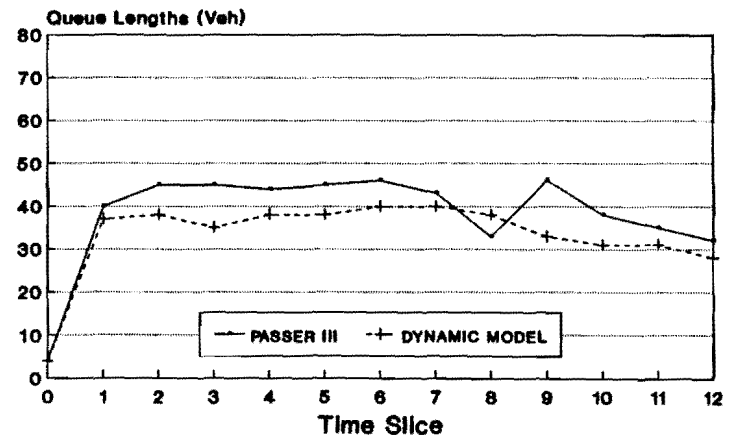
(d) Approach 4

Figure 6-3. Queues by TRAF-NETSIM at TUDI (Case 1)

Queues by Input-Output Analysis

100
80
60
40
20
0

45 Degree Line

1
1

0.60
1

Regression Line

2

R$^2$ = .82

0    20    40    60    80    100

Queues by TRAF-NETSIM

(a) PASSER III

Queues by Input-Output Analysis

100
80
60
40
20
0

45 Degree Line

1
1

0.67
1

Regression Line

R$^2$ = .87

0    20    40    60    80    100
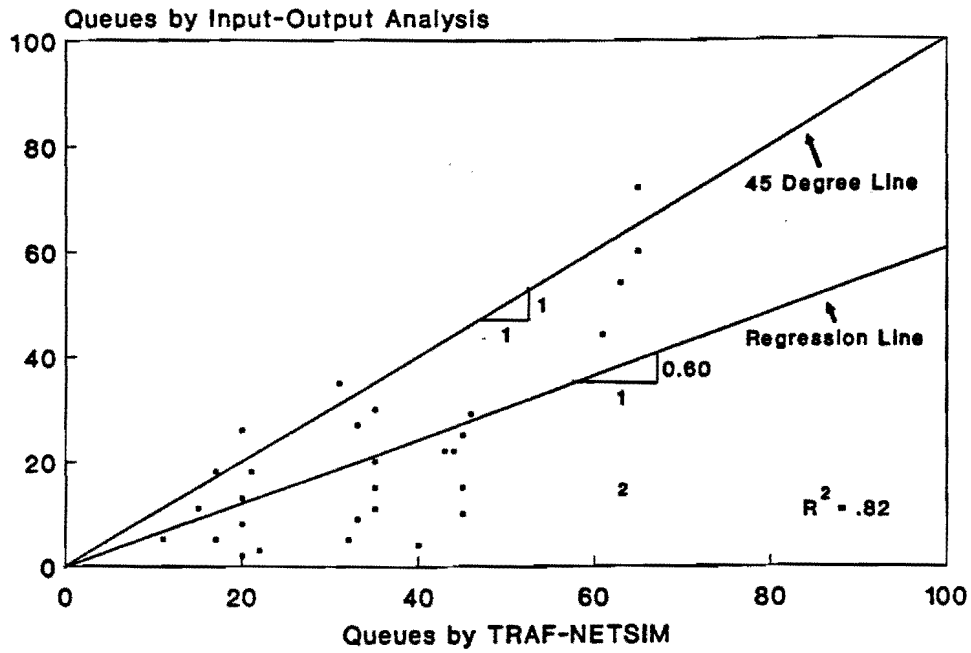
Queues by TRAF-NETSIM
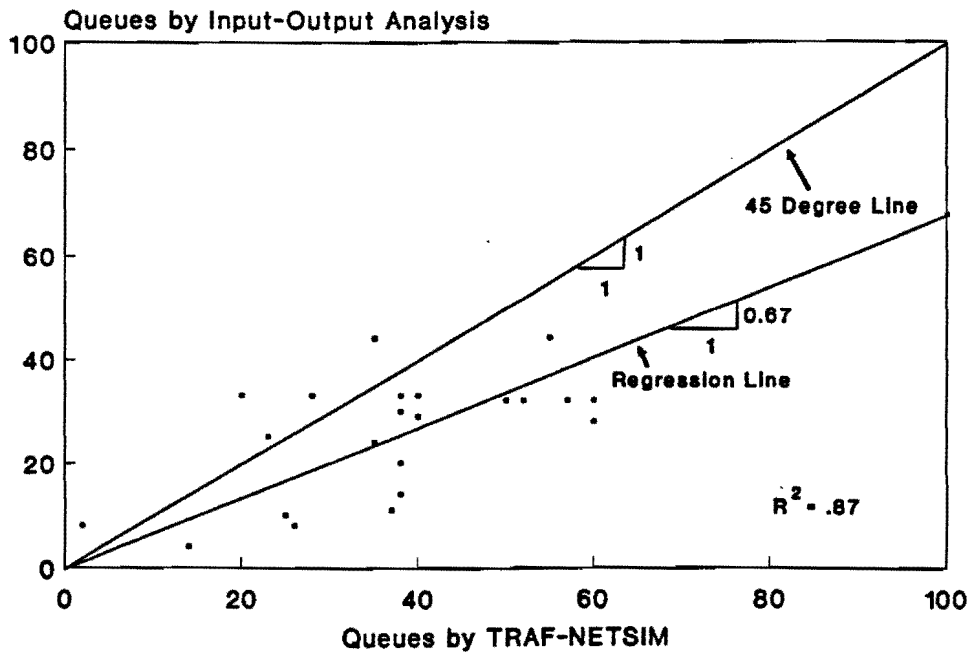
(b) Dynamic Model

Figure 6-4. Comparisons of Queue Estimation by Input-Output Analysis versus TRAF-NETSIM

**Queue Length on Approach 3 (vehicles)**

Max Queue < 93
Max Queue < 50

Time Slice

(a) Queue Profile on Approach 3



**Green Time for Approach 3 (seconds)**

Max Queue < 93
Max Queue < 50

Time Slice
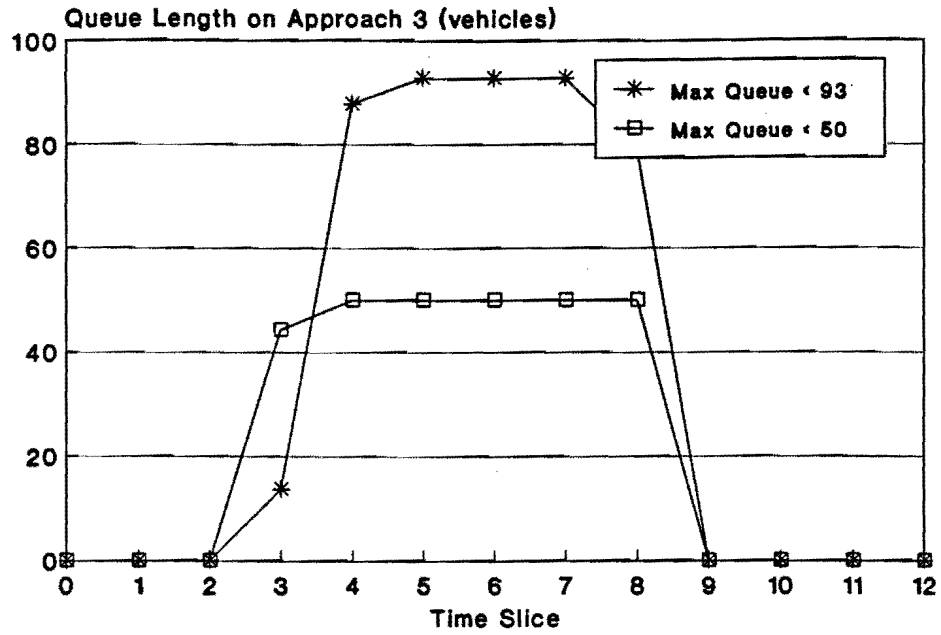
(b) Green Time for Approach 3

Figure 6-5.  Relationship between Queue Constraint and Green Time

is that the Input-Output model estimates queues based on uniform traffic demand only, and does not consider the effect random demand has on queue length estimation. The $\beta$ factor in Equation 22 should be adjusted based on this result. From the regression analysis, a value of .65 appears to be reasonable for the $\beta$ factor.

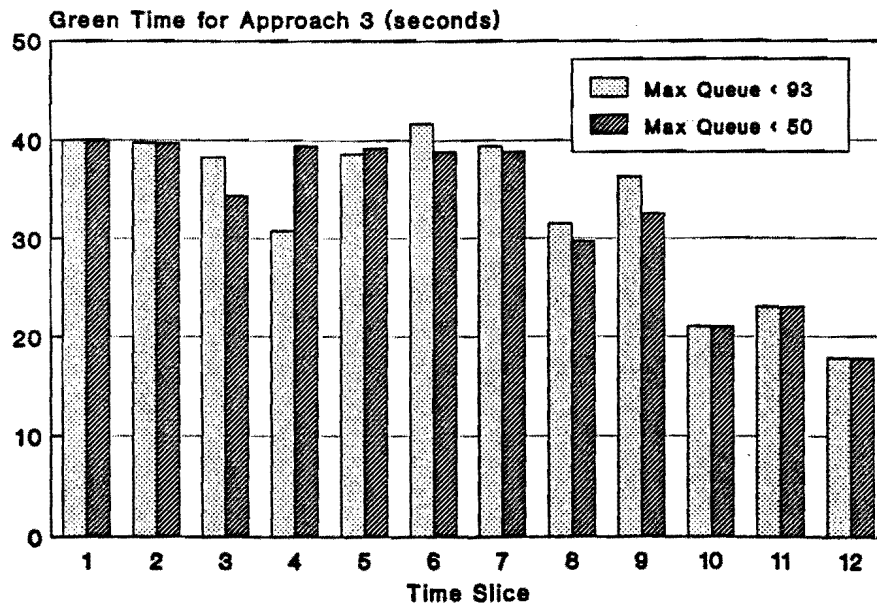Figure 6-5 illustrates how signal timing responds to queue length constraints. Figure 6-5(a) shows queue profiles on Approach 3 of Case 1. Two different queue constraints were applied: 93 and 50 vehicles. Figure 6-5(b) presents the green times of Approach 3 produced by the dynamic model. In the 50-vehicle queue constraint case, queue on Approach 3 reaches its upper bound at the end of Time Slice 4. To prevent queue spillback, the dynamic model assigns large green time to the 50-vehicle queue constraint case compared to the 93-vehicle case.

## 6.2.2 Three-Level Diamond Interchange

The dynamic model controlling the oversaturated three-level diamond interchange was evaluated by comparing it to the conventional model. The 4-phase 4-overlap strategy was selected as the conventional control strategy, while the dynamic model utilized the two-phase clearance strategy. Three cases were prepared for the evaluation and these cases are not identical to those of the conventional diamond interchange:

Case 1. $v/c = 1.1$, Alternate peak time - Pattern 1,
Case 2. $v/c = 1.1$, Alternate peak time - Pattern 2, and
Case 3. $v/c = 1.3$, Simultaneous peak time.

The volume-to-capacity ratio ($v/c$) was calculated from the application of the 4-phase 4-overlap strategy. The peak hour volumes (PHV) in Cases 1 and 2 were slightly higher than the interchange capacity. The PHV was increased for Case 3. Alternate peak time in Case 1 meant that peak demands on the external approaches did not occur simultaneously. The PHV of Approaches 1 and 2 occurred between Time Slices 2 and 5, and for Approaches 3 and 4 the PHV occurred between Time Slices 5 and 8. In Case 2, Approaches 1 and 3 had the same peak time; Approaches 2 and 4 had the same peak time. Simultaneous peak time in Case 1 meant that the peak demands on the four external approaches occurred almost at the same time.

A short cycle length (45 seconds) was used for the dynamic model in order to reduce queue spillback onto the internal links since long cycle lengths might cause queue spillback problem at internal links in the two-phase two-clearance strategy. A range of cycle lengths was tested using TRAF-NETSIM. The resulting traffic conditions were observed using the GTRAF animation display. A 45-cycle length appeared to be reasonable for the given three-level diamond interchange. The 45-cycle length is not too short because individual signals in the three-level diamond interchange have only two phases.

The saturation adjustment factor $\alpha$ in Equation 19 is critical in the three-level diamond interchange problems because lane configurations of internal approaches are very

71

complicated, resulting in under-utilization of available lanes. Performances of signal timings derived from a range of the α factor was examined using the TRAF-NETSIM results and the GTRAF graphic animation. Starting at one, the α-factor was reduced by increments of 0.1. An α-factor of 0.7 was found appropriate for the test cases.

An 80-second cycle length with 11 seconds of one-way overlap was used for the 4-phase 4-overlap strategy. In this strategy, long cycle lengths do not cause a queue spillback problem from the internal links into the intersections because the 4-phase 4-overlap strategy guarantees perfect progression on the internal links. Detailed traffic information on the three test cases is presented in Appendix C. Appendix D presents the optimal signal timing produced by the dynamic model for all test cases.

Signal timing plans were generated for the three cases using a 4-phase 4-overlap strategy and the modified dynamic model. The timing plans were simulated using TRAF-NETSIM. Results of the simulation are summarized in Table 6-3. The dynamic model increased total travel and vehicle discharge consistently when compared to the 4-phase 4-overlap strategy. That is, the dynamic model increased system productivity. This model decreased delay by 21 percent in Case 1 and 20 percent in Case 2, while increasing delay by three percent in Case 3. This result means the dynamic model performed better in the alternate peak time than did the 4-phase 4-overlap strategy. These results are similar to the conventional diamond interchange. A large number of stops were observed in the application of the dynamic model. The increased number of stops was an expected result because the 2-phase clearance strategy used in the dynamic model forced vehicles to stop in the internal links. The 4-phase 4-overlap strategy did not result in any queue spillback on the internal links, while the dynamic model produced a small amount of spillback in the heavy demand case.

Figure 6-6 shows queue lengths on external approaches estimated by the Input-Output Analysis for Case 1. The dynamic model produced shorter queues than the 4-phase 4-overlap strategy. The reason is that the dynamic model assigns more green time to the external approaches than the 4-phase 4-overlap strategy. Queues estimated by TRAF-NETSIM for Case 1 are shown in Figure 6-7. Queue profiles estimated by the two control strategies showed somewhat similar trends, but the Input-Output queue estimator used in the dynamic model consistently understimated queue lengths on all approaches. This performance was similar to that observed with the conventional diamond interchange.

The Input-Output model used in the dynamic model assumes queue length to be the difference between input rate and output rate. The output rate in the Input-Output model was assumed to be constant, even if this rate were somewhat reduced due to traffic conditions at the downstream links. The fact that the Input-Output model significantly underestimated queue lengths indicates that vehicle discharge from upstream signals was being impeded to some degree by the stopped vehicles on the internal links of the three-level diamond interchange. TRAF-NETSIM can handle this kind of situation in the simulation process. Queue profiles for the other test cases are presented in Appendix E.

TABLE 6-3 COMPARISON OF PERFORMANCES BETWEEN 4-PHASE-OVERLAP AND DYNAMIC MODEL USING TRAF-NETSIM

| | Total Travel (veh-mile) | Vehicles Discharged | Delay (min/veh) | Stops per Trip | Queue Backup(sec) |
|---|---|---|---|---|---|
| Case 1. V/C = 1.1, Alternate Peak Time - Pattern 1 | | | | | |
| 4-Phase-Overlap | 12,589 | 18,782 | 4.14 | 1.4 | 0 |
| DYNAMIC MODEL | 12,635 | 18,904 | 3.29 | 2.2 | 0 |
| % DIFFERENCE | + 0.4 | + 0.6 | - 21 | + 57 | |
| Improve ?[1] | yes | yes | yes | no | |
| Case 2. V/C = 1.1, Alternate Peak Time - Pattern 2 | | | | | |
| 4-Phase-Overlap | 12,547 | 18,767 | 4.03 | 1.4 | 0 |
| DYNAMIC MODEL | 12,734 | 18,981 | 3.22 | 2.1 | 0 |
| % DIFFERENCE | + 1.4 | + 1.1 | - 20 | + 50 | |
| Improve ? | yes | yes | yes | no | |
| Case 3. V/C = 1.3, Simultaneous Peak Time | | | | | |
| 4-Phase-Overlap | 12,547 | 18,767 | 4.44 | 1.4 | 0 |
| DYNAMIC MODEL | 12,743 | 18,981 | 4.57 | 2.2 | 8 |
| % DIFFERENCE | + 1.6 | + 1.1 | + 3 | + 57 | |
| Improve ? | yes | yes | no | no | |

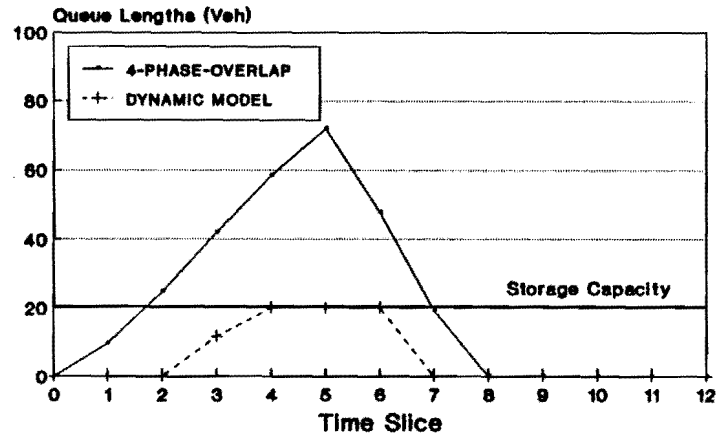1) Results of Wilcoxon rank-sum test
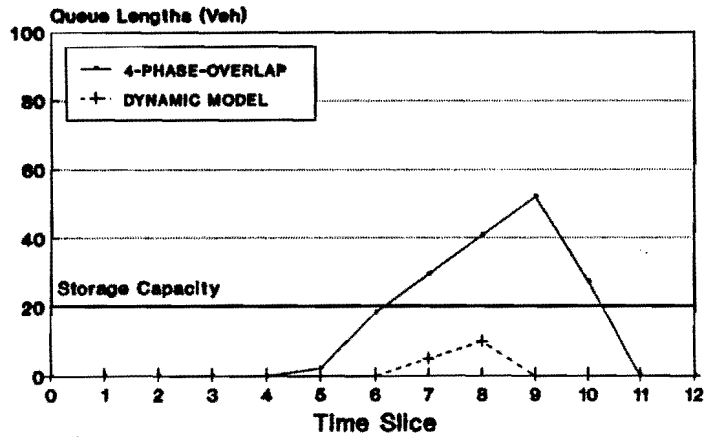   Research Hypothesis: Dynamic Model improved system performance.
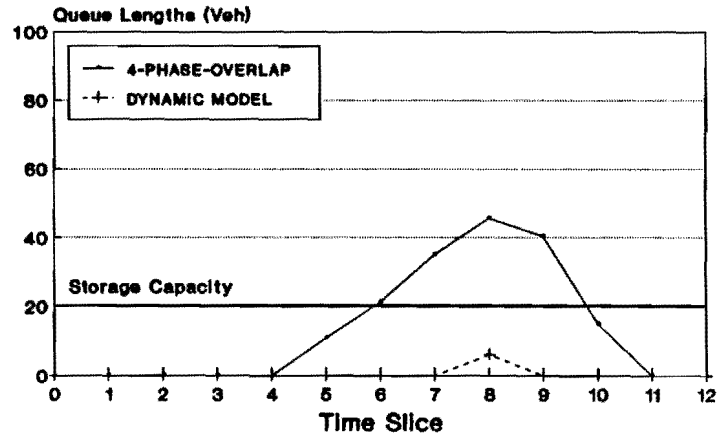   Significance Level = 0.05
   Sample Size = 5
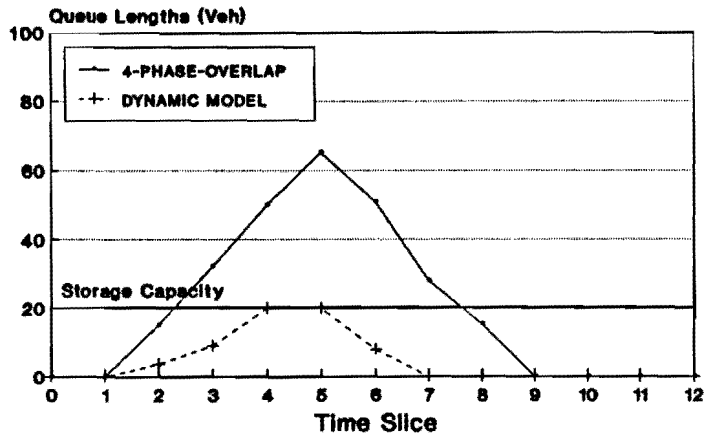
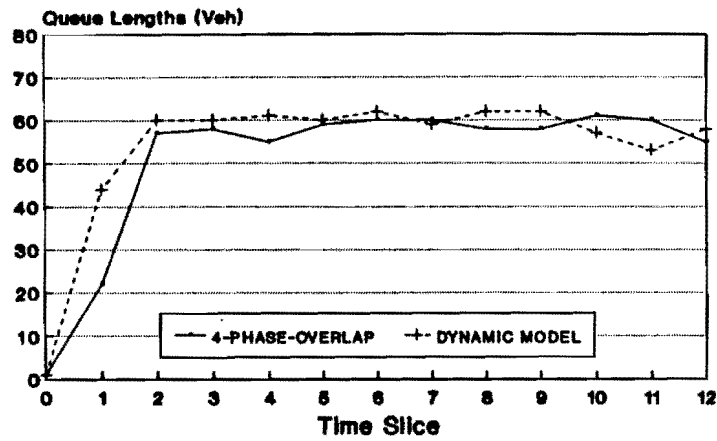(a) Approach 1



(b) Approach 2


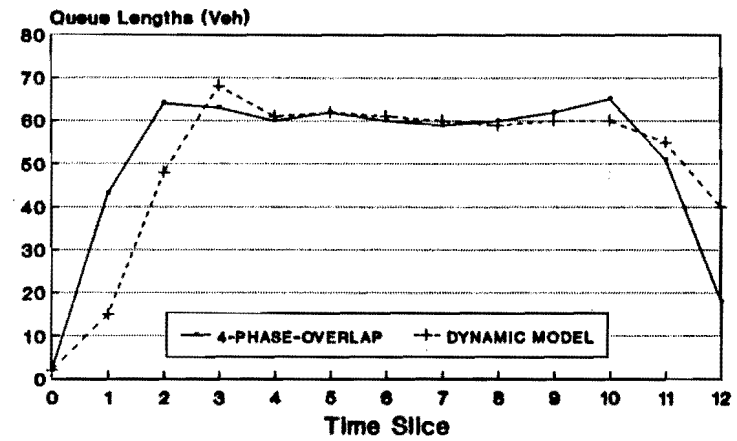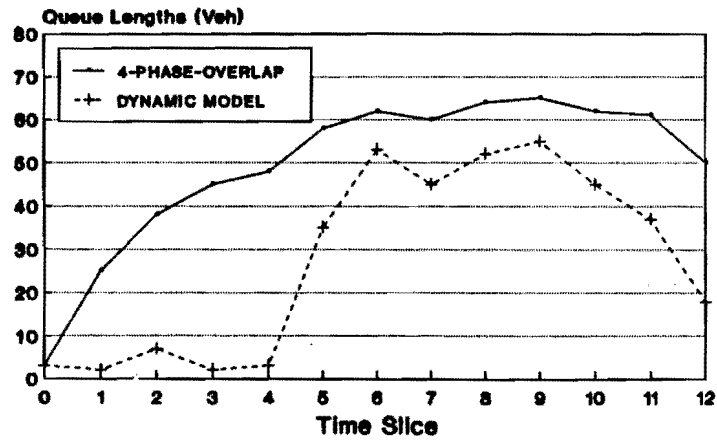
(c) Approach 3



(d) Approach 4

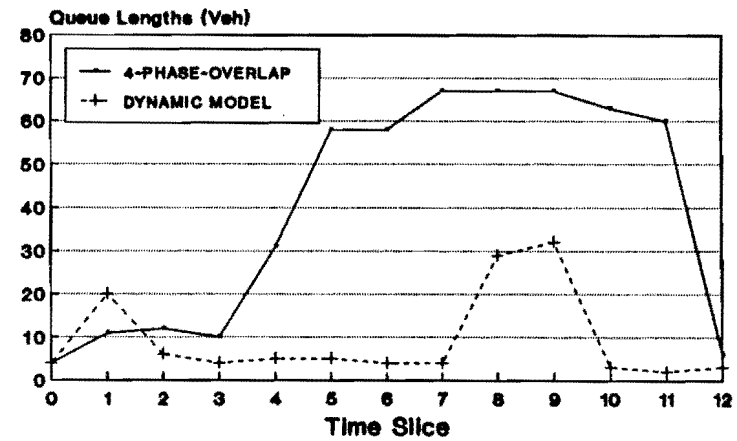Figure 6-6.   Queues by Input-Output Analysis TLDI (Case 1)

(a) Approach 1



(b) Approach 2



(c) Approach 3



(d) Approach 4

Figure 6-7.  Queues by TRAF-NETSIM at TLDI (Case 1)

# 7. IMPLEMENTATION

The dynamic optimization models developed in this study can provide effective traffic signal control for oversaturated signalized intersections. These models were designed for practical use in traffic engineering. The optimal solutions generated by them are applicable to actual signal controllers. To aid in the field application of the models, some additional features should be added and some implementation points noted, as described in the following sections.

## 7.1 PROCEDURE FOR SIGNAL TIMING DESIGN

Because the input-output processor of data for the dynamic model was not developed in this research, the entire data processing procedures presently must be performed manually, except for solving the MILP problem. Step-by-step procedures for signal timing design using the dynamic model are as follows:

Step 1.    Determine control period and time-slice duration,

Step 2.    Prepare input data,

Step 3.    Determine initial queue storage capacity,

Step 4.    Prepare MILP formulation,

Step 5.    Solve MILP problem,

Step 6.    If feasible solution, go to STEP 7; otherwise, adjust the queue storage capacity and go to STEP 4, and

Step 7.    Interpret and implement output.

Step 1 is the determination of the control period and time-slice duration. The dynamic model was designed for oversaturated traffic conditions. The control period should cover the oversaturated period that begins at the onset of queue-formation and ends when these queues dissipate. The time-slice duration should be determined carefully. A 15-minute time slice was used in this study and is recommended for future applications. The 15-minute time slice has been used in freeway on-ramp control (5). If time-slice duration are too short, severe fluctuations of traffic demands and needlessly frequent changes in signal plans may result. On the other hand, if the duration is too long, the result will not be sensitive to time-varying traffic demand.

In Step 2, input data should be prepared for the MILP formulation. The following input data are required for the dynamic model:

1. Time-slice traffic demands ($V_{ij}$), vps,
2. Saturation flow ($S_{ij}$), vps,
3. Time-slice turning percentages ($P_{ikj}$),
4. System cycle length (C), seconds,

76

5. Adjustment factors ($\alpha$, $\beta$), and
6. Queue storage capacity ($N_i$), vehicles.

The dynamic model requires the input data to adequately represent traffic and geometric characteristics, as do conventional static models. Additionally, the dynamic model requires time-slice traffic volumes encompassing the entire control period. The user should take an average of several daily observations for input volumes. Cycle length cannot be optimized in the dynamic model. If the optimization of cycle length were modeled in the dynamic model, it would become a nonlinear optimization problem, which would be very difficult to solve. Consequently, cycle length should be determined using the static model.

The saturation flows on internal links are adjusted using the factor $\alpha$ in Equation 19. This adjustment is necessary when the lane configurations on internal links are so complex that vehicles cannot fully utilize the available lanes. No adjustment factors were needed for the conventional diamond interchange due to its simple lane configuration. In the three-level diamond interchange, the adjustment of the $\alpha$ factor is important. An $\alpha$-factor of 0.7 was used for the three-level diamond interchange problem. This factor was calibrated using TRAF-NETSIM simulation.

Step 3 is the determination of the queue storage capacities ($N_i$) for external approaches using the following equation:

$$\text{Storage Capacity} = \frac{\text{(Link Length, feet)} \times \text{(Number of Lanes)}}{\text{(Vehicle Storage Length, feet)}} \tag{27}$$

In actual input coding, it is desirable to use a queue storage capacity less than the actual capacity calculated from Equation 27 so as to provide a storage buffer to absorb some natural fluctuations in demand. The queue storage adjustment factor, $\beta$, in Equation 22 should be calibrated. The dynamic model tends to underestimate queue lengths because it does not consider the effect of random variation in traffic demand on queue estimation. From the regression analysis shown in Figure 6-4, the value of .65 appears to be reasonable for the $\beta$ factor.

Steps 4 and 5 are to prepare the MILP formulation and then solve the formulation using special software for mathematical programming. Because several software packages are currently available to solve the optimization problem, the software package should be chosen with care, based on its features. MAXBAND (*31*) uses MPCODE (*33*) to solve its MILP problem. LINDO (*34*) was easy to use, compared with MPCODE. This study used LINDO to solve the MILP problem of the dynamic model. Both mainframe and PC versions are currently available. LINDO is proprietary and costs about $1,400 per copy for the PC version. A example of a LINDO formulation is presented in Appendix B.

Step 6 requires feedback. As discussed in Chapter 5, the dynamic model sometimes fails to produce a feasible solution. Infeasibility occurs when the queue storage capacities, determined in Step 3, are unrealistically small for the given traffic demand. Users must adjust the queue constraints on one or more approaches in order to resolve the infeasibility. Then, one should return to Step 4 and modify the constraints in the MILP formulation corresponding to the queue constraints.

When the dynamic model cannot produce a feasible solution due to extremely heavy traffic demand, the following modifications should be considered:

1.    Relax the queue constraints for one or more approaches,
2.    Reduce the traffic demand by metering, or
3.    Increase the interchange capacity.

The first option to resolve infeasibility is to relax the queue constraints for the less critical approaches. For instance, the conventional diamond interchange has four external approaches. Two of them are connected to the freeway mainline, and the others are connected to intersections. Queue spillback to the freeway mainline results in more serious operation and safety problems than would queue spillback into in upstream intersection. The queue constraints for arterial approaches should be relaxed. The adjusted queue constraints are applied to the MILP problem in Step 4.

The dynamic model may produce long queue lengths for those approaches having the relaxed queue constraints; that is, the arterial approaches to the conventional diamond interchange. If this long queue is not desirable, the second method should be considered. Traffic volume of arterial approaches can be reduced by adjusting signal timing of upstream intersections.

In the three-level diamond interchange, all external approaches are connected to the freeway mainline. There is no space to relax queue constraints. Geometric improvements of the interchange should be considered to resolve the infeasibility problem.

The dynamic model can be regarded as a low-cost transportation improvement technique. This model is effective in relieving congestion within a traffic demand range that the queue storage capacity of the roadway system can accommodate. Beyond this range, however, no model is very helpful, and major geometric improvements should be considered to solve the remaining congestion problems.

In this research, the signal timing design procedures were performed manually, which were very time consuming and tedious. It is felt that a general purpose preprocessor program should be developed for the convenient use of coding data into the dynamic model. This program could be a member of the PASSER family, complementing the present family of undersaturated traffic models.

## 7.2 COMPUTER REQUIREMENTS

The dynamic model, as an off-line signal timing tool, would need a computer to solve MILP problems. An IBM PC-compatible computer is required to optimize signal timing using LINDO and to simulate the signal timing using TRAF-NETSIM. A math coprocessor is essential for executing LINDO and TRAF-NETSIM. Because the dynamic model was designed as an off-line signal timing tool, an extensive computer system and detectors are not required.

# 8. CONCLUSIONS AND RECOMMENDATIONS

## 8.1    CONCLUSIONS

Dynamic optimization models were developed for signal control of oversaturated diamond interchanges. The traffic control objective of the model was to provide maximum system productivity as well as minimum system delay for selected roadway systems. The dynamic models were evaluated using the TRAF-NETSIM simulation program.

Conclusions drawn from this research on oversaturated traffic conditions are described as follows:

1.    The dynamic model produces an optimal signal timing plan for traffic control of the signalized interchange during oversaturated traffic conditions.

2.    The dynamic model consistently outperforms conventional models with regard to system productivity. This conclusion was drawn from the TRAF-NETSIM simulation. Total travel and vehicle discharge in the TRAF-NETSIM output indicated increased productivity of the control systems.

3.    The dynamic model reduced total system delay from eight percent to 23 percent, for most test cases, while it increased delay slightly for a few test cases. The dynamic model generally increases the number of stops as compared to the conventional models because it more fully utilizes the forward storage capacity of the signalized network.

4.    Queue management on external approaches is a primary concern in the traffic control of congested conventional diamond interchanges and three-level diamond interchanges. The capability of queue management is a unique feature of the dynamic model. This capability was demonstrated by the Input-Output analysis and the TRAF-NETSIM simulation. The dynamic model is superior to the conventional models in queue management for congested interchanges.

5.    The dynamic model controls queue lengths through efficient and timely changes of signal timing plans as demand changes. The frequent change of signal timing may cause unexpected operational problems, however. Traffic control strategies presented in this research were designed to minimize the transitional delay. The control strategies appear to be effective in reducing this delay.

6.    The dynamic model is regarded as a low-cost transportation improvement technique. This model is effective in relieving congestion within the traffic demand range that the queue storage capacity of the roadway system can accommodate. Beyond this

acceptable range, however, the model is not very helpful, and major geometric

80

improvements should be considered to solve the remaining congestion problems.

7. TRAF-NETSIM was used as an evaluation tool to test the control strategies developed for oversaturated traffic conditions. Its ability to simulate queue spillback and intersection blockage was very important in evaluating the traffic control of the oversaturated conditions. It was found that TRAF-NETSIM was able to simulate these phenomena. The graphic presentation of the dynamic simulation process greatly aided the interpretation of operational results.

8. LINDO was used to solve the MILP problems. LINDO successfully solved the large-size optimization problems. For example, the MILP formulation for the three-level diamond interchange consists of 492 constraints, 144 general variables, and 72 integer variables for three-hour control period, i.e., 12 time slices. LINDO is also convenient to use due to its user-friendly features.

## 8.2 RECOMMENDATIONS

This research was an initial attempt to employ a dynamic optimization model for signal control of oversaturated signalized interchanges. Based on the simulation results, the dynamic model showed improved performance, and its applicability from a practical viewpoint was demonstrated successfully. Further studies are recommended to enhance the dynamic model, as follows:

1. Field validation of queue management control is recommended to confirm the benefits estimated by TRAF-NETSIM for the dynamic model.

2. The dynamic model has a weakness in signal timing during undersaturated time slices. Slack green times exist when all competing approaches are undersaturated. The dynamic model should be improved by introducing a routine to efficiently allocate these slack green times. This problem can be solved using a two-step optimization procedure like PASSER II-87 (30).

3. The data input formulas for LINDO were prepared by a manual method, which was time-consuming and tedious. An input-output processor should be developed for general use by traffic engineers.

4. TRAF-NETSIM appeared to produce acceptable results in the simulation of congested traffic conditions. Studies are recommended to verify the reliability of its simulation results for congested traffic conditions through field tests.

5. The idea of queue management can be further extended to the area of the freeway on-ramp control. The queues formed on the on-ramps due to metering often overflow onto the surface streets. Using the queue management idea, these excessive queues could be controlled up to allowable limits.

# REFERENCES

1. L.J. Pignataro et al. Traffic Control in Oversaturated Street Networks. *NCHRP* Report 194, TRB, National Research Council, Washington, D.C., 1978.

2. D.B. Fambro et al. *A Report on the User's Manual for the Microcomputer Version of PASSER III-88.* Report FHWA/TX-88/478-1, Texas State Dept. of Highway and Public Transportation, Austin, Texas, 1988.

3. C.E. Wallace et al. *TRANSYT-7F User's Manual.* Transportation Research Center, University of Florida, Gainesville, Florida, 1988.

4. J.A. Wattleworth and D.S. Berry. Peak-Period Control of a Freeway System--Some Theoretical Investigations. *Highway Research Record* 89, HRB, National Research Council, Washington, D.C., 1965, pp. 1-25.

5. T. Imada and A.D. May. *FREQ8PE: A Freeway Corridor Simulation and Ramp Metering Optimization Model.* Report UCB-ITS-RR-85-10, Institute of Transportation Studies, Univ. of California, Berkeley, California, 1985.

6. FHWA. *TRAF-NETSIM User's Manual.* FHWA, U.S. Department of Transportation, Washington, D.C., 1988.

7. J.A. Bonneson and C.J. Messer. *A National Survey of Single-Point Urban Interchanges.* Report FHWA/TX-88/1148-1, Texas Transportation Institute, Texas A&M University System, College Station, Texas, 1989.

8. F.V. Webster. *Traffic Signal Settings.* Road Research Technical Paper 39, Her Majesty's Stationary Office, London, England, 1958.

9. F.V. Webster and F.M. Cobbe. *Traffic Signals.* Road Research Technical Paper 56, Her Majesty's Stationary Office, London, England, 1966.

10. D.C. Gazis and R.B. Potts. The Oversaturated Intersection. *Proc. 2nd Int. Symp. on the Theory of Road Traffic Flow,* Organization for Economic Co-operation and Development, Paris, France, 1965, pp. 221-237.

11. D.C. Gazis. Optimal Control of a System of Oversaturated Intersections. *Operations Research,* Vol. 12, 1964, pp. 815-831.

12. M.G. Singh and H. Tamura. Modelling and Hierarchical Optimization for Oversaturated Urban Road Traffic Networks. *Int. J. Control,* Vol. 20, No. 6, 1974, pp. 913-934.

13. P.G. Michalopoulos. Oversaturated Signal Systems with Queue Length Constraints-I. Single Intersection. *Transportation Research*, Vol. 11, 1977, pp. 413-421.

14. P.G. Michalopoulos and G. Stephanopoulos. An Algorithm for Real-Time Control of Critical Intersections. *Traffic Engineering and Control*, Vol. 20, 1979, pp. 9-15.

15. P.G. Michalopoulos et al. An Application of Shock Wave Theory to Traffic Signal Control. *Transportation Research*, Vol. 15B, 1981, pp. 35-51.

16. D. Longley. A Control Strategy for a Congested Computer Controlled Traffic Network. *Transportation Research*, Vol. 2, 1968, pp. 391-408.

17. R.L. Gordon. A Technique for Control of Traffic at Critical Intersections. *Transportation Science*, Vol. 4, 1969, pp. 279-287.

18. OECD, *Traffic Control in Saturated Conditions*. Organization for Economic Co-operation and Development, Paris, France, 1981.

19. Strategies to Alleviate Traffic Congestion. *Proc. ITE's 1987 National Conference*, ITE, Washington, D.C., 1988.

20. T. Shibata and T. Yamamoto. Detection and Control of Congestion in Urban Road Networks. *Traffic Engineering and Control*, Vol. 25, No. 9, 1984, pp. 438-444.

21. A. K. Rathi. A Control Scheme for High Traffic Density Sectors. *Transportation Research*, Vol. 22B, No. 2, 1988, pp. 81-101.

22. E.B. Lieberman. *Development of an Internal Metering Control Policy for Arterials Experiencing Saturated Conditions*. Unpublished Report, KLD Associates, Inc., New York, 1989.

23. D.I. Robertson. *TRANSYT: A Traffic Network Study Tool*. Road Research Laboratory Report No. RL-253, Grothorne, Berkshire, England, 1969.

24. D. Gibson and P. Ross. Simulation of Traffic in Street Networks. *Public Roads*, Vol. 41, No. 2, 1977.

25. W.D. Labrum et al. Analyzing Intersection Performance With NETSIM. *Public Roads*, Vol. 42, No. 1, 1978.

26. S.L. Cohen and G. Euler. Signal Cycle Length and Fuel Consumption and Emissions. *Transportation Research Record* 667, TRB, National Research Council, Washington, D.C., 1978.

27. W.D. Laburm and R.M. Farr. *Traffic Network Simulation with NETSIM--In a Small Urban Grid.* Technology Sharing Report, FHWA-1P-80-XX, FHWA, U.S. Department of Transportation, Washington, D.C.,1978.

28. S. Wong. TRAF-NETSIM: How It Works, What It Does. *ITE Journal,* Vol. 60, No. 4, ITE, Washington, D.C., April 1990, pp. 22-27.

29. B. Andrews and E. Lieberman. *GTRAF User Guide.* Report FHWA-RD-87, FHWA, U.S. Department of Transportation, Washington, D.C., 1988.

30. E.C.P. Chang, J.C. Lei, and C.J. Messer. *Arterial Signal Timing Optimization Using PASSER II-87 - Microcomputer User's Guide.* Report TTI-2-18-86-467-1, Texas Transportation Institute, Texas A&M University System, College Station, Texas, 1988.

31. C.J. Messer et al. *Optimization of Left Turn Phase Sequence in Signalized Networks Using MAXBAND 86 - Volume 2. User's Manual.* Report FHWA/RD-84/, FHWA, U.S. Department of Transportation, Washington, D.C., 1986.

32. H. Tsay and L. Lin. New Algorithm for Solving the Maximum Progression Bandwidth. *Transportation Research Record* 1194, TRB, National Research Council, Washington D.C., 1988.

33. A.S. Land and S. Powell. *FORTRAN Codes for Mathematical Programming.* John Wiley & Sons, Ltd., London, England, 1973.

34. L. Schrage. *User's Manual for Linear, Integer and Quadratic Programming with LINDO.* 3rd ed., The Scientific Press, Redwood City, California, 1986.

35. C.J. Messer and D.J. Berry. Effects of Design Alternatives on Quality of Service at Signalized Diamond Interchanges. *Transportation Research Record* 538, TRB, National Research Council, Washington, D.C., 1975.

36. C.H. Knapp et al. Simulation and Control of Traffic on a Diamond Interchange. *Transportation Research Record* 644, TRB, National Research Council, Washington, D.C., 1977.

37. D.R. Drew. *Traffic Theory and Control.* McGraw-Hill Book Company, New York, New York, 1968, pp. 393-399.

38. W.L. Hays. *Statistics.* 3rd ed., CBS College Publishing, New York, New York, 1981, pp. 590-591.
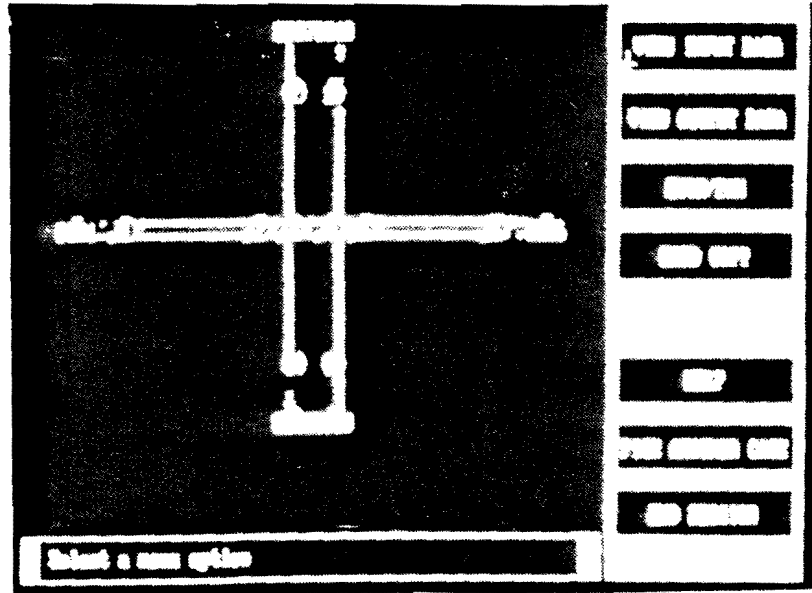
APPENDIX A

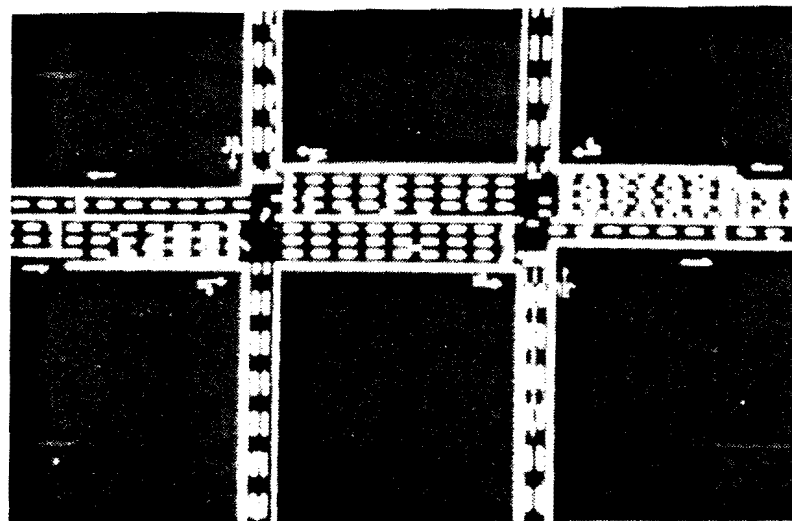Examples of GTRAF Graphic Displays

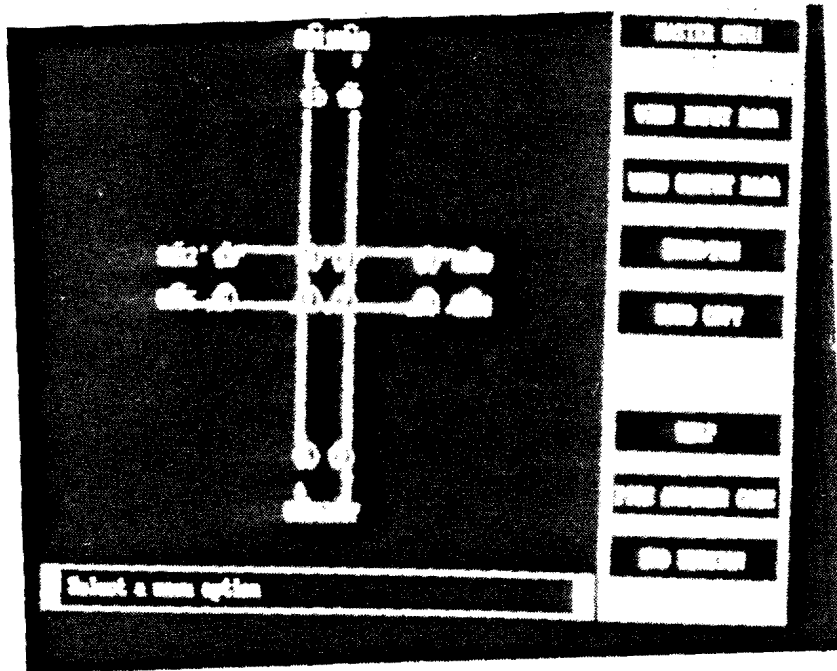# APPENDIX A. EXAMPLES OF GTRAF GRAPHIC DISPLAYS
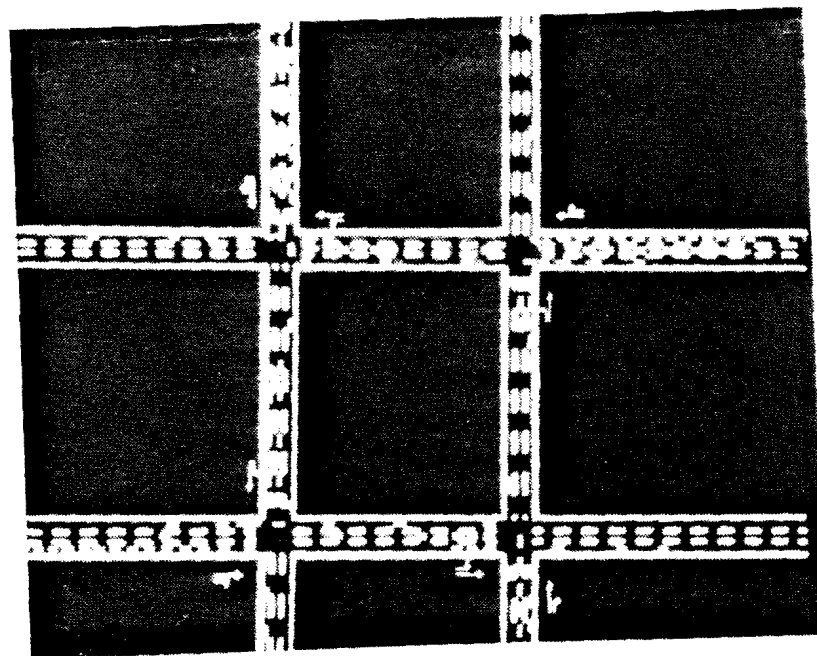


(a) Link-Node Diagram



(b) Graphic Animation Display

Figure A-1. GTRAF Display of TUDI

(a) Link-Node Diagram



(b) Graphic Animation Display

Figure A-2. GTRAF Display of TLDI

87

APPENDIX B

Examples of MILP Formulation, TUDI, Case 1

# APPENDIX B.  EXAMPLES OF MILP FORMULATION, CDI, CASE 1

```
MIN
  1530L11+1530L12+1530L13+1530L14+1530L15+1530L16
+1530L17+1530L18+1530L19+1530L110+1530L111+1530L112
+900L21+900L22+900L23+900L24+900L25+900L26
+900L27+900L28+900L29+900L210+900L211+900L212
+1350L31+1350L32+1350L33+1350L34+1350L35+1350L36
+1350L37+1350L38+1350L39+1350L310+1350L311+1350L312
+900L41+900L42+900L43+900L44+900L45+900L46
+900L47+900L48+900L49+900L410+900L411+900L412
SUBJECT TO
L1=90
L2=99
L3=63
L4=99
V11 = .215
V12 = .193
V13 = .228
V14 = .228
V15 = .228
V16 = .233
V17 = .233
V18 = .222
V19 = .193
V110 = .165
V111 = .169
V112 = .190
V21 = .299
V22 = .333
V23 = .306
V24 = .347
V25 = .347
V26 = .340
V27 = .343
V28 = .299
V29 = .304
V210 = .264
V211 = .251
V212 = .172
V31 = .445
V32 = .442
V33 = .444
V34 = .447
V35 = .436
V36 = .432
V37 = .432
V38 = .331
V39 = .292
V310 = .234
V311 = .256
V312 = .198
```

```
V41 = .347
V42 = .353
V43 = .350
V44 = .356
V45 = .342
V46 = .347
V47 = .309
V48 = .290
V49 = .307
V410 = .263
V411 = .241
V412 = .263
G11 + G21 + G61 = .867
G31 + G41 + G71 = .867
G12 + G22 + G62 = .867
G32 + G42 + G72 = .867
G13 + G23 + G63 = .867
G33 + G43 + G73 = .867
G14 + G24 + G64 = .867
G34 + G44 + G74 = .867
G15 + G25 + G65 = .867
G35 + G45 + G75 = .867
G16 + G26 + G66 = .867
G36 + G46 + G76 = .867
G17 + G27 + G67 = .867
G37 + G47 + G77 = .867
G18 + G28 + G68 = .867
G38 + G48 + G78 = .867
G19 + G29 + G69 = .867
G39 + G49 + G79 = .867
G110+ G210+ G610= .867
G310+ G410+ G710= .867
G111+ G211+ G611= .867
G311+ G411+ G711= .867
G112+ G212+ G612= .867
G312+ G412+ G712= .867
G61 + G71 = .667
G62 + G72 = .667
G63 + G73 = .667
G64 + G74 = .667
G65 + G75 = .667
G66 + G76 = .667
G67 + G77 = .667
G68 + G78 = .667
G69 + G79 = .667
G610+ G710= .667
G611+ G711= .667
G612+ G712= .667
G11 - G71 <0
G12 - G72 <0
```

```
G13  - G73  <0
G14  - G74  <0
G15  - G75  <0
G16  - G76  <0
G17  - G77  <0
G18  - G78  <0
G19  - G79  <0
G110- G710<0
G111- G711<0
G112- G712<0
G31  - G61  <0
G32  - G62  <0
G33  - G63  <0
G34  - G64  <0
G35  - G65  <0
G36  - G66  <0
G37  - G67  <0
G38  - G68  <0
G39  - G69  <0
G310- G610<0
G311- G611<0
G312- G612<0
L11  - L1  <=    0
L12  - L1  <=    0
L13  - L1  <=    0
L14  - L1  <=    0
L15  - L1  <=    0
L16  - L1  <=    0
L17  - L1  <=    0
L18  - L1  <=    0
L19  - L1  <=    0
L110- L1  <=    0
L111- L1  <=    0
L112- L1  <=    0
L21  - L2  <=    0
L22  - L2  <=    0
L23  - L2  <=    0
L24  - L2  <=    0
L25  - L2  <=    0
L26  - L2  <=    0
L27  - L2  <=    0
L28  - L2  <=    0
L29  - L2  <=    0
L210- L2  <=    0
L211- L2  <=    0
L212- L2  <=    0
L31  - L3  <=    0
L32  - L3  <=    0
L33  - L3  <=    0
L34  - L3  <=    0
```

```
L35 - L3 <=    0
L36 - L3 <=    0
L37 - L3 <=    0
L38 - L3 <=    0
L39 - L3 <=    0
L310- L3 <=    0
L311- L3 <=    0
L312- L3 <=    0
L41 - L4 <=    0
L42 - L4 <=    0
L43 - L4 <=    0
L44 - L4 <=    0
L45 - L4 <=    0
L46 - L4 <=    0
L47 - L4 <=    0
L48 - L4 <=    0
L49 - L4 <=    0
L410- L4 <=    0
L411- L4 <=    0
L412- L4 <=    0
L11 >=    0
L12 >=    0
L13 >=    0
L14 >=    0
L15 >=    0
L16 >=    0
L17 >=    0
L18 >=    0
L19 >=    0
L110>=    0
L111>=    0
L112>=    0
L21 >=    0
L22 >=    0
L23 >=    0
L24 >=    0
L25 >=    0
L26 >=    0
L27 >=    0
L28 >=    0
L29 >=    0
L210>=    0
L211>=    0
L212>=    0
L31 >=    0
L32 >=    0
L33 >=    0
L34 >=    0
L35 >=    0
L36 >=    0
```

```
L37 >=     0
L38 >=     0
L39 >=     0
L310>=     0
L311>=     0
L312>=     0
L41 >=     0
L42 >=     0
L43 >=     0
L44 >=     0
L45 >=     0
L46 >=     0
L47 >=     0
L48 >=     0
L49 >=     0
L410>=     0
L411>=     0
L412>=     0
-L11       -900G11  +900V11  <=     0
-L12 +L11  -900G12  +900V12  <=     0
-L13 +L12  -900G13  +900V13  <=     0
-L14 +L13  -900G14  +900V14  <=     0
-L15 +L14  -900G15  +900V15  <=     0
-L16 +L15  -900G16  +900V16  <=     0
-L17 +L16  -900G17  +900V17  <=     0
-L18 +L17  -900G18  +900V18  <=     0
-L19 +L18  -900G19  +900V19  <=     0
-L110+L19  -900G110 +900V110<=     0
-L111+L110-900G111  +900V111<=     0
-L112+L111-900G112  +900V112<=     0
-L21       -1350G21 +900V21  <=     0
-L22 +L21  -1350G22 +900V22  <=     0
-L23 +L22  -1350G23 +900V23  <=     0
-L24 +L23  -1350G24 +900V24  <=     0
-L25 +L24  -1350G25 +900V25  <=     0
-L26 +L25  -1350G26 +900V26  <=     0
-L27 +L26  -1350G27 +900V27  <=     0
-L28 +L27  -1350G28 +900V28  <=     0
-L29 +L28  -1350G29 +900V29  <=     0
-L210+L29  -1350G210 +900V210<=    0
-L211+L210-1350G211 +900V211<=    0
-L212+L211-1350G212 +900V212<=    0
-L31       -900G31+900V31  <=    0
-L32 +L31  -900G32+900V32  <=    0
-L33 +L32  -900G33+900V33  <=    0
-L34 +L33  -900G34+900V34  <=    0
-L35 +L34  -900G35+900V35  <=    0
-L36 +L35  -900G36+900V36  <=    0
-L37 +L36  -900G37+900V37  <=    0
-L38 +L37  -900G38+900V38  <=    0
```

```
-L39 +L38 -900G39+900V39  <=    0
-L310+L39 -900G310+900V310<=    0
-L311+L310-900G311+900V311<=    0
-L312+L311-900G312+900V312<=    0
-L41       -1350G41+900V41  <=    0
-L42 +L41 -1350G42+900V42  <=    0
-L43 +L42 -1350G43+900V43  <=    0
-L44 +L43 -1350G44+900V44  <=    0
-L45 +L44 -1350G45+900V45  <=    0
-L46 +L45 -1350G46+900V46  <=    0
-L47 +L46 -1350G47+900V47  <=    0
-L48 +L47 -1350G48+900V48  <=    0
-L49 +L48 -1350G49+900V49  <=    0
-L410+L49 -1350G410+900V410<=    0
-L411+L410-1350G411+900V411<=    0
-L412+L411-1350G412+900V412<=    0
-1000 Z11 + L11 <=    0
-1000 Z12 + L12 <=    0
-1000 Z13 + L13 <=    0
-1000 Z14 + L14 <=    0
-1000 Z15 + L15 <=    0
-1000 Z16 + L16 <=    0
-1000 Z17 + L17 <=    0
-1000 Z18 + L18 <=    0
-1000 Z19 + L19 <=    0
-1000 Z110+ L110<=    0
-1000 Z111+ L111<=    0
-1000 Z112+ L112<=    0
-1000 Z21 + L21 <=    0
-1000 Z22 + L22 <=    0
-1000 Z23 + L23 <=    0
-1000 Z24 + L24 <=    0
-1000 Z25 + L25 <=    0
-1000 Z26 + L26 <=    0
-1000 Z27 + L27 <=    0
-1000 Z28 + L28 <=    0
-1000 Z29 + L29 <=    0
-1000 Z210+ L210<=    0
-1000 Z211+ L211<=    0
-1000 Z212+ L212<=    0
-1000 Z31 + L31 <=    0
-1000 Z32 + L32 <=    0
-1000 Z33 + L33 <=    0
-1000 Z34 + L34 <=    0
-1000 Z35 + L35 <=    0
-1000 Z36 + L36 <=    0
-1000 Z37 + L37 <=    0
-1000 Z38 + L38 <=    0
-1000 Z39 + L39 <=    0
-1000 Z310+ L310<=    0
```

```
-1000 Z311+ L311<=    0
-1000 Z312+ L312<=    0
-1000 Z41 + L41 <=    0
-1000 Z42 + L42 <=    0
-1000 Z43 + L43 <=    0
-1000 Z44 + L44 <=    0
-1000 Z45 + L45 <=    0
-1000 Z46 + L46 <=    0
-1000 Z47 + L47 <=    0
-1000 Z48 + L48 <=    0
-1000 Z49 + L49 <=    0
-1000 Z410+ L410<=    0
-1000 Z411+ L411<=    0
-1000 Z412+ L412<=    0
-1000Z11 -L11         -900G11+900V11 >= - 1000
-1000Z12 -L12 +L11 -900G12+900V12 >= - 1000
-1000Z13 -L13 +L12 -900G13+900V13 >= - 1000
-1000Z14 -L14 +L13 -900G14+900V14 >= - 1000
-1000Z15 -L15 +L14 -900G15+900V15 >= - 1000
-1000Z16 -L16 +L15 -900G16+900V16 >= - 1000
-1000Z17 -L17 +L16 -900G17+900V17 >= - 1000
-1000Z18 -L18 +L17 -900G18+900V18 >= - 1000
-1000Z19 -L19 +L18 -900G19+900V19 >= - 1000
-1000Z110-L110+L19 -900G110+900V110>= - 1000
-1000Z111-L111+L110-900G111+900V111>= - 1000
-1000Z112-L112+L111-900G112+900V112>= - 1000
-1000Z21 -L21         -1350G21+900V21 >= - 1000
-1000Z22 -L22 +L21 -1350G22+900V22 >= - 1000
-1000Z23 -L23 +L22 -1350G23+900V23 >= - 1000
-1000Z24 -L24 +L23 -1350G24+900V24 >= - 1000
-1000Z25 -L25 +L24 -1350G25+900V25 >= - 1000
-1000Z26 -L26 +L25 -1350G26+900V26 >= - 1000
-1000Z27 -L27 +L26 -1350G27+900V27 >= - 1000
-1000Z28 -L28 +L27 -1350G28+900V28 >= - 1000
-1000Z29 -L29 +L28 -1350G29+900V29 >= - 1000
-1000Z210-L210+L29 -1350G210+900V210>= - 1000
-1000Z211-L211+L210-1350G211+900V211>= - 1000
-1000Z212-L212+L211-1350G212+900V212>= - 1000
-1000Z31 -L31         -900G31+900V31 >= - 1000
-1000Z32 -L32 +L31 -900G32+900V32 >= - 1000
-1000Z33 -L33 +L32 -900G33+900V33 >= - 1000
-1000Z34 -L34 +L33 -900G34+900V34 >= - 1000
-1000Z35 -L35 +L34 -900G35+900V35 >= - 1000
-1000Z36 -L36 +L35 -900G36+900V36 >= - 1000
-1000Z37 -L37 +L36 -900G37+900V37 >= - 1000
-1000Z38 -L38 +L37 -900G38+900V38 >= - 1000
-1000Z39 -L39 +L38 -900G39+900V39 >= - 1000
-1000Z310-L310+L39 -900G310+900V310>= - 1000
-1000Z311-L311+L310-900G311+900V311>= - 1000
-1000Z312-L312+L311-900G312+900V312>= - 1000
```

```
-1000Z41 -L41      -1350G41+900V41 >= - 1000
-1000Z42 -L42 +L41 -1350G42+900V42 >= - 1000
-1000Z43 -L43 +L42 -1350G43+900V43 >= - 1000
-1000Z44 -L44 +L43 -1350G44+900V44 >= - 1000
-1000Z45 -L45 +L44 -1350G45+900V45 >= - 1000
-1000Z46 -L46 +L45 -1350G46+900V46 >= - 1000
-1000Z47 -L47 +L46 -1350G47+900V47 >= - 1000
-1000Z48 -L48 +L47 -1350G48+900V48 >= - 1000
-1000Z49 -L49 +L48 -1350G49+900V49 >= - 1000
-1000Z410-L410+L49 -1350G410+900V410>= - 1000
-1000Z411-L411+L410-1350G411+900V411>= - 1000
-1000Z412-L412+L411-1350G412+900V412>= - 1000
END
  INTE        Z11
  INTE        Z12
  INTE        Z13
  INTE        Z14
  INTE        Z15
  INTE        Z16
  INTE        Z17
  INTE        Z18
  INTE        Z19
  INTE        Z110
  INTE        Z111
  INTE        Z112
  INTE        Z21
  INTE        Z22
  INTE        Z23
  INTE        Z24
  INTE        Z25
  INTE        Z26
  INTE        Z27
  INTE        Z28
  INTE        Z29
  INTE        Z210
  INTE        Z211
  INTE        Z212
  INTE        Z31
  INTE        Z32
  INTE        Z33
  INTE        Z34
  INTE        Z35
  INTE        Z36
  INTE        Z37
  INTE        Z38
  INTE        Z39
  INTE        Z310
  INTE        Z311
  INTE        Z312
  INTE        Z41
```

```
INTE        Z42
INTE        Z43
INTE        Z44
INTE        Z45
INTE        Z46
INTE        Z47
INTE        Z48
INTE        Z49
INTE        Z410
INTE        Z411
INTE        Z412
```

# APPENDIX C

Traffic Data for Case in Evaluation of Dynamic Model

# APPENDIX C. TRAFFIC DATA USED IN EVALUATING DYNAMIC MODEL

(a) Input Volume (vph)

| | Case 1 Approach | | | | Case 2 Approach | | | | Case 3 Approach | | | |
|------|------|------|------|------|------|------|------|------|------|------|------|------|
| Time | 1 | 2 | 3 | 4 | 1 | 2 | 3 | 4 | 1 | 2 | 3 | 4 |
| 1 | 1191 | 1076 | 2715 | 1249 | 1290 | 1220 | 2580 | 1249 | 1392 | 1440 | 1344 | 1874 |
| 2 | 1069 | 1199 | 2697 | 1271 | 1260 | 1152 | 2580 | 1271 | 1338 | 1188 | 1860 | 1906 |
| 3 | 1263 | 1102 | 2709 | 1260 | 1260 | 1260 | 2604 | 1195 | 1080 | 1674 | 2100 | 1134 |
| 4 | 1263 | 1249 | 2727 | 1282 | 1140 | 1192 | 2562 | 1246 | 1368 | 2279 | 1320 | 1800 |
| 5 | 1263 | 1249 | 2660 | 1231 | 1200 | 1591 | 2496 | 1231 | 1140 | 1602 | 2496 | 648 |
| 6 | 1290 | 1224 | 2636 | 1249 | 1398 | 1836 | 2292 | 1249 | 1398 | 1674 | 1260 | 1512 |
| 7 | 1290 | 1235 | 2636 | 1112 | 1398 | 1800 | 2112 | 1184 | 2100 | 1242 | 1140 | 1314 |
| 8 | 1230 | 1076 | 2020 | 1044 | 1308 | 1796 | 1926 | 1044 | 1152 | 1800 | 2106 | 810 |
| 9 | 1069 | 1094 | 1782 | 1105 | 1398 | 1728 | 1872 | 1141 | 1158 | 1642 | 1620 | 1350 |
| 10 | 914 | 950 | 1428 | 947 | 1350 | 1620 | 1764 | 1055 | 1200 | 1458 | 1764 | 1220 |
| 11 | 936 | 904 | 1562 | 868 | 1014 | 1152 | 1536 | 1084 | 1194 | 1355 | 1536 | 1375 |
| 12 | 1052 | 619 | 1208 | 947 | 1140 | 1123 | 1188 | 767 | 1140 | 1145 | 1188 | 1150 |

(b) Turning Percentage (%)
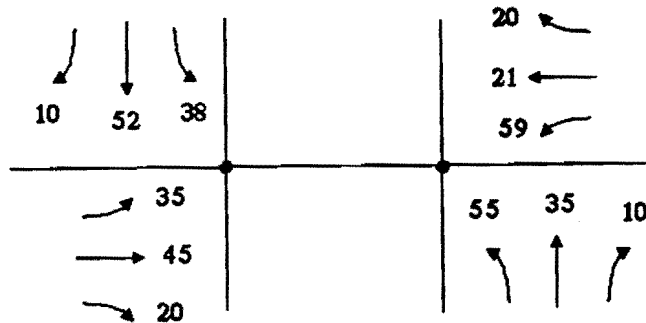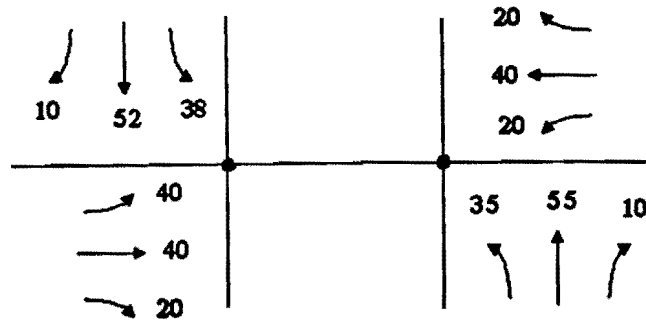


Figure C-1. Traffic Data for TUDI

99

# APPENDIX D

## Signal Timings Produced by Dynamic Model

# APPENDIX D.  SIGNAL TIMINGS PRODUCED BY DYNAMIC MODEL

## 1.  Signal Timing for TUDI

### Case 1

| Time Slice | LEFT INT A | B | C | RIGHT INT A | B | C |
|---|---|---|---|---|---|---|
| 1 | 19 | 18 | 41 | 40 | 19 | 19 |
| 2 | 18 | 18 | 42 | 40 | 20 | 18 |
| 3 | 21 | 18 | 39 | 34 | 23 | 21 |
| 4 | 20 | 18 | 40 | 40 | 18 | 20 |
| 5 | 20 | 19 | 39 | 39 | 18 | 21 |
| 6 | 16 | 20 | 42 | 39 | 21 | 18 |
| 7 | 18 | 21 | 39 | 39 | 18 | 21 |
| 8 | 29 | 19 | 30 | 30 | 18 | 30 |
| 9 | 17 | 22 | 39 | 33 | 24 | 21 |
| 10 | 19 | 19 | 40 | 38 | 20 | 20 |
| 11 | 19 | 19 | 40 | 38 | 20 | 20 |
| 12 | 19 | 19 | 40 | 38 | 20 | 20 |

### Case 2

| Time Slice | LEFT INT A | B | C | RIGHT INT A | B | C |
|---|---|---|---|---|---|---|
| 1 | 19 | 18 | 41 | 39 | 20 | 19 |
| 2 | 19 | 20 | 39 | 38 | 19 | 21 |
| 3 | 19 | 20 | 39 | 39 | 18 | 21 |
| 4 | 17 | 23 | 38 | 38 | 18 | 22 |
| 5 | 18 | 22 | 38 | 37 | 19 | 22 |
| 6 | 15 | 26 | 37 | 34 | 21 | 23 |
| 7 | 24 | 26 | 28 | 27 | 19 | 32 |
| 8 | 19 | 30 | 29 | 29 | 18 | 31 |
| 9 | 16 | 29 | 33 | 33 | 18 | 27 |
| 10 | 20 | 27 | 31 | 31 | 18 | 29 |
| 11 | 24 | 22 | 32 | 23 | 27 | 28 |
| 12 | 19 | 30 | 29 | 29 | 18 | 31 |

### Case 3

| Time Slice | LEFT INT A | B | C | RIGHT INT A | B | C |
|---|---|---|---|---|---|---|
| 1 | 21 | 24 | 33 | 22 | 29 | 27 |
| 2 | 20 | 20 | 38 | 28 | 28 | 22 |
| 3 | 16 | 28 | 34 | 30 | 22 | 26 |
| 4 | 19 | 31 | 28 | 21 | 25 | 32 |
| 5 | 19 | 29 | 30 | 30 | 18 | 30 |
| 6 | 21 | 33 | 24 | 21 | 21 | 36 |
| 7 | 31 | 21 | 26 | 22 | 22 | 34 |
| 8 | 17 | 29 | 32 | 32 | 18 | 28 |
| 9 | 17 | 32 | 29 | 25 | 22 | 31 |
| 10 | 18 | 24 | 36 | 33 | 21 | 24 |
| 11 | 18 | 23 | 37 | 32 | 23 | 23 |
| 12 | 18 | 23 | 37 | 32 | 23 | 23 |

2. Signal Timing for TLDI

## Case 1

|  | Int 1 | | Int 2 | | Int 3 | | Int 4 | |
|---|---|---|---|---|---|---|---|---|
|  | Ph 1 | Ph 2 | Ph 1 | Ph 2 | Ph 1 | Ph 2 | Ph 1 | Ph 2 |
| Time Slice | | | | | | | | |
| 1 | 16 | 21 | 21 | 16 | 14 | 23 | 10 | 27 |
| 2 | 20 | 17 | 17 | 20 | 13 | 24 | 15 | 22 |
| 3 | 21 | 16 | 16 | 21 | 13 | 24 | 16 | 21 |
| 4 | 19 | 18 | 18 | 19 | 13 | 24 | 15 | 22 |
| 5 | 20 | 17 | 17 | 20 | 13 | 24 | 16 | 21 |
| 6 | 18 | 19 | 15 | 22 | 14 | 23 | 19 | 18 |
| 7 | 18 | 19 | 13 | 24 | 16 | 21 | 19 | 18 |
| 8 | 18 | 19 | 19 | 18 | 14 | 24 | 13 | 24 |
| 9 | 17 | 20 | 20 | 17 | 14 | 23 | 13 | 24 |
| 10 | 21 | 16 | 16 | 21 | 13 | 24 | 16 | 21 |
| 11 | 25 | 12 | 12 | 25 | 9 | 28 | 12 | 25 |
| 12 | 21 | 16 | 16 | 21 | 13 | 24 | 16 | 21 |

## Case 2

|  | Int 1 | | Int 2 | | Int 3 | | Int 4 | |
|---|---|---|---|---|---|---|---|---|
|  | Ph 1 | Ph 2 | Ph 1 | Ph 2 | Ph 1 | Ph 2 | Ph 1 | Ph 2 |
| 1 | 16 | 16 | 16 | 16 | 14 | 18 | 16 | 16 |
| 2 | 20 | 12 | 12 | 20 | 14 | 18 | 12 | 20 |
| 3 | 20 | 12 | 12 | 20 | 14 | 18 | 12 | 20 |
| 4 | 18 | 14 | 14 | 18 | 14 | 18 | 14 | 18 |
| 5 | 18 | 14 | 14 | 18 | 14 | 18 | 14 | 18 |
| 6 | 16 | 16 | 16 | 16 | 14 | 18 | 16 | 16 |
| 7 | 16 | 16 | 16 | 16 | 14 | 18 | 16 | 16 |
| 8 | 16 | 16 | 16 | 16 | 14 | 18 | 16 | 16 |
| 9 | 16 | 16 | 16 | 16 | 14 | 18 | 16 | 16 |
| 10 | 16 | 16 | 16 | 16 | 14 | 18 | 16 | 16 |
| 11 | 13 | 19 | 19 | 13 | 8 | 24 | 14 | 18 |
| 12 | 13 | 19 | 19 | 13 | 13 | 19 | 13 | 19 |

## Case 3

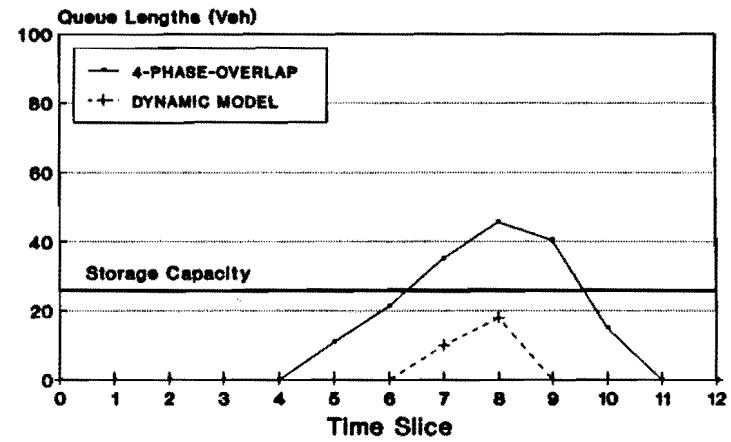|  | Int 1 | | Int 2 | | Int 3 | | Int 4 | |
|---|---|---|---|---|---|---|---|---|
|  | Ph 1 | Ph 2 | Ph 1 | Ph 2 | Ph 1 | Ph 2 | Ph 1 | Ph 2 |
| 1 | 17 | 15 | 15 | 17 | 11 | 21 | 15 | 17 |
| 2 | 21 | 11 | 11 | 21 | 14 | 18 | 10 | 22 |
| 3 | 20 | 12 | 12 | 20 | 14 | 18 | 11 | 21 |
| 4 | 19 | 13 | 13 | 19 | 14 | 18 | 13 | 19 |
| 5 | 20 | 12 | 12 | 20 | 14 | 18 | 12 | 20 |
| 6 | 19 | 13 | 13 | 19 | 14 | 18 | 13 | 19 |
| 7 | 16 | 16 | 16 | 16 | 14 | 18 | 16 | 16 |
| 8 | 15 | 17 | 17 | 15 | 15 | 17 | 14 | 18 |
| 9 | 17 | 15 | 15 | 17 | 11 | 21 | 15 | 17 |
| 10 | 16 | 16 | 16 | 16 | 14 | 18 | 16 | 16 |
| 11 | 20 | 12 | 12 | 20 | 9 | 23 | 12 | 20 |
| 12 | 15 | 17 | 17 | 15 | 15 | 17 | 8 | 24 |

APPENDIX E

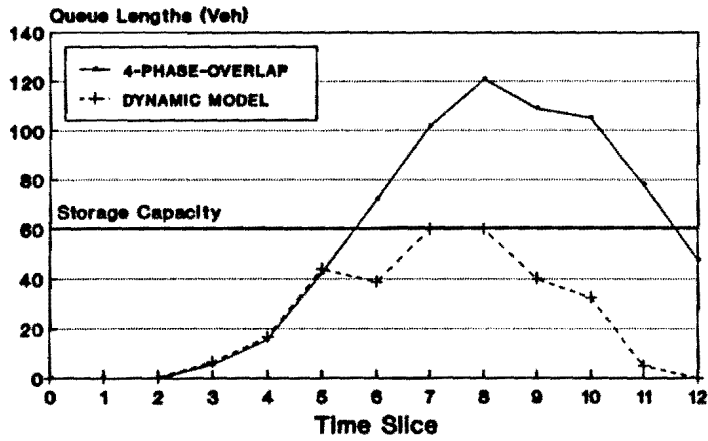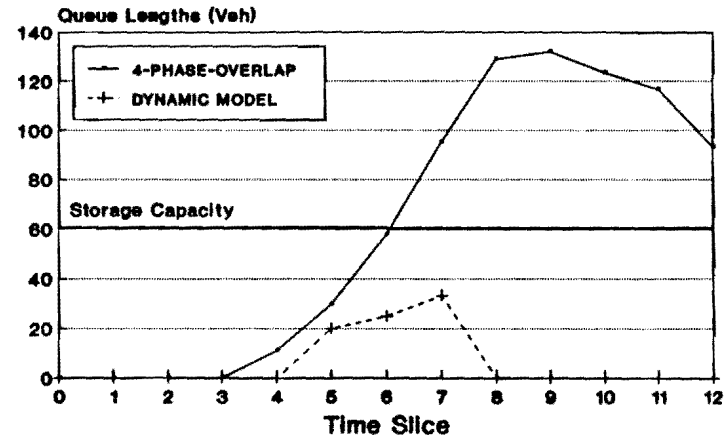Queue Profiles
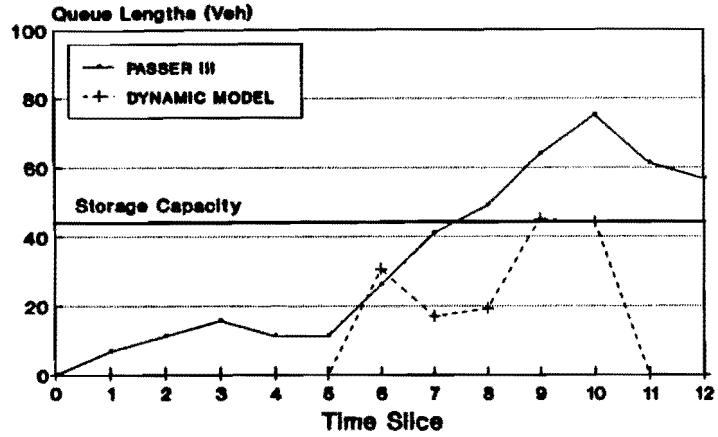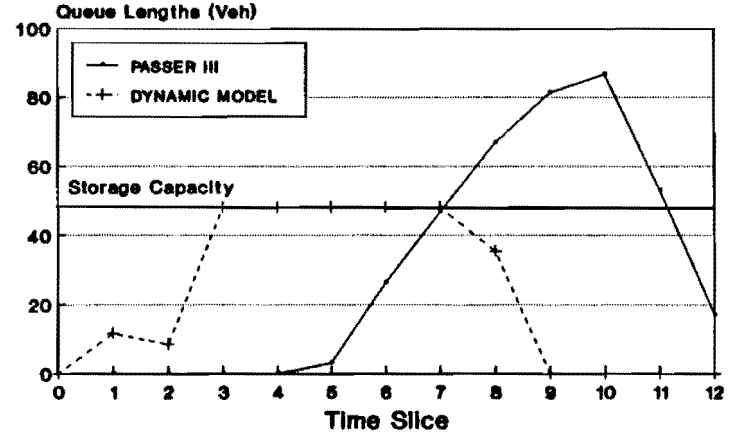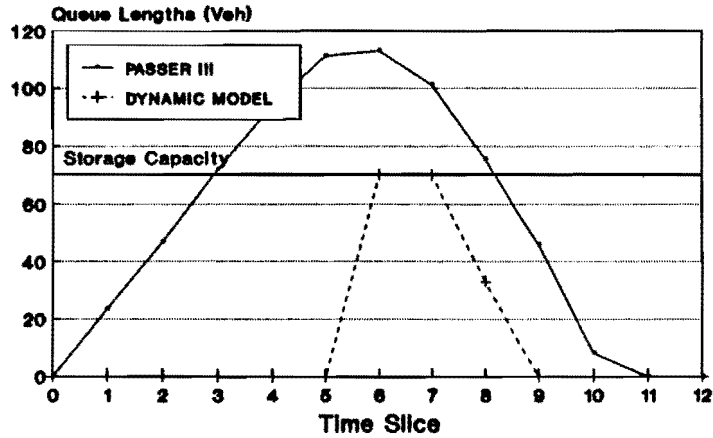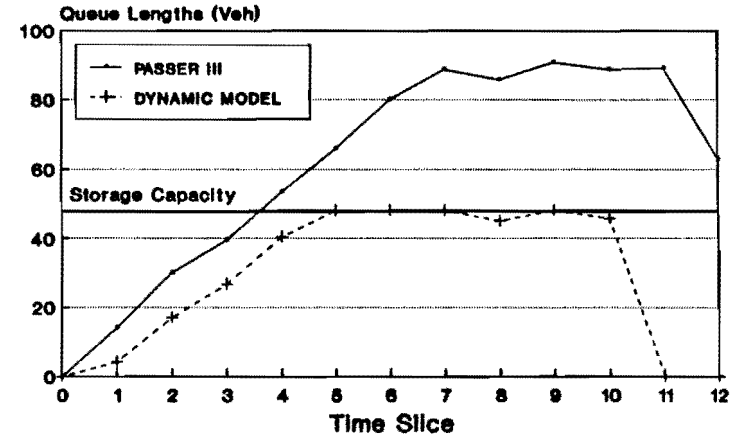
Figure E-1. Queues by Input-Output Analysis, TUDI, Case 2

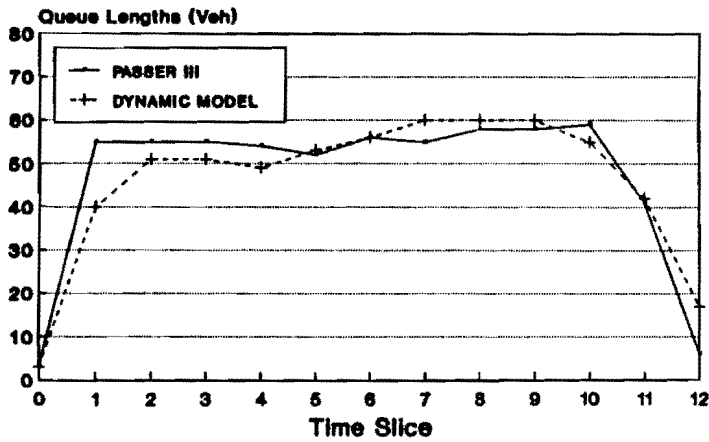## APPROACH 1

Queue Lengths (Veh)



## APPROACH 2

Queue Lengths (Veh)



## APPROACH 3

Queue Lengths (Veh)



## APPROACH 4

Queue Lengths (Veh)
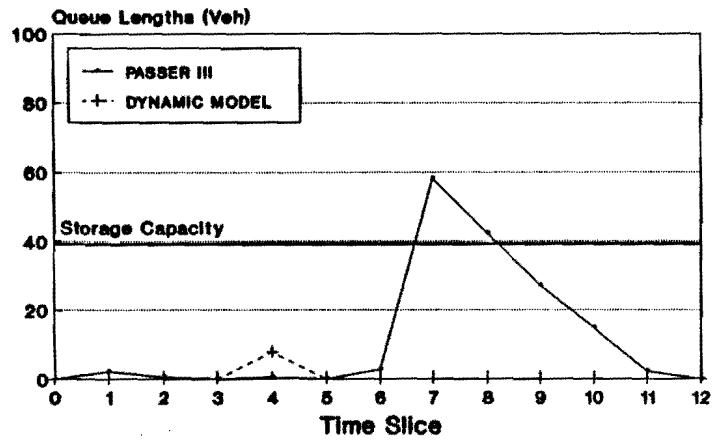


Figure E-2.  Queues by Input-Output Analysis, TUDI, Case 3

## APPROACH 1

Queue Lengths (Veh)

- 4-PHASE-OVERLAP
- DYNAMIC MODEL

Storage Capacity

Time Slice

## APPROACH 2

Queue Lengths (Veh)

- 4-PHASE-OVERLAP
- DYNAMIC MODEL

Storage Capacity

Time Slice

## APPROACH 3

Queue Lengths (Veh)

- 4-PHASE-OVERLAP
- DYNAMIC MODEL

Storage Capacity

Time Slice

## APPROACH 4

Queue Lengths (Veh)

- 4-PHASE-OVERLAP
- DYNAMIC MODEL

Storage Capacity

Time Slice
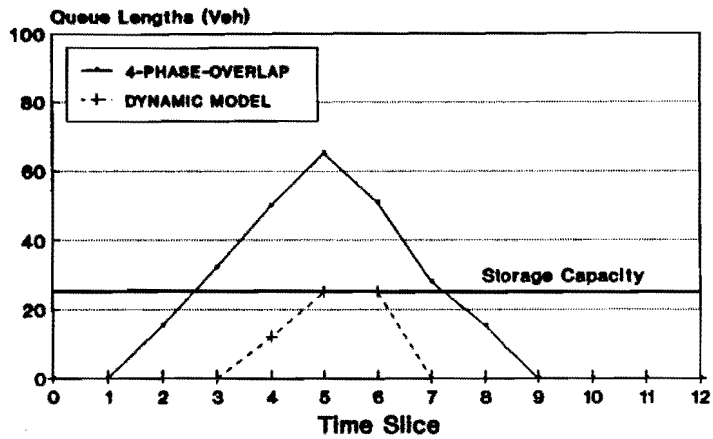
Figure E-3. Queues by Input-Output Analysis, TLDI, Case 2

# APPROACH 1

Queue Lengths (Veh)



# APPROACH 2

Queue Lengths (Veh)



# APPROACH 3

Queue Lengths (Veh)



# APPROACH 4

Queue Lengths (Veh)
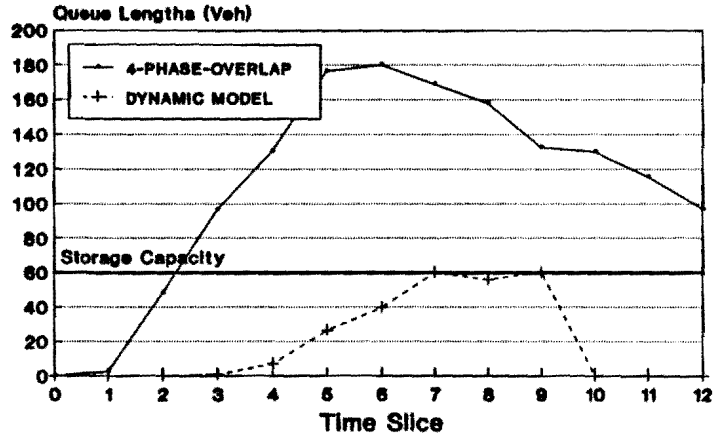


Figure E-4.  Queues by Input-Output Analysis,TLDI,Case 3

# APPROACH 1
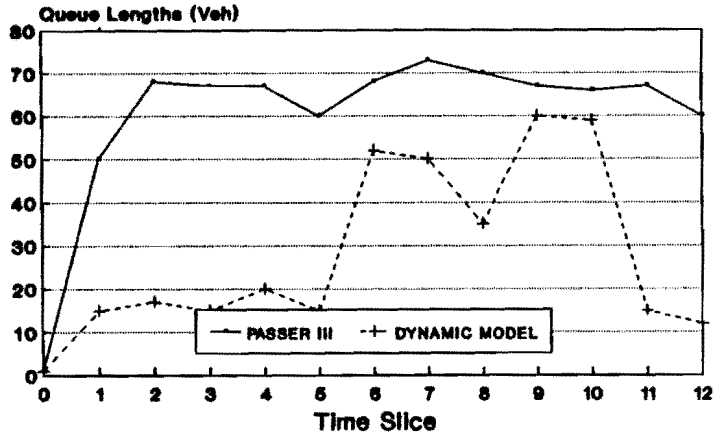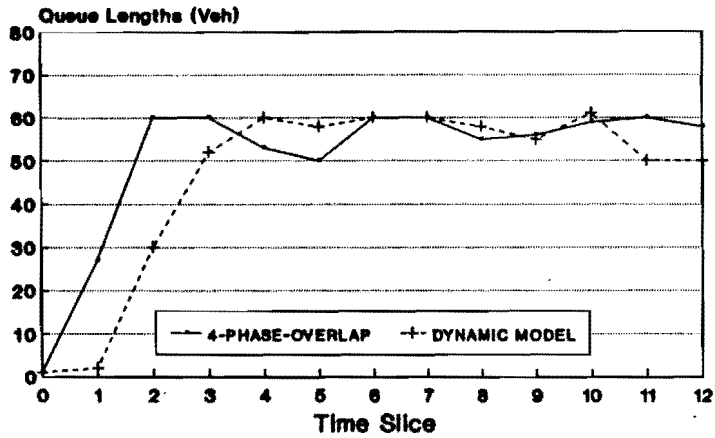


# APPROACH 2
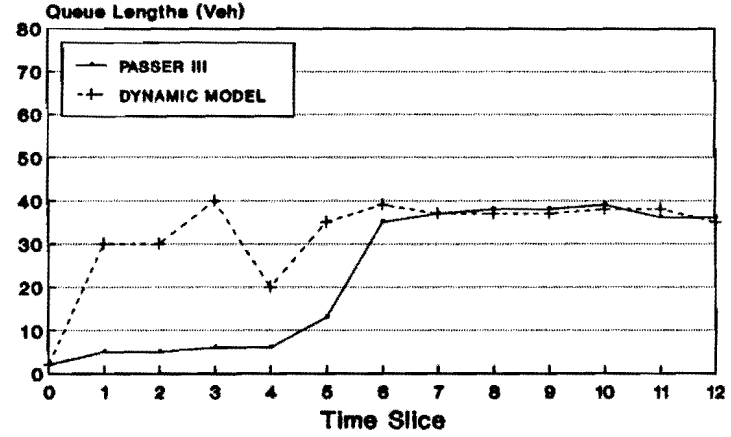


# APPROACH 3
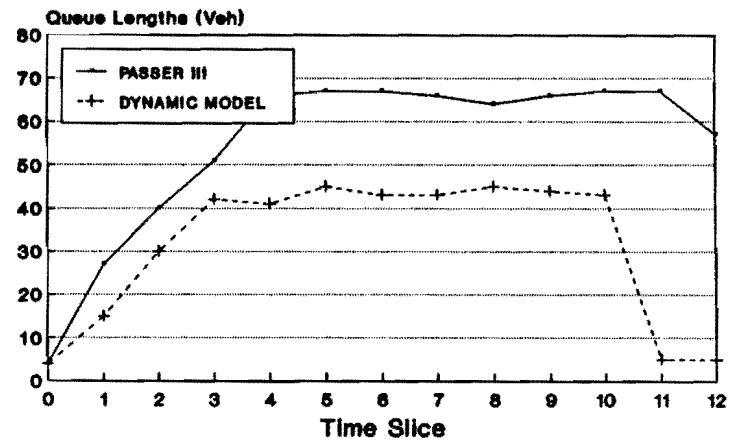


# APPROACH 4



Figure E-5.  Queues by TRAF-NETSIM, TLDI, Case 2
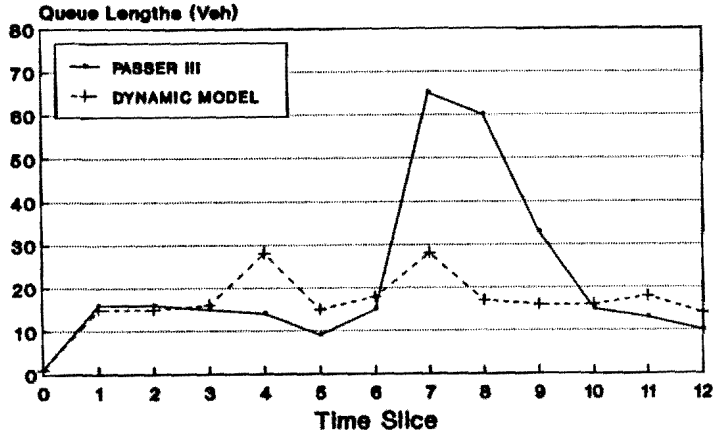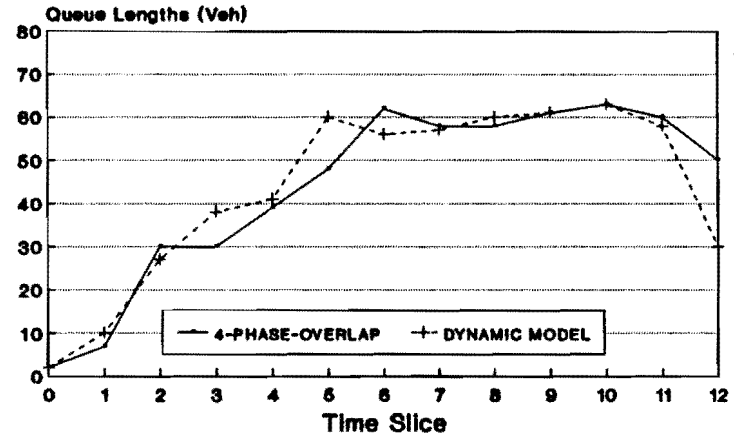
## APPROACH 1



## APPROACH 2
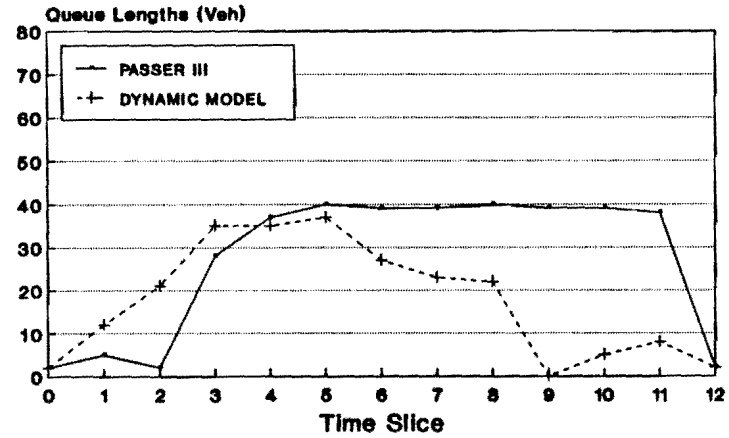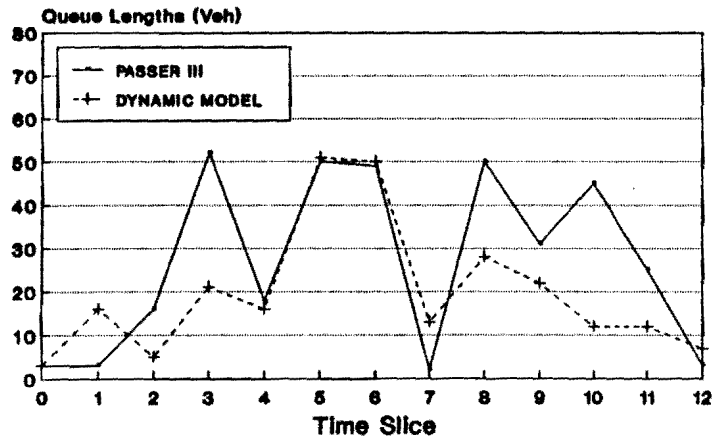


## APPROACH 3
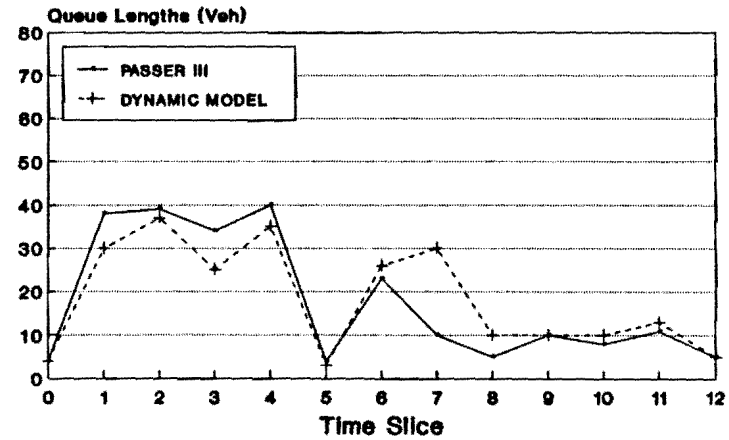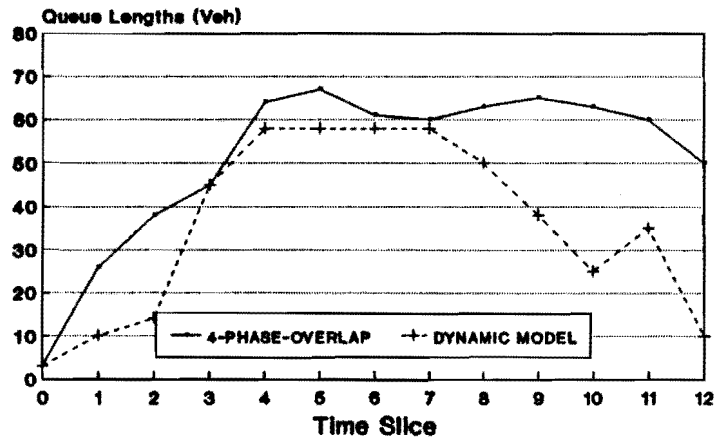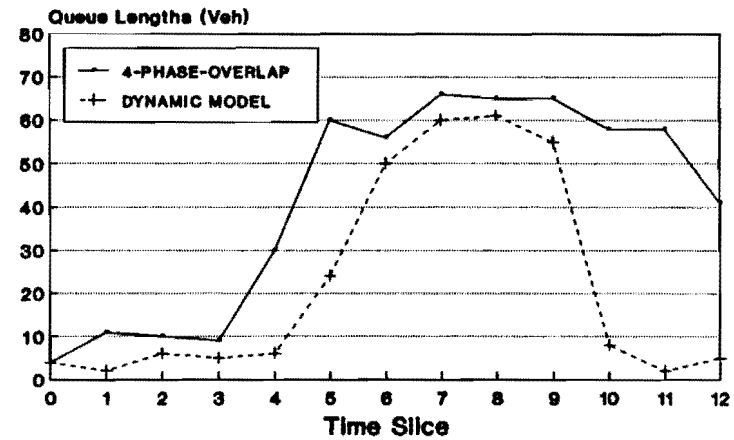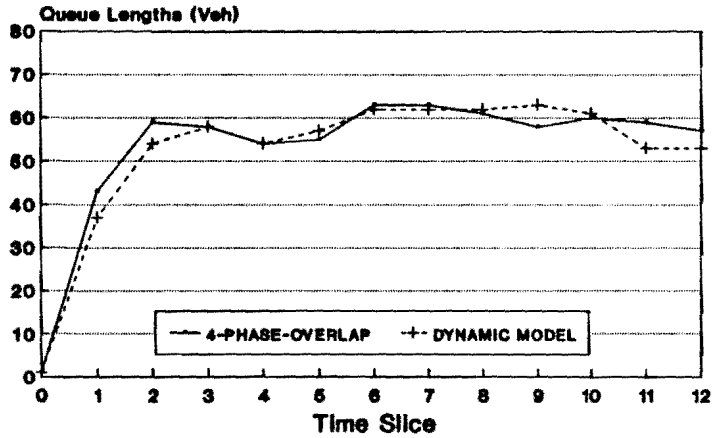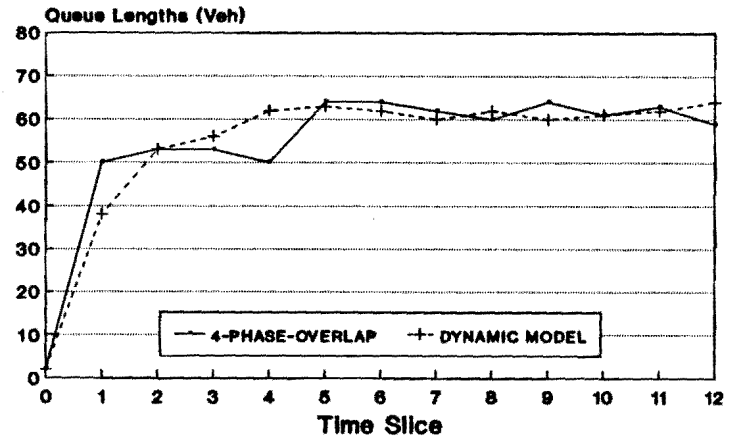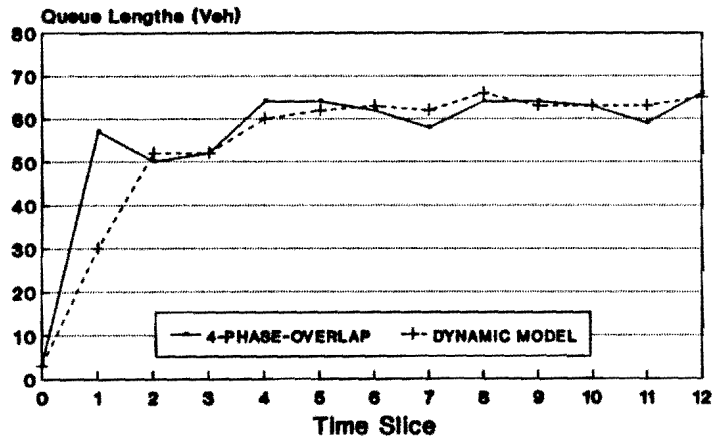


## APPROACH 4



Figure E-6.  Queues by TRAF-NETSIM, TLDI, Case 3

## APPROACH 1

Queue Lengths (Veh)



Time Slice

## APPROACH 2

Queue Lengths (Veh)



Time Slice

## APPROACH 3

Queue Lengths (Veh)



Time Slice

## APPROACH 4

Queue Lengths (Veh)



Time Slice

Figure E-7.  Queues by TRAF-NETSIM, TLDI, Case 2

## APPROACH 1



**Queue Lengths (Veh)**

Time Slice

Legend: 4-PHASE-OVERLAP · DYNAMIC MODEL

## APPROACH 2



**Queue Lengths (Veh)**

Time Slice

Legend: 4-PHASE-OVERLAP · DYNAMIC MODEL

## APPROACH 3



**Queue Lengths (Veh)**

Time Slice

Legend: 4-PHASE-OVERLAP · DYNAMIC MODEL

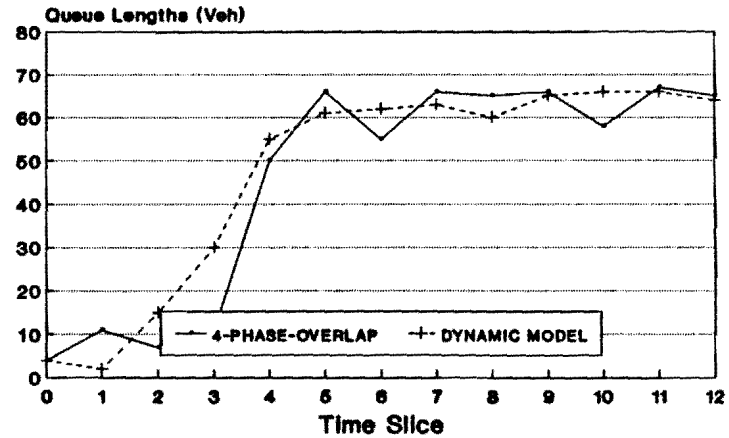## APPROACH 4



**Queue Lengths (Veh)**

Time Slice

Legend: 4-PHASE-OVERLAP · DYNAMIC MODEL

Figure E-8. Queues by TRAF-NETSIM, TLDI, Case 3